

**AN INVESTIGATION ON THE OPTIMIZATION
DOMAIN OF BIOLOGICAL GROWTH
METHOD**

**A THESIS SUBMITTED TO THE GRADUATE
SCHOOL OF APPLIED SCIENCES
OF
NEAR EAST UNIVERSITY**

**By
AYOUB MOFTAH MILAD YAHYA**

**In Partial Fulfilment of the Requirements for
the Degree of Master of Science
in
Mechanical Engineering**

NICOSIA 2017

**AYOUB MOFTAH MILAD
YAHYA**

**AN INVESTIGATION ON THE OPTIMIZATION
DOMAIN OF BIOLOGICAL GROWTH METHOD**

**NUE
2107**

**AN INVESTIGATION ON THE OPTIMIZATION
DOMAIN OF BIOLOGICAL GROWTH
METHOD**

**A THESIS SUBMITTED TO THE GRADUATE
SCHOOL OF APPLIED SCIENCES
OF
NEAR EAST UNIVERSITY**

**By
AYOUB MOFTAH MILAD YAHYA**

**In Partial Fulfilment of the Requirements for
the Degree of Master of Science
in
Mechanical Engineering**

NICOSIA 2017

**AYOUB MOFTAH MILAD YAHYA: AN INVESTIGATION ON THE
OPTIMIZATION DOMAIN OF BIOLOGICAL GROWTH METHOD**

**Approval of Director of Graduate School of
Applied Sciences**

Prof. Dr. Nadire CAVUS

**We certify that this thesis is satisfactory for the award of the degree of Master of
Science in Mechanical Engineering**

Examining Committee in Charge:

Prof. Dr. Mahmut A. Savas Committee Chairman, Department of Mechanical
Engineering, NEU

Assist. Prof. Dr. Ali Evcil Supervisor, Department of Mechanical Engineering,
NEU

Assist. Prof. Dr. Ehsan Kiani Department of Automotive Engineering, NEU

I hereby declare that all information in this document has been obtained and presented in accordance with academic rules and ethical conduct. I also declare that, as required by these rules and conduct, I have fully cited and referenced all material and results that are not original to this work.

Name, Last name: AYOUB YAHYA

Signature:

Date:

ACKNOWLEDGEMENTS

First, thanks to God alone for letting me to complete my Master Thesis success.

I would like to thanks to my supervisor, Assist. Prof. Dr. Ali Evcil for his patient guidance, encouragement and advice he has provided throughout my time as student. I have been extremely lucky to have a supervisor who cared so much about my work, and who responded to my questions and queries so promptly. In particular, I would like to thank Dogukan Evcil for his contribution during the software development.

Finally, I must express my very profound gratitude to my parents for providing me with unfailing support and continuous encouragement throughout my years of study and through the process of researching and writing this thesis. This accomplishment would not have been possible without them. Thank you.

To my parents...

ABSTRACT

The aim of the study was to investigate the effect of domain thickness in Biological Growth Method which is a tool used in structural shape optimization. The method was implemented by using MARC-MENTAT student version as the finite element code, pre- and post-processor. A small software called Biological Growth Interface (BGI) was developed to control and modify the data in the input and output files. The procedure was verified by conducting the parametric study of the plate with a hole problem discussed in the literature. The analyses were extended up to 40 mm domain thickness. It was observed that the number of iterations required for optimization decreased as the magnification factor and domain thickness increased. However, satisfactory results were obtained from the analyses resulted after more than 5 iterations.

It can be concluded that the method works with reasonable accuracy with an automatic mesh with large enough elements to prevent distortion and aspect ratio problems, an optimization domain selected roughly but including the remarkable stress changes around the hole boundary, a reference stress equal to the stress level far away from the hole and a low magnification factor to guarantee enough number of iterations for acceptable results.

Keywords: Biological growth method; domain thickness; finite element analysis; shape optimization; plane with a hole

ÖZET

Çalışmanın amacı, yapısal şekil optimizasyonunda kullanılan Biyolojik Büyüme Metodunda, etkinlik alan kalınlığının etkisini araştırmaktır. Metod MARC-MENTAT sonlu eleman paketinin öğrenci versiyonu kullanılarak uygulanmıştır. Biological Growth Interface (BGI) olarak isimlendirilen küçük bir ara yazılım girdi ve çıktı dosyalarındaki bilgileri kontrol etmek ve düzenlemek amacı ile oluşturulmuştur. Yöntem, literatürde yer alan delikli plakanın parametrik çalışması ile doğrulanmıştır. Etkin alanın kalınlığı 40 mm'ye kadar artırılarak sonuçlar incelenmiştir. Büyüklük faktörü ve etkin alan kalınlığı arttıkça iterasyon sayısının azaldığı, ancak 5 iterasyondan fazla süren analizlerin tatminkar sonuç verdiği gözlenmiştir.

Metodun, otomatik sonlu eleman ağı kullanarak kabul edilebilir sonuçlar verebileceği gösterilmiştir. Bunun için elemanların boyutları şekillerindeki bozulmaları tolere edecek büyüklükte olmalı ve etkin alan seçimi delik çevresindeki gerilim yığılmalarını içine alacak şekilde yapılmalıdır. Referans gerilme delikten uzakta yer alan nominal gerilme olarak alınabilir. Yeterli sayıda iterasyon ise büyüklük faktörünü azaltarak elde edilebilir.

Anahtar Kelimeler: Biyolojik büyüme metodu; alan kalınlığı; sonlu eleman analizi; şekil optimizasyonu; delikli plaka

TABLE OF CONTENTS

ACKNOWLEDGMENTS	ii
ABSTRACT	iv
ÖZET	v
TABLE OF CONTENTS	vi
LIST OF TABLES	viii
LIST OF FIGURES	ix
LIST OF SYMBOLS USED	xiii
CHAPTER 1: INTRODUCTION	1
CHAPTER 2: LITERATURE REVIEW	
2.1 Biological Growth Method	4
2.2 History	4
2.3 The Fundamental Procedure for the Method	7
2.4 Some Different Applications (2D, 3D)	10
2.4.1 Applications (2D)	11
2.4.2 Applications (3D)	13
CHAPTER 3: METHODOLOGY	
3.1 Optimization Tools	15
3.1.1 MARC-MENTAT student version (2016.0.0.SE)	15
3.1.2 Biological Growth Interface	15
3.2 Modelling	15
3.3 Optimization	16
CHAPTER 4: RESULTS AND DISCUSSION	
4.1 Verification of Biological Growth Method	23
4.2 Optimization of a Plate with a Hole with Domain Thickness 20 mm	42
4.3 Optimization of a Plate with a Hole with Domain Thickness 30 mm	56

4.4 Optimization of a Plate with a Hole with Domain Thickness 40 mm	69
4.4 Optimization of a Plate with a Hole with Auto-Mesh	80
CHAPTER 5: CONCLUSIONS AND FUTURE WORK	84
REFERENCES.....	86
APPENDICES	
Appendix 1: StressV1.dat.....	89
Appendix 2: StressV1.out.....	94
Appendix 3: ThermalV1.dat.....	120
Appendix 4: ThermalV1.out.....	127

LIST OF TABLES

Table 3.1: Format of file StressVi.dat	19
Table 3.2: Format of file StressVi.out	20
Table 3.3: Format of file ThermalVi.dat	21
Table 3.4: Format of file ThermalVi.out	22
Table 4.1: Optimization parameters	24
Table 4.2: Summary and comparison of results with domain thickness 10mm.....	41
Table 4.3: Summary of results with domain thickness 20mm.....	55
Table 4.4: Summary of results with domain thickness 30mm.....	68
Table 4.5: Summary of results with domain thickness 40mm.....	79
Table 4.6: Summary of results with auto-mesh	83

LIST OF FIGURES

Figure 2.1: A cantilever beam under end shear load	11
Figure 2.2: A square plate with hole under biaxial loading	12
Figure 2.3: Plate-with-a-hole	13
Figure 2.4: Plate-with-a-hole (3D)	14
Figure 3.1: Flow chart of Biological Growth Method used	17
Figure 4.1: Description of the problem	23
Figure 4.2: Finite element discretization of one-quarter of the plate	23
Figure 4.3: Finite element model for stress (left) and thermal (right) analyses (D=10mm).....	24
Figure 4.4: von Mises stresses (left) and thermal deformations (right) of the original shape (D=10mm).....	24
Figure 4.5: Optimization results of a plate with a hole (D=10 mm, K = 250, $\sigma_{ref} = 10$ MPa).....	26
Figure 4.6: Optimization results of a plate with a hole (D=10 mm, K = 275, $\sigma_{ref} = 10$ MPa).....	27
Figure 4.7: Optimization results of a plate with a hole (D=10 mm, K = 500, $\sigma_{ref} = 10$ MPa).....	28
Figure 4.8: Optimization results of a plate with a hole (D=10 mm, K = 750, $\sigma_{ref} = 10$ MPa).....	29
Figure 4.9: Optimization results of a plate with a hole (D=10 mm, K=1000, $\sigma_{ref} = 10$ MPa).....	30
Figure 4.10: Optimization results of a plate with a hole (D=10 mm, K=250, $\sigma_{ref} = 40$ MPa).....	31
Figure 4.11: Optimization results of a plate with a hole (D=10 mm, K=275, $\sigma_{ref} = 40$ MPa).....	32
Figure 4.12: Optimization results of a plate with a hole (D=10 mm, K=500, $\sigma_{ref} = 40$ MPa).....	33
Figure 4.13: Optimization results of a plate with a hole (D=10 mm, K=750, $\sigma_{ref} = 40$ MPa).....	34
Figure 4.14: Optimization results of a plate with a hole (D=10 mm, K=1000, $\sigma_{ref}=40$ MPa).....	35
Figure 4.15: Optimization results of a plate with a hole (D=10 mm, K=250, $\sigma_{ref} = 60$ MPa).....	36

Figure 4.16: Optimization results of a plate with a hole (D=10 mm, K=275, $\sigma_{ref} = 60$ MPa).....	37
Figure 4.17: Optimization results of a plate with a hole (D=10 mm, K=500, $\sigma_{ref} = 60$ MPa).....	38
Figure 4.18: Optimization results of a plate with a hole (D=10 mm, K=750, $\sigma_{ref} = 60$ MPa).....	39
Figure 4.19: Optimization results of a plate with a hole (D=10 mm, K=1000, $\sigma_{ref}=60$ MPa).....	40
Figure 4.20: Finite element model for stress (left) and thermal (right) analyses (D=20mm).....	42
Figure 4.21: von Mises stresses (left) and thermal deformations (right) of the original shape (D=20mm).....	42
Figure 4.22: Optimization results of a plate with a hole (D=20 mm, K=250, $\sigma_{ref} =10$ MPa).....	43
Figure 4.23: Optimization results of a plate with a hole (D=20 mm, K =275, $\sigma_{ref} =10$ MPa).....	44
Figure 4.24: Optimization results of a plate with a hole (D=20 mm, K =500, $\sigma_{ref} =10$ MPa).....	45
Figure 4.25: Optimization results of a plate with a hole (D=20 mm, K=250, $\sigma_{ref} = 40$ MPa).....	46
Figure 4.26: Optimization results of a plate with a hole (D=20 mm, K=275, $\sigma_{ref} = 40$ MPa).....	47
Figure 4.27: Optimization results of a plate with a hole (D=20 mm, K=500, $\sigma_{ref} = 40$ MPa).....	48
Figure 4.28: Optimization results of a plate with a hole (D=20 mm, K=750, $\sigma_{ref} = 40$ MPa).....	49
Figure 4.29: Optimization results of a plate with a hole (D=20 mm, K=250, $\sigma_{ref} = 60$ MPa).....	50
Figure 4.30: Optimization results of a plate with a hole (D=20 mm, K=275, $\sigma_{ref} = 60$ MPa).....	51
Figure 4.31: Optimization results of a plate with a hole (D=20 mm, K=500, $\sigma_{ref} = 60$ MPa).....	52
Figure 4.32: Optimization results of a plate with a hole (D=20 mm, K=750, $\sigma_{ref} = 60$ MPa).....	53
Figure 4.33: Optimization results of a plate with a hole (D=20 mm, K=1000, $\sigma_{ref}=60$ MPa).....	54

Figure 4.34: Finite element model for stress (left) and thermal (right) analyses (D=30mm).....	56
Figure 4.35: von Mises stresses (left) and thermal deformations (right) of the original shape (D=30mm).....	56
Figure 4.36: Optimization results of a plate with a hole (D=30 mm, K=250, σ_{ref} =10MPa).....	57
Figure 4.37: Optimization results of a plate with a hole (D=30 mm, K =275, σ_{ref} =10MPa).....	58
Figure 4.38: Optimization results of a plate with a hole (D=30 mm, K =500, σ_{ref} =10MPa).....	59
Figure 4.39: Optimization results of a plate with a hole (D=30 mm, K=250, σ_{ref} = 40 MPa).....	60
Figure 4.40: Optimization results of a plate with a hole (D=30 mm, K=275, σ_{ref} = 40 MPa).....	61
Figure 4.41: Optimization results of a plate with a hole (D=30 mm, K=500, σ_{ref} = 40 MPa).....	62
Figure 4.42: Optimization results of a plate with a hole (D=30 mm, K=250, σ_{ref} = 60 MPa).....	63
Figure 4.43: Optimization results of a plate with a hole (D=30 mm, K=275, σ_{ref} = 60 MPa).....	64
Figure 4.44: Optimization results of a plate with a hole (D=30 mm, K=500, σ_{ref} = 60 MPa).....	65
Figure 4.45: Optimization results of a plate with a hole (D=30 mm, K=750, σ_{ref} = 60 MPa).....	66
Figure 4.46: Optimization results of a plate with a hole (D=30 mm, K=1000, σ_{ref} =60 MPa).....	67
Figure 4.47: Finite element model for stress (left) and thermal (right) analyses (D=40mm).....	69
Figure 4.48: von Mises stresses (left) and thermal deformations (right) of the original shape (D=40mm).....	69
Figure 4.49: Optimization results of a plate with a hole (D=40 mm, K=250, σ_{ref} =10MPa).....	70
Figure 4.50: Optimization results of a plate with a hole (D=40 mm, K =275, σ_{ref} =10MPa).....	71
Figure 4.51: Optimization results of a plate with a hole (D=40 mm, K=100, σ_{ref} = 40 MPa).....	72

Figure 4.52: Optimization results of a plate with a hole (D=40 mm, K=200, $\sigma_{\text{ref}} = 40$ MPa).....	73
Figure 4.53: Optimization results of a plate with a hole (D=40 mm, K=250, $\sigma_{\text{ref}} = 40$ MPa).....	74
Figure 4.54: Optimization results of a plate with a hole (D=40 mm, K=275, $\sigma_{\text{ref}} = 40$ MPa).....	75
Figure 4.55: Optimization results of a plate with a hole (D=40 mm, K=250, $\sigma_{\text{ref}} = 60$ MPa).....	76
Figure 4.56: Optimization results of a plate with a hole (D=40 mm, K=275, $\sigma_{\text{ref}} = 60$ MPa).....	77
Figure 4.57: Optimization results of a plate with a hole (D=40 mm, K=500, $\sigma_{\text{ref}} = 60$ MPa).....	78
Figure 4.58: Finite element model for stress (left) and thermal (right) analyses (Auto-mesh).....	80
Figure 4.59: von Mises stresses (left) and thermal deformations (right) of the original shape (Auto-mesh).....	80
Figure 4.60: Optimization results of a plate with a hole (Auto-mesh, K=200, $\sigma_{\text{ref}} = 10$ MPa).....	81
Figure 4.61: Optimization results of a plate with a hole (Auto-mesh, K=250, $\sigma_{\text{ref}} = 10$ MPa).....	82

List of Abbreviations and Symbols

2D	Two Dimension
3D	Three Dimension
BEM	Boundary Element Method
BGI	Biological Growth Interface
BGM	Biological Growth Method
D	Optimization domain
FEM	Finite Element Method
E	Actual Young's modulus
E_{red}	Reduced Young's modulus
k	Magnification factor
u, v, w	Displacement components
x, y, z	Cartesian coordinates
$\varepsilon_x, \varepsilon_y, \varepsilon_z$	Normal components of the infinitesimal strain tensor
$\sigma_x, \sigma_y, \sigma_z$	Normal components of Cauchy stress tensor
σ_{vm}	Equivalent von Mises stress
σ_{ref}	Reference stress
$\Delta\vartheta$	Temperature difference
Δt	Time span
β	Proportionality factor
Γ	Optimization boundary
α	Thermal expansion coefficient
ζ	Conversion factor
ν	Poisson's ratio

CHAPTER 1

INTRODUCTION

Optimization is known as the is a way through which a function can either be minimized or maximized. Optimization problems inserted are in any modeling and as well as in the designing. For identifying a model, there is a need of minimizing the distance that is between the model predictions made and the experiments which take place. Modelling can regularly be explained or expressed as a minimization of energy. For instance, the balance of a preservationist framework can be acquired by limiting its aggregate potential energy. What's more, obviously, is that the ideal plan is additionally concerned regarding the criteria of performance which is to be maximized.

Structural optimization is one of the most important because it looks for the best option out of all the designs for structure and it looks at both extremes of the design while selecting which are of minimization and maximization. Its function is to minimize the cost and the usage of material which is used for the project, and at the same time it is to make sure that the safety is taken into consideration and kept at maximum level, and also another concern is of maximizing the performance. For the design of the structure to be optimized in engineering, there are three different types structural optimization which is size, shape and topology optimization their detailed explanation is as follow:

Size optimization process selects the domain of the structure which is to be fixed, fixes it and once the process takes place, it cannot change the domain of the structure. The variables of design sizing can be in two states meaning that it can either be continuous or discrete. This process of size optimization is mostly known the application of optimization which takes place at the stage of design details.

Shape of the exterior boundary surfaces or arches is selected in the shape optimization. Examples which are known for this problem comprise of locating the border of the structure, locating the area of junctions of a skeletal structure, locating the best standards for parameters, which characterize the center surface of a shell structure. This process of shape optimization is known the application of optimization, and it is the initial design stage.

For finding the best layout for the structure according to the defined design topology optimization is used. Unlike the other optimization methodologies, topology optimization uses a grand or universal structure as its preliminary design. The issues which are identified are conditions of support, applied loads, structure volume which is to be constructed and other restrictions which might be considered by the designer of the structure. This optimization type is most tough amongst other two types (Tang, 2011).

Biological Growth Method (BGM) was introduced by Mattheck (1990), who had carried out observations in nature to come up with this method. According to BGM, if optimization were to be applied in nature, it would be done via swelling or shrinking of the outermost layer that produces the leveling of the local stress of the material. Then again, Mattheck characterizes ideal shape as the one that demonstrates a condition of consistent stress at part of, or the entirety of, the surface of the material (Cardona et al., 2006).

Hrennikoff, McHenry, and Newmark were the first ones who had started the development of Finite Element Method (FEM) in structural mechanics in 1940s. They made use of a mesh created by rods and beams for the solution of stresses in ongoing solids. Conrants which was in a lecture from 1941, it had given proposition which was a method for problems of the torsional model, it recommended for making use of piecewise polynomial interpolation over triangular sub-regions. As the development in the technological fields progressed, computers had come into being, and through the use of a computer it became possible for writing and solving the stiffness equations in the form of a matrix. The matrix of stiffness equation for the beam, truss, and various elements had been presented in a study carried out by Turner,

Clough, Topp, and Martin in 1956. Clough was the one who had come up with the finite element and was credited for it. A great deal of work had been put into the development of finite element method. This work has been carried into the fields related to the formulation of the elements and as well as the implementation of a computer. There are number of developments which have been achieved in the computer technology such as the hardware, accurate solutions for matrix, efficiency in matrix solver, graphics which help to ease the visual of the process stages, generation of mesh, and as well as in the stages which take place after the processing (Budynas & Nisbett, 2008).

Boundary Element Method (BEM) is a technique which is used for conversion of equations governing into equivalent integrals. It uses the associations from vector calculus which relate to Gauss-Green or the divergence theorem, which include both surface and volume integrals, are converted to integral equations which do not consist of volume integrals concerning the unknown response. The last conversion includes few known solutions (fundamental solutions) related to the original differential equation.

The aim of the study was to implement the biological growth method using finite element software MSC Marc-Mentat student version and to investigate the effects of domain thickness on the method. A parametric study, also including the domain thickness among others, was conducted. A much more simpler and faster analysis technique was the expected outcome.

CHAPTER 2

LITERATURE REVIEW

2.1 Biological Growth Method

Biological Growth Method (BGM) was introduced by Mattheck (1990), who had carried out observations in nature on trees, their joints, deer antlers etc., in order to come up with the method. According to him natural substances are able to optimize their shapes and structures depending on the load themselves. He has defined optimum shape as “the one that shows a state of constant stress at part of or the whole of the surface of the component.” According to BGM, if optimization was to be applied in nature, it would be done via swelling or shrinking of most outer layer that produces the levelling of local stress of the material (Wessel et al., 2004).

2.2 History

The best example for shape optimization in a natural and simple state would be of bones and trees. They tend to bring change in their structure according to the external loads which are put upon them, this change takes place to reduce the stress.

Computer –Aided Shape Optimization (CAO) was developed by Mattheck and Burkhardt (1990), algorithm by simulating tree growth to optimize mechanical engineering structures. The method assumed that in all structures considered, a state of constant stress at the surface of the biological 'component' was always given the natural loading case applied. This technique is therefore equivalent to a procedure which material is added at overloaded places in the structure and is not added (or even removed) at places with stresses below the reference stress until the optimal shape attained (Mattheck, 1991).

An optimization algorithm known as Soft Kill Option (SKO) was proposed by Baumgartner et al. (1992), this algorithm was developed in order to locate the optimum structural topology depending on the replication of reconciling bone mineralization by having to change Young's modulus depending on the calculated stress distribution. According to Mattheck

and Burkhardt (1990), the optimum topology which is obtained can be made use of in order to create a new model of finite element for the subsequent shape optimization with the help of CAO to even out the contours and for the reduction of stress which remain (Baumgartner et al., 1992).

It was Chen and Tsai (1993) who had broadened the approaches for simulated biological growth with the help of fabricated temperature loading in order to lessen the stress concentration which was subjected to area limitations or to lessen area (weight) subjected to stress limitations.

According to Tekkaya and Guneri (1996), implementation of biological growth methodology was a part of experiential method and calculated systematically the impact of parameters that manage the process of optimization, on the procedure of optimization when minimizing the concentration of stress of a squared plate that initially contained circular hole under biaxial tensions.

A mixed method which was of experimental and evolutionary methods was proposed by Le Rice Le Riche and Cailletaud (1998), it was created to come up with the solution for the problems of shape optimization. In improvement of designs biological growth had been measured as an efficient approach yet the problem it faced was that it was not able to produce a global optimum shape. Evolutionary or genetic algorithms (Hajela, 1990; Jenkins, 1991; Rajeev and Krishnamoorthy, 1992) are able to manage problems related to nonconvex and find the global optimal shape but as large problems are in question then the calculated cost would be very high. Hence, mixture of the evolutionary approach and biological growth method was considered to an efficient and cost effective approach. As the outcomes were in agreement with the results of Le Riche and Cailletaud (Le Riche, & Cailletaud, 1998).

Cai, et al., (1998) developed and proposed a method which for the structural shape optimization, this method added the Boundary Element Method (BEM) with biological growth optimization method. The method proposed was considered to be correct as it had proven couple of examples. It came out to be an efficient, simple and effective method for shape optimization. Carolina et al., (2004) noted the implementation of BGM with BEM. Boundary-only along with the accuracy for the dislocation and stress solutions are the most

special and known intrinsic characteristic of BEM which make this method efficient and effective for the solutions of shape optimization problems (Wessel et al., 2004).

An adjusted approach of biological growth method was presented by Tian & Shangjin (2004), this approach is able to get the shape optimization of structure through a complex geometry solution. This solution has three parts to it. First, there is no use of node coordinates in the modification of FEM model, the structure's boundary is defined with the help of B-spline curve. Second, there is a cost function which is created in order to allow the structural weight to be decreased to its minimal level, which is subject to limitations of stress and geometrical. Therefore, there is an improvement in the biological growth method which allows it to optimize the design of the complex geometry. Third, as the evolution of shape optimization takes place, there is a method which is related to the penalty, it deals with anyone who violates the constraint settings. This adjusted approach had been tested and was successfully implemented for the shape optimization of centrifugal impellers (Tian & Shangjin, 2004).

A new approach had been presented for the shape optimization for three dimensional and damage tolerant structures by Peng & Jones (2008). This approach makes use of a new method, which is known as Failure Analysis of Structures (FAST), it is applied to get the estimation of the stress-intensity factor for the cracks at a notch. CAD and FAST codes are made use of in the development of methodology and software which are used for the automation damage-tolerance calculations. In order to find the location of worst cracks, modeling of number of cracks by the fractured critical edges of the structure is done by the help of FAST. FAST is later used for the evaluation of damage-tolerance objective functions for the algorithms of optimization. To understanding the problem which is being faced by optimization with fatigue life is done via stress-based biological growth method. Hence, by the help of numerical examples this has proven that a stress-optimized structure is not essentially going to provide the longest fatigue life (Peng & Jones, 2009).

Over the past years there has been various methods proposed, adaptive biological method is an example which was proposed for the reduction of cost and for improving accuracy (Zehsaz, Torkpanpouri & Paykani, 2013). In the study carried out by Zehsaz, Tokpanpouri, and Paykani (2013), influences of step factor, control points coordination and number of

control points in the convergence rate were taken into consideration. ANSYS Parametric Design language (APDL) was used for writing the codes, In APDL, parameters being studied are taken as inputs and it gives the best shape for the components which are being studied. The results of the study had shed light upon attaining successful optimization showed that step factor must be kept within a certain range in order to attain the successful optimization. Another way for attaining optimized shape is by making use of any coordinate system which is used for defining control points and as well as having to select any direction for stimulus vector of algorithm. Moreover, if the number of control points are increased, it can cause creation of non-uniformities in the studied boundaries. Having to attain the acceptable accuracy is impossible because of the formation of saw form at the studied boundary known as “saw position” (Zehsaz, Torkpanpouri & Paykani, 2013).

2.3 The Fundamental Procedure for the Method

Biological Growth Method (BGM) function is defined as:

$$\text{Minimize } [\sigma_{vm}(x, y, z) - \sigma_{ref}] \quad \forall (x, y, z) \in D \quad (2.1)$$

where $\sigma_{vm}(x, y, z)$ is the von Mises stress at any point at the optimization domain D and σ_{ref} is known as the reference stress. And through the reference stress the von Mises stress distribution tends to clear away. In correspondence to the growth of biological structures under loads, it is proposed that (2.1) can be satisfied if the optimization domain changes its shape according to:

$$\varepsilon_{sw}^{\dot{}}(x, y, z) = \beta[\sigma_{vr}(x, y, z) - \sigma_{ref}] \quad (2.2)$$

Where $\varepsilon_{sw}^{\dot{}}(x, y, z)$ is the volumetric swelling strain-rate which is proportional to the driving function, i.e. the deviation of the von. Mises stress from the reference stress at a generic location in the optimization domain. The proportionality factor is given by β . The volumetric swelling scheme can be attained with the use of an Euler integration scheme for a timespan of Δt as shown below:

$$\varepsilon_{sw}(x, y, z) = \beta[\sigma_{vr}(x, y, z) - \sigma_{ref}]\Delta t \quad \forall (x, y, z) \in D \quad (2.3)$$

An elegant method to implement the swelling equation (2.3) is by means of a thermal analogy. It can be shown that this analogy is based on the generalized Hooke's law (shear strains are discarded):

$$\begin{aligned}\varepsilon_x &= \frac{1}{E} [\sigma_x - \nu (\sigma_y + \sigma_z)] + \alpha \Delta\vartheta \\ \varepsilon_y &= \frac{1}{E} [\sigma_y - \nu (\sigma_x + \sigma_z)] + \alpha \Delta\vartheta \\ \varepsilon_z &= \frac{1}{E} [\sigma_z - \nu (\sigma_y + \sigma_x)] + \alpha \Delta\vartheta\end{aligned}\tag{2.4}$$

Here, ε_x , ε_y and ε_z are strain components, normal components of stresses are depicted by σ_x , σ_y and σ_z that are part of the Cauchy stress tensor, Poisson's ratio is depicted by ν , the coefficient of thermal expansion is represented by α and $\Delta\vartheta$ represents the change in the temperature. Now, if the mechanical loads on the structure to be optimized are removed and a great reduction in the Young's modulus E of the optimization domain is made, then abandonment of the first parts of the strains can be done even by keeping the same boundary conditions of the real problems, Therefore,

$$\varepsilon_x \approx \varepsilon_y \approx \varepsilon_z \approx \alpha \Delta\vartheta\tag{2.5}$$

In the optimization domain D , if thermal expansion is just defined to be as non-zero, then, from equation (2.5)

$$\varepsilon_{sw}(x, y, z) = \alpha \Delta\vartheta(x, y, z) \quad \forall (x, y, z) \in D\tag{2.6}$$

Comparison of equation (2.3) with equation (2.6) indicates the correspondence

$$\Delta t \quad \Leftrightarrow \quad \alpha\tag{2.7}$$

$$\beta [\sigma_{vm}(x, y, z) - \sigma_{ref}] \quad \Leftrightarrow \quad \Delta\vartheta(x, y, z)\tag{2.7}$$

Equations (2.6) and (2.7) are the basic relations of the thermal analogy for the swelling phenomenon given in equations (2.2) and

$$(2.3)$$

Mathematical framework shown above for the optimization and its parameters is explained below:

1. First the optimization boundary has to be selected which is depicted by Γ .

2. Size of the region D which has to be optimized has to be decided that is constrained from by Γ .
3. The mechanical analysis has to be conducted via:
 - a. Provided the conditions of mechanical loading;
 - b. Provided the conditions of essential boundary;
 - c. And properties of the original material.

Von Mises stress distribution of the optimization region D is found through this analysis.

4. The mechanical analysis can be carried via:
 - a. Thermal loads

$$\Delta\vartheta(x, y, z) = \zeta [\sigma_{vm}(x, y, z) - \sigma_{ref}] \quad (2.8)$$

Conversion factor is depicted by ζ , with having unit's degrees temperature per stress. And reference stress is depicted by σ_{ref}

- b. For the optimization, non-zero α which is the thermal expansion coefficient must be used and for other regions, zero expansion coefficient can be used.
- c. For the D (optimization domain), Young's modulus E_{red} is significantly reduced.

Through this calculation the displacements u, v, w can be provisioned along the optimization surface Γ which bounds D.

5. The optimization boundary Γ must be update with:

$$\begin{aligned} X &= x + k u(x, y, z) \\ Y &= y + k v(x, y, z) \\ Z &= z + k w(x, y, z) \end{aligned} \tag{2.9}$$

Here K represents a magnification factor that is essential for the acceleration convergence.

It is necessary to repeat steps 3 to 5 until there is no change noted and detected in the driving function. It must be noted that this procedure enables interfering of the user at the steps 1 and 2.

There has to be total of seven parameters which are to be set during the implication of the method. From these parameters, similar results are shown by ζ , α and k : All of these parameters tend to behave like magnification factors. Hence, this study, has only taken k into consideration, while ζ considered as unity, and the definite thermal expansion coefficient is α . The reduced Young's modulus has only a minor effect on the results as long as it is considerably small preventing any constraints owing to static indeterminacy. For this reason, the value of E_{red} is set equal to 1/400 of the actual Young's modulus of the material. On the other hand, selection of the optimization boundary Γ is an engineering decision and depends on the problem in hand, so that it is selected intuitively for the analysis problem described in the next section. (Tekkaya & Güneri, 1996).

2.4 Some Different Applications (2D, 3D)

In this section some applications from previous scientific papers were discussed.

2.4.1 Applications (2D)

- **Cantilever beam under top shear loading**

A cantilever beam under top uniform distributed shear loading, as shown below in Figure 1, is chosen as the first example. The length and the width of the beam are 5 m and 1.2 m, respectively. 6 MN/m is the value of the top shear loading. 210 GPa and 0.3 is the value for the Young's modulus and Poisson (Chen, & Tsai, 1993).

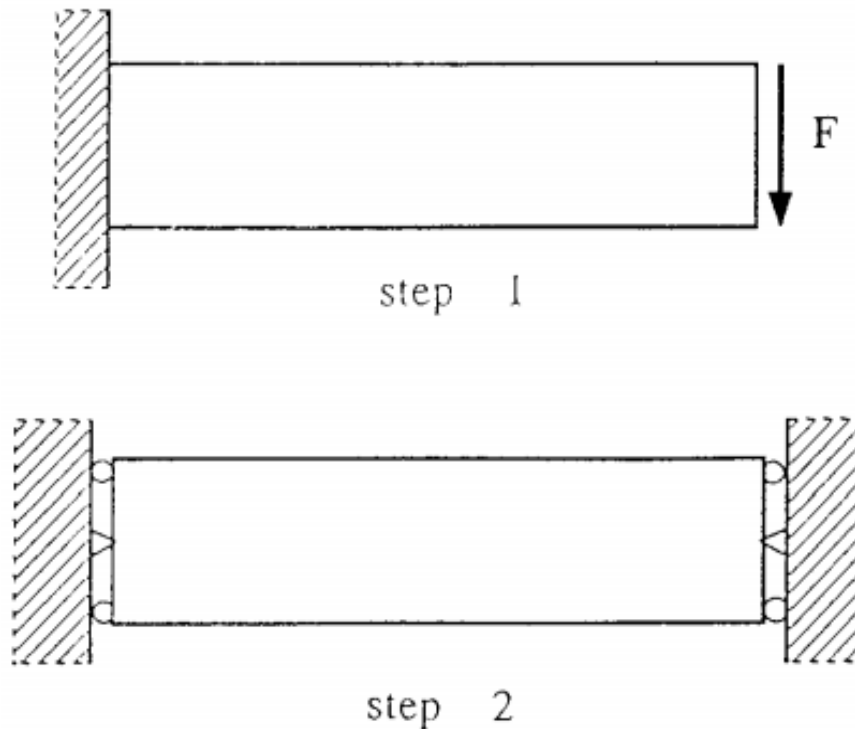


Figure 2.1: A cantilever beam under end shear load

- **Square plate with a hole under biaxial tension**

It can be seen in the figure 2, there is a square plate which has a hole that is there to even tensile loads by its edges. The emphasis of the stress is on the pinnacles of the hole. The main aim of the optimization is to come up with a shape which could be given to the hole in order to minimize the stress which is in the boundary hole elements. The plate is of 12 in length and the hole is of 2 in length. Young's modulus is 30×10^6 psi (69 GPa), Poisson's ratio is 0.3 and load P is 10 lb/in (1750 N/m) (Chen, & Tsai, 1993).

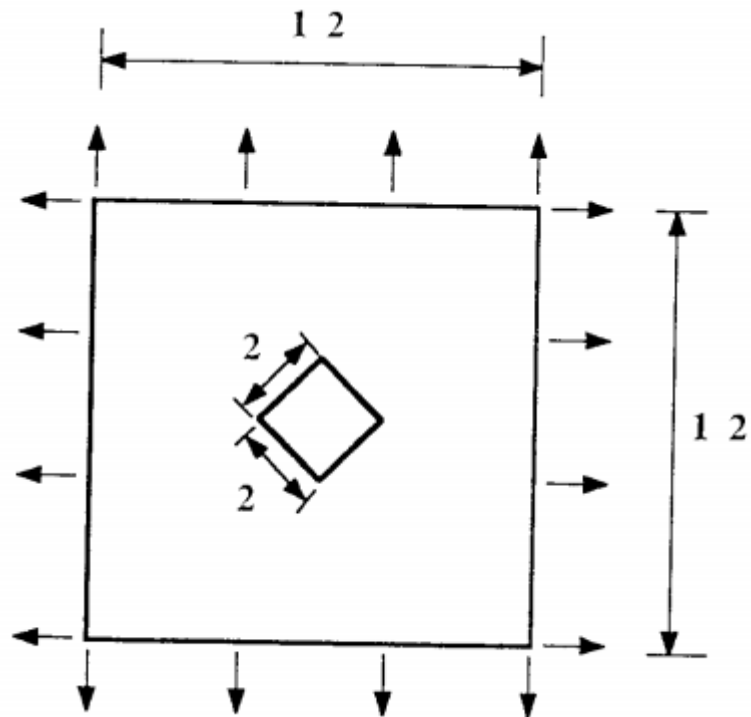


Figure 2.2: A square plate with hole under biaxial loading

- **Plate-with-a-hole problem**

The plate considered is a square with dimensions 300×300 mm as shown in Figure 3 with a center hole of diameter 80 mm and thickness of 5 mm. The material is presumed to be a standard steel which has the Young's modulus of 210 GPa and its Poisson's ratio is 0.3. The applied stress along the sides perpendicular to the x-axis is taken as 45 MPa and along the sides perpendicular to they-axis is taken as 22.5 MPa. The stress state is taken two-dimensional (Tekkaya & Güneri, 1996).

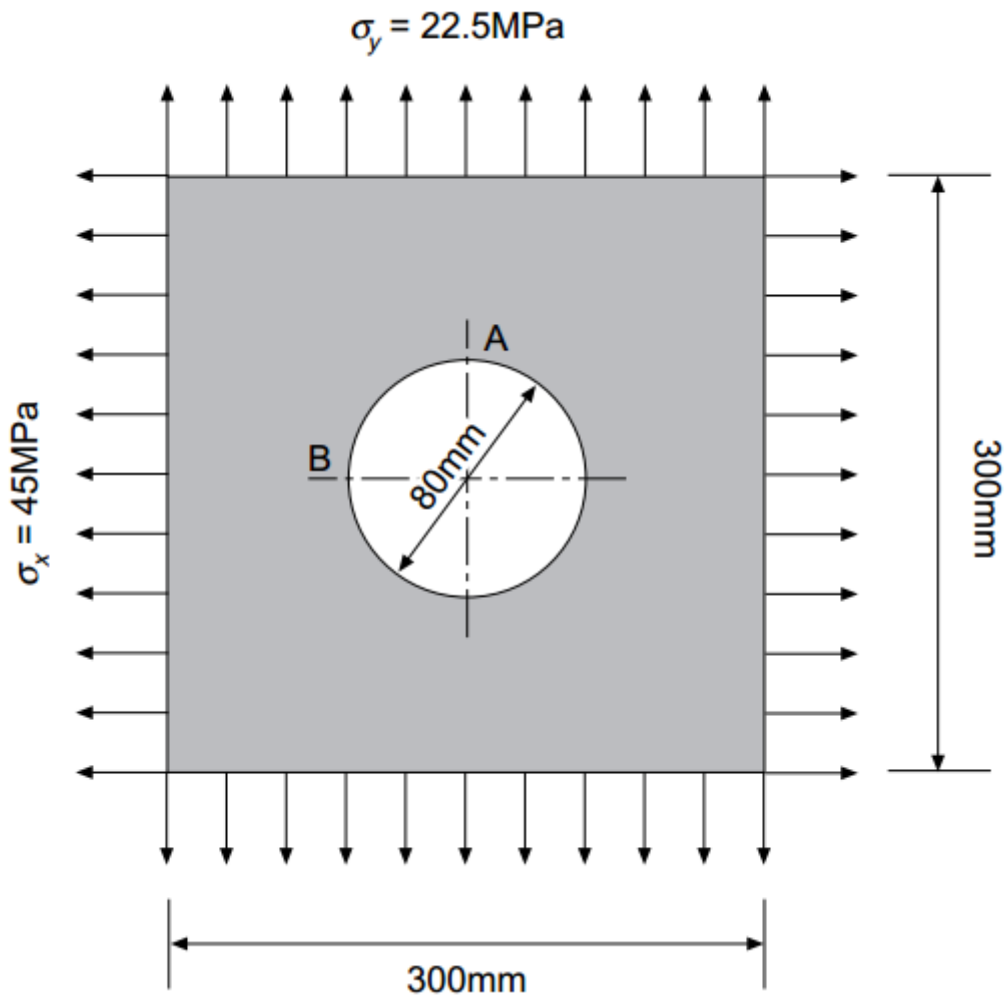


Figure 2.3: Plate-with-a-hole

2.4.2 Applications (3D)

- **Plate-with-a-hole problem**

Figure 4 given below shows a 3-D plate with a hole and it has a continuous in-plane tension of 100 MPa in the direction of x. As there is a symmetry, only a quarter part of the plate is ideal. In this example, the stress concentration factor is of 3 which is located at curve of the hole where it crosses y-axis. The externally applied tensile stress and the reference Mises stress are set to be the same, and for the ending of the loop criterion 2 was selected. Criterion 2 was selected because criterion 1 was not a good option because it could reach only zero-

driving force as the hole grows together. And value of Poisson ratio which would require a fine mesh at the vertex on the main axis of the transient ellipse during the remolding phase is of $\nu=0.0$ (Mattheck, & Moldenhauer, 1990).

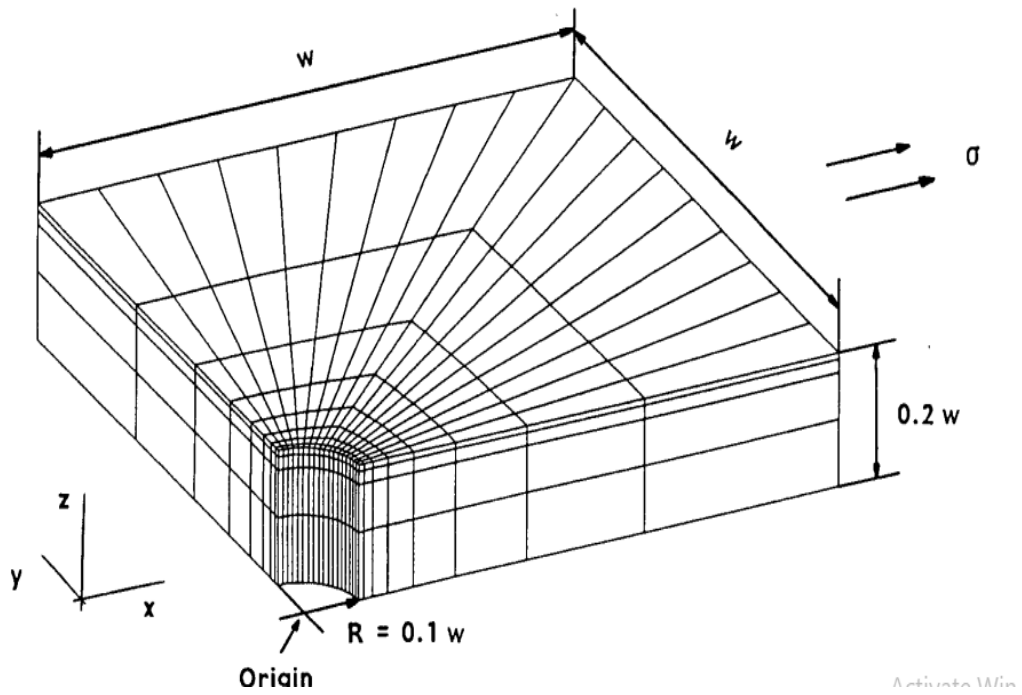


Figure 2.4: Plate-with-a-hole (3D)

CHAPTER 3

METHODOLOGY

The methodology used in the study involves the adaptation of the biological growth method for shape optimization to the student version of a commercial finite element code with the aid of a software developed. The flowchart of the procedure is shown in Figure 3.1 together with the tools used.

3.1 Optimization Tools

3.1.1 Marc-Mentat student version (2016.0.0.SE)

MARC-MENTAT student version is a limited and combined application of MARC finite element software and MENTAT pre- and post-processor. MENTAT is a powerful tool to generate finite element models, run MARC and interpret the results obtained. MARC can be run externally if the required data file is readily available.

3.1.2 Biological Growth Interface

Biological Growth Interface (BGI) is a software developed during the study using Java to transfer the required data between the input and output files created by MARC and MENTAT. It is also used to input the optimization parameters during the optimization process.

3.2 Modelling

MARC-MENTAT student version (2016.0.0 SE) were used as pre-processor to form the models. The models could be saved as *.mud or *.mfd files. The mesh, displacement boundary condition, geometric properties and element types of structural and thermal analyses models were the same. The elements and nodes of the domain to be optimized were defined. The two models deviate from each other as described below.

In the stress analysis model, force boundary conditions were applied. The material properties were given as it is for the material under consideration. von Mises stresses were selected to be given as output.

In the thermal analysis model, the material properties were defined. However, the Young's modulus was defined as 525 MPa (softer) for the domain elements. Displacements were selected to be given as output.

The data files (*.dat), needed to run MARC finite element software externally, were generated by running MARC via the application MARC-MENTAT student version (2016.0.0 SE) using the model files (*.mud or *.mfd) formed. The data file for the stress analysis is ready to run within the first iteration and therefore its name was given as *V1.dat. However, thermal boundary conditions were missing in the thermal analysis data file and must be added during the first iteration. The name of the thermal analysis file therefore was given as *V0.dat.

3.3 Optimization

The optimization iterations were conducted by Biological Growth Interface (BGI) software developed. After each iteration BGI stops and waits for new data set for the next iteration. At the beginning of each iteration it is required to enter the data files and three optimization parameters, namely, stress reference, stress-temperature factor and magnification factor. There is no need to re-enter the parameters if they will remain the same. However, data files for stress analysis (*stressVi.dat*) and thermal analysis (*thermalVi-1.dat*) must be updated after each iteration. Before the first iteration, BGI does the necessary changes to *thermalV0.dat* file to include the thermal boundary conditions, assigned as $\Delta T = 0$ to the nodes defined in the set Domain Nodes.

BGI then calls MARC to conduct the stress analysis using the file *stressVi.dat*. The files *stressVi.out*, *stressVi.t16*, *stressVi.t19* are created as outputs. *.t16 (binary) and *.t19 (ASCII) files can be used to visualize the results using MENTAT as post-processor. The results obtained are also listed in *.out file.

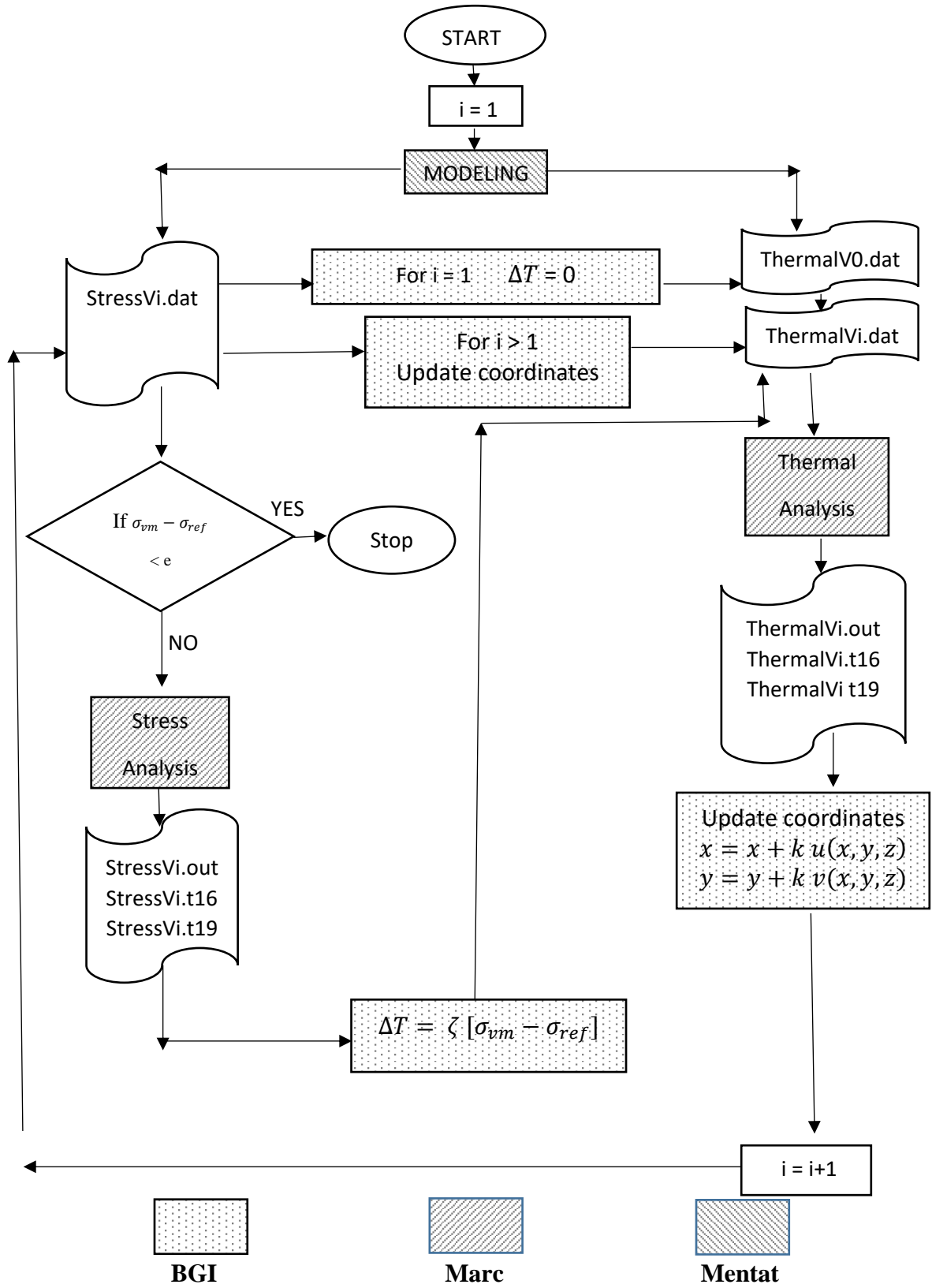


Figure 3.1: Flow chart of Biological Growth Method used

BGI then opens the *stressVi.out* file and reads the von Mises stresses at every integration point. BGI finds the integration points around each node listed in the set Domain Nodes and takes the averages of their von Mises stresses to calculate the nodal von Mises stresses. The differences between the von Mises stresses and the reference stress multiplied by stress-temperature factor are assigned as temperature differences ($\Delta T = \zeta [\sigma_{vm} - \sigma_{ref}]$) to the nodes in the set Domain Nodes in the file *thermalVi-1.dat* and the file is saved as *thermalVi.dat*.

BGI calls MARC again to run *thermalVi.dat* and the files *thermalVi.out*, *thermalVi.t16*, *thermalVi.t19* are created as outputs similar to that of stress analysis. The deflections of the nodes in the set Domain Nodes are obtained from the *thermalVi.out* file and the coordinates of these nodes were updated in *stressVi.dat* file to form *stressVi+1.dat* file.

BGI now pauses and waits for a command for further optimization. The user is now expected to analyze the results and decide to continue or to stop. To continue, it is required to change the file names as *stressVi+1.dat* and *thermalVi.dat* and click on the run button.

The format of the *stressVi.dat*, *stressVi.out*, *thermalVi.dat* and *thermalVi.out* files are given in Table 3.1, Table 3.2, Table 3.3 and Table 3.4, respectively. Sample files are also presented in Appendix A1 to A4

Table 3.1 :Format of file StressVi.dat

Title	Line	Column	Explanation
sizing		1	--
		2	Total number of elements
		3	Total number of nodes
		4	--
connectivity	1		--
	others	1	Element number
		2	Element type
		3	1 st elemental node
		4	2 nd elemental node
		5	3 rd elemental node
		6	4 th elemental node
coordinates	1		--
	others	1	Nodes Numbers
		2	The coordinates of the point in the axis X
		3	The coordinates of the point in the axis Y
		4	The coordinates of the point in the axis Z
define node set apply#_nodes		1-N	Nodes defined in the in apply#-nodes set
Define ndsq set Domain_Nodes		1-N	Nodes defined in the Domain nodes set
Define element set Domain_elements		1-N	Elements defined in the Domain elements set
isotropic	1		Material type
	2		--
	3	1	Young's modulus
		2	Poisson's ratio
	7		Nodes numbers
geometry	1		---
	2	1	Thickness
	3		Nodes numbers
fixed temperature	1-6		Data about displacement boundary conditions
fixed disp	1-6		Data about displacement boundary conditions

Table 3.2 :Format of file stressVi.out

Title	Line	Column	Explanation
sizing		1	--
		2	Total number of elements
		3	Total number of nodes
		4	--
elements		1	Element type
tresca	1	2	Element no
mises		4	Integration point
	2	2	Section thickness
	3	3	Values von Mises stress
total displacements	1		--
	2		--
	3	1	Node number
		2	Displacement in x-direction
		3	Displacement in y-direction
		4	Node number
		5	Displacement in x-direction
		6	Displacement in y-direction
		7	Node number
		8	Displacement in x-direction
		9	Displacement in y-direction
total equivalent nodal forces	1		--
	2		--
	3	1	Node number
		2	Result in x-direction
		3	Result in y-direction
		4	Node number
		5	Result in x-direction
		6	Result in y-direction
		7	Node number
		8	Result in x-direction
		9	Result in y-direction
reaction forces at fixed boundary conditions	1		--
	2		--
	3	1	Node number
		2	Result in x-direction
		3	Result in y-direction
		4	Node number
		5	Result in x-direction
		6	Result in y-direction
		7	Node number
		8	Result in x-direction
		9	Result in y-direction

Table 3.3 :Format of file thermalVi.dat

Title	Line	Column	Explanation
Sizing		1	--
		2	Total number of elements
		3	Total number of nodes
		4	--
Connectivity	1		--
	others	1	Element number
		2	Element type
		3	1 st elemental node
		4	2 nd elemental node
		5	3 rd elemental node
coordinates	1		--
	others	1	Nodes numbers
		2	The coordinates of the point in the axis X
		3	The coordinates of the point in the axis Y
	4	The coordinates of the point in the axis Z	
define node set apply#_nodes		1-N	Nodes defined in apply#-nodes set
define node set applyT_nodes		1-N	Nodes defined in applyT#-nodes set for thermal BG
define ndsq set Domain_Nodes		1-N	Nodes defined in the Domain nodes set
define element set Domain_elements		1-N	Elements defined in the Domain elements set
isotropic	1		Material type
	2		--
	3	1	Young's modulus
		2	Poisson's ratio
		3	--
		4	thermal expansion
		7	Nodes numbers
geometry	1		---
	2	1	Thickness
	3		Nodes numbers
fixed temperature	1-6		Data about displacement boundary conditions
fixed disp	1-6		Data about displacement boundary conditions

Table 3.4 :Format of file thermalVi.out

Title	Line	Column	Explanation
sizing		1	--
		2	Total number of elements
		3	Total number of nodes
		4	--
elements		1	Element type
Tresca	1	2	Element no
mises		4	integration point
	2	2	section thickness
	3	3	Values von mises stress
total displacements	1		--
	2		--
	3	1	Node number
		2	Displacement in x-direction
		3	Displacement in y-direction
		4	Node number
		5	Displacement in x-direction
		6	Displacement in y-direction
		7	Node number
		8	Displacement in x-direction
		9	Displacement in y-direction
total equivalent nodal forces	1		--
	2		--
	3	1	Node number
		2	Result in x-direction
		3	Result in y-direction
		4	Node number
		5	Result in x-direction
		6	Result in y-direction
		7	Node number
		8	Result in x-direction
		9	Result in y-direction
reaction forces at fixed boundary conditions			(Same as total equivalent nodal forces)
total nodal temperatures	1		--
	2	1	Node number
		2	Temperature of node
		3	Node number
		4	Temperature of node
		5	Node number
		6	Temperature of node
		7	Node number
		8	Temperature of node
		9	Node number
		10	Temperature of node

CHAPTER 4

RESULTS AND DISCUSSIONS

4.1 Verification of Biological Growth Method

Verification of the method was done by using the plane with a hole problem under bi-axial loading as shown in Figure 4.1 and described by Tekkaya (1996). The thickness of the plane was taken as 5 mm. Due to symmetry one-fourth of the plane was modeled and symmetry boundary conditions were applied as shown in Figure 4.2.

Optimization parameters are given in Table 4.1. Domain thickness of 10 mm is used for the verification of the model. The analyses with domain thicknesses from 20 to 40 mm were further examined and will be discussed after the verification section.

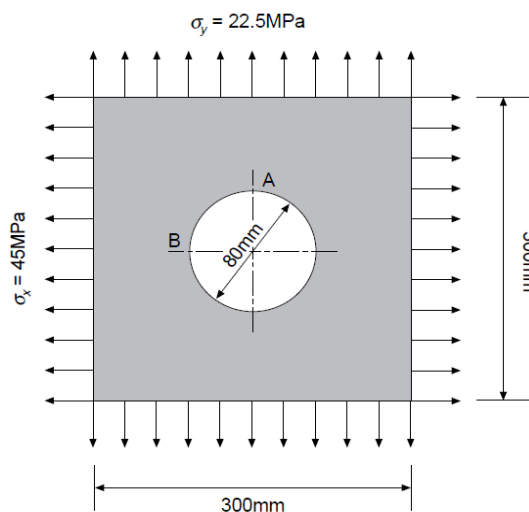


Figure 4.1: Description of the problem

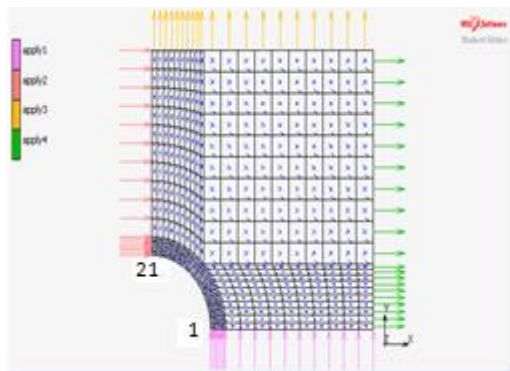


Figure 4.2: Finite element discretization of one-quarter of the plate

Table 4.1: Optimization parameters

Optimization boundary, Γ	Hole boundary
Stress-temperature factor, ζ	1°C/MPa
Reduced Young's modulus, E_{red}	525 MPa (1/400 of original E)
Thermal expansion coefficient, α	0.0000108 m/m/°C
Reference stress, σ_{ref}	10, 40, 60 MPa
Magnification factor, \mathbf{K}	250, 275, 500, 750, 1000
Domain thickness, \mathbf{D}	10, 20, 30, 40 mm

The finite element models and the boundary conditions for stress and thermal analysis are shown in Figure 4.3 for domain thickness 10 mm. The von Mises stresses of stress analysis and total deflections of the thermal expansion analysis of the original shape can be seen in Figure 4.4. The stress far away from the concentration zones is about 40 MPa. This value of stress would exist in the plate without the hole. The maximum and minimum von Mises stresses were around 130 MPa and 10 MPa respectively.

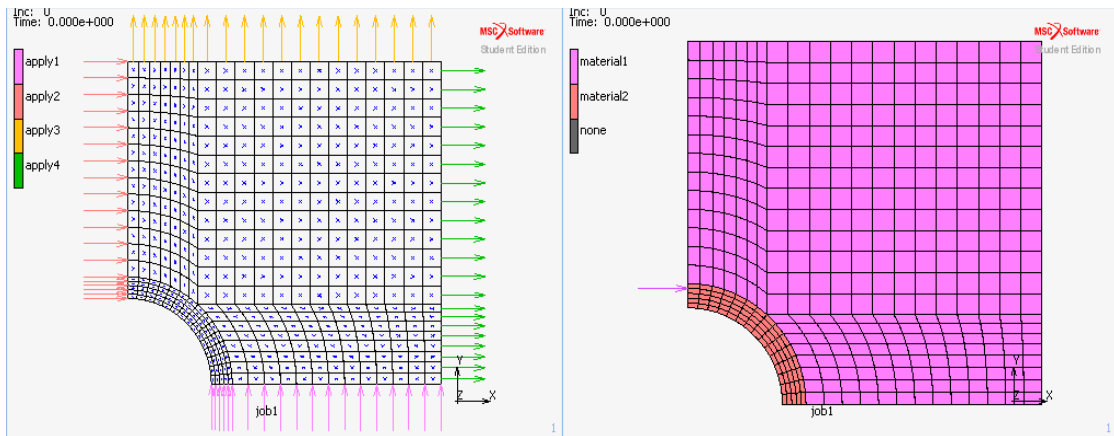


Figure 4.3: Finite element model for stress (left) and thermal (right) analysis (D=10mm)

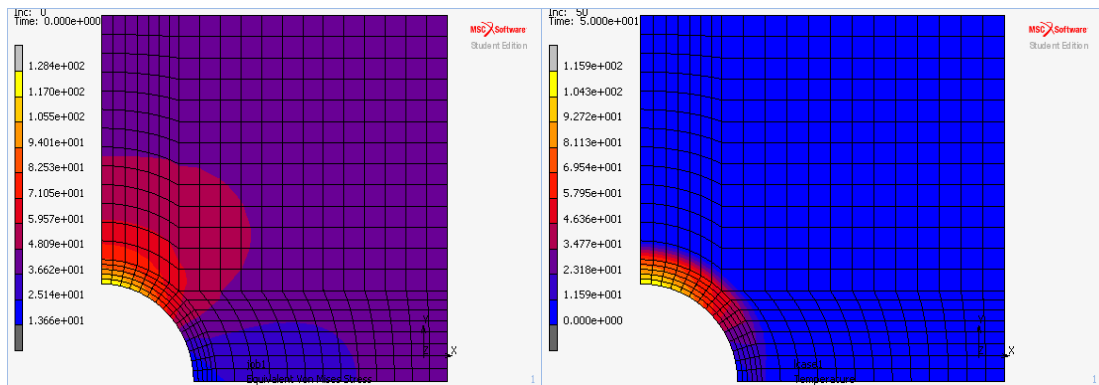


Figure 4.4: von Mises stresses (left) and thermal deformations (right) of the original shape

For domain thickness $D = 10$ mm, fifteen optimization analyses were conducted including the combinations of reference stresses $\sigma_{\text{ref}} = 10, 40$ and 60 MPa and magnification factor $k = 250, 275, 500, 750$ and 1000 . The results obtained including (a) von Mises stress distributions of the plate after first and last iterations, (b) the change of von Mises stresses by iterations along the hole boundary, (c) the change of ellipse axes ratio by iterations are presented in Figures 4.5 to 4.19.

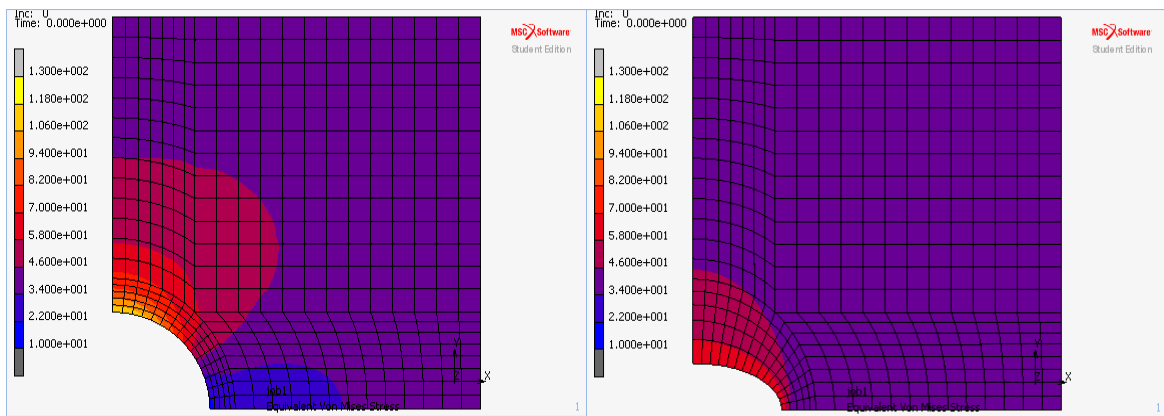
Generally, it was observed that the maximum von Mises stress of about 130 MPa at the beginning of the optimization analysis close to the hole boundary dropped down to the values around 70 MPa as the hole changed its shape to an ellipse with an ellipse axes ratio of around 2 .

The results obtained were summarized in Table 4.3 together with results obtained by Tekkaya (1996) for comparison. It should be noted at this point that the main difference between the present study and Tekkaya (1996) was in the first the coordinated of the nodes in the domain set were only modified after every iteration according to the thermal deflections. However, in the second the coordinates of the nodes on the boundary of the hole were modified. A new mesh was regenerated after each iteration keeping the thickness of the domain as constant. In the present study, the thickness of the domain does not remain constant but changes during the optimization process, as it can also be seen in the figures. Even with this remarkable difference between the two studies, the results are still in good agreement with each other, verifying the methodology used.

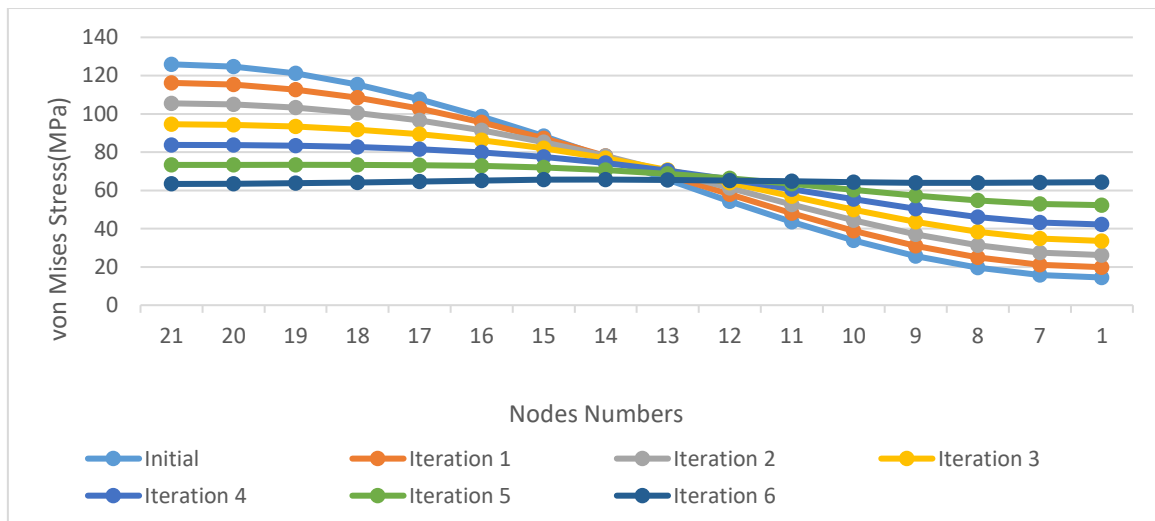
Number of iterations required for convergence decreased with increasing value of magnification factor. Very high magnification values caused iteration numbers as low as 2 for convergence. These values were considered as not trustable since the method does not have enough number of steps to regulate the optimum shape. This might be the reason why the analyses were not conducted by Tekkaya (1996) for $\sigma_{\text{ref}} = 10$ MPa and $k = 750$ and 1000 . The results of these combinations showed that the convergence occurs in 2 iterations. Even the results for $k = 750$ were reasonable, the result for $k = 1000$ could not be accepted.

As the reference stress value was increased towards the expected final stress value, the number of iterations were increased. The final maximum von Mises stress values were obtained around 70 MPa for $\sigma_{\text{ref}} = 40$ MPa and $\sigma_{\text{ref}} = 60$ MPa. For $\sigma_{\text{ref}} = 10$ MPa these values are lower and vary between 65 and 70 MPa. It may be concluded that even though a σ_{ref} equal to the expected final maximum stress will give the best result, a value around the stress level some distance away from the stress concentration will be satisfactory.

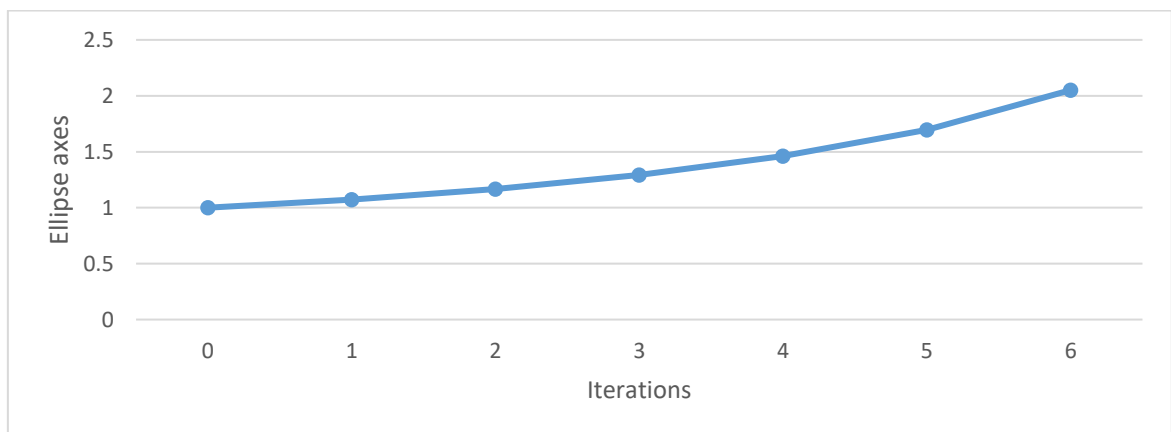
Having determined the effect of reference stress and magnification factor on the performance of the optimization procedure, it was challenging to examine the effect of domain thickness which was not investigated by Tekkaya (1996). In the following sections domain thicknesses $20, 30$ and 40 mm were examined. The aim was to determine if it was possible to develop a way to simplify the modelling procedure.



(a) von Mises stresses for first and last iterations: Iteration 1 (left), Iteration 6 (right)

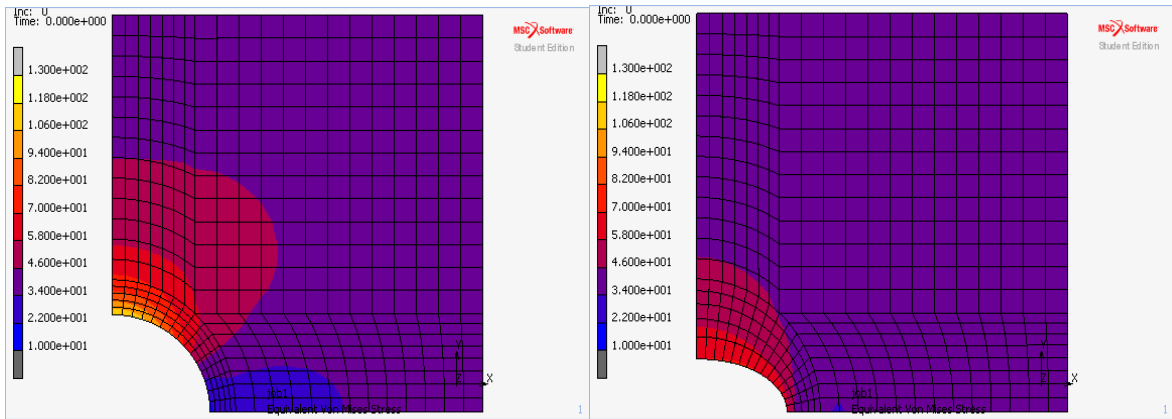


(b) Variation of von Mises stress distribution along the hole boundary

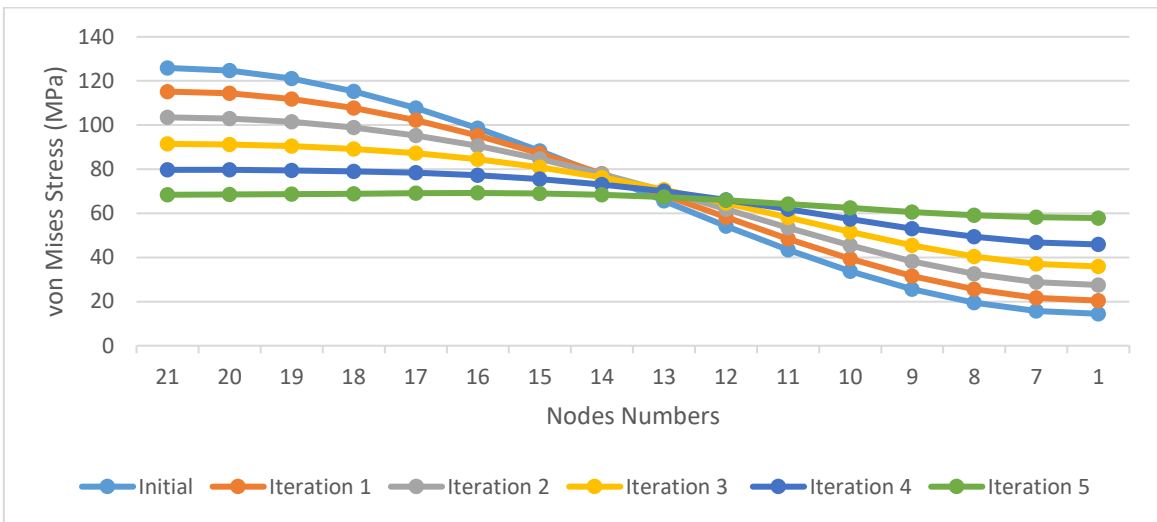


(c) Variation of ellipse axes ratio

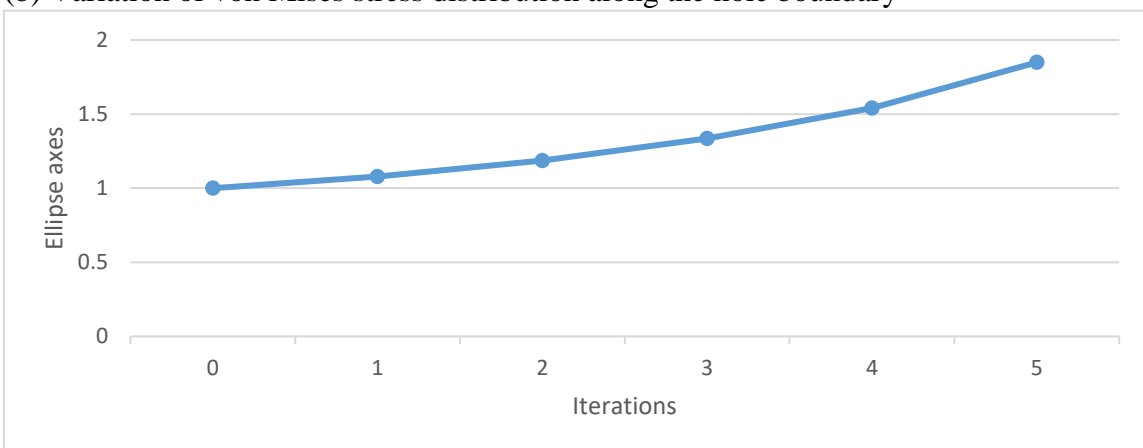
Figure 4.5: Optimization results of a plate with a hole ($D=10$ mm, $K = 250$, $\sigma_{ref} = 10$ MPa)



(a) von Mises stresses for first and last iterations: Iteration 1 (left), Iteration 5 (right)

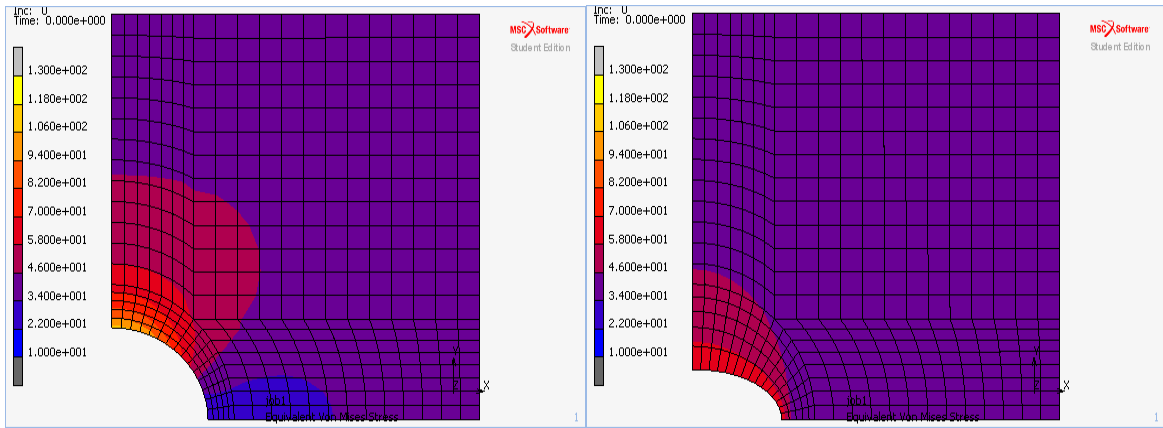


(b) Variation of von Mises stress distribution along the hole boundary

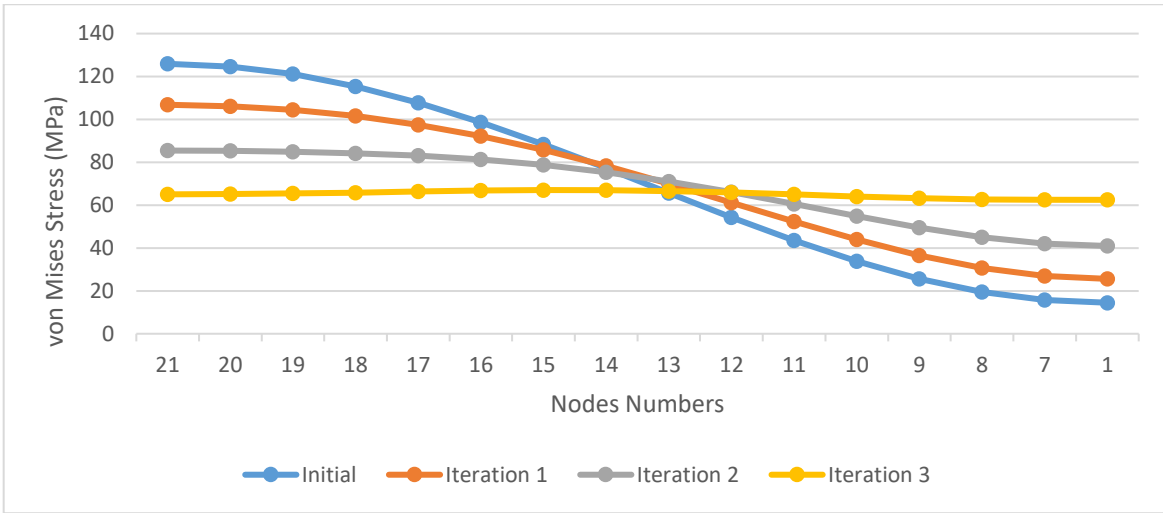


(c) Variation of ellipse axes ratio

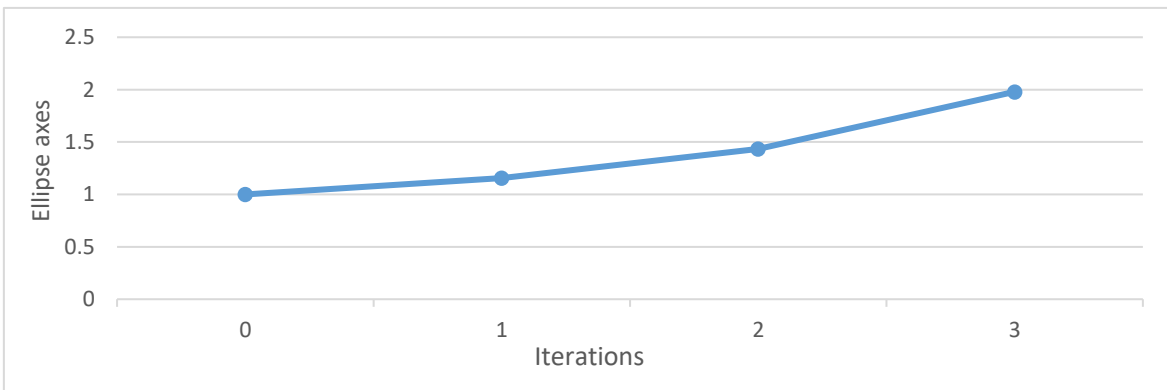
Figure 4.6: Optimization results of a plate with a hole ($D=10$ mm, $K = 275$, $\sigma_{ref} = 10$ MPa)



(a) von Mises stresses for first and last iterations: Iteration 1 (left), Iteration 3 (right)

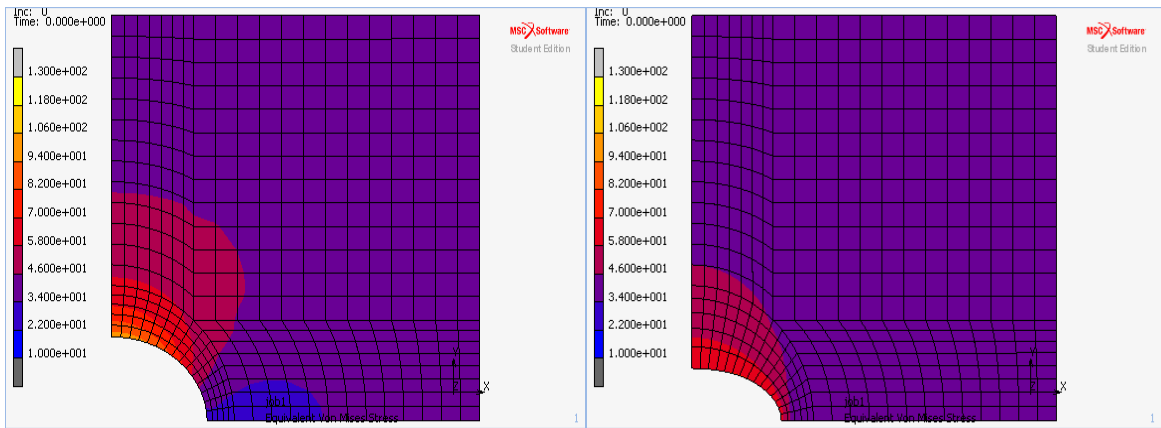


(b) Variation of von Mises stress distribution along the hole boundary

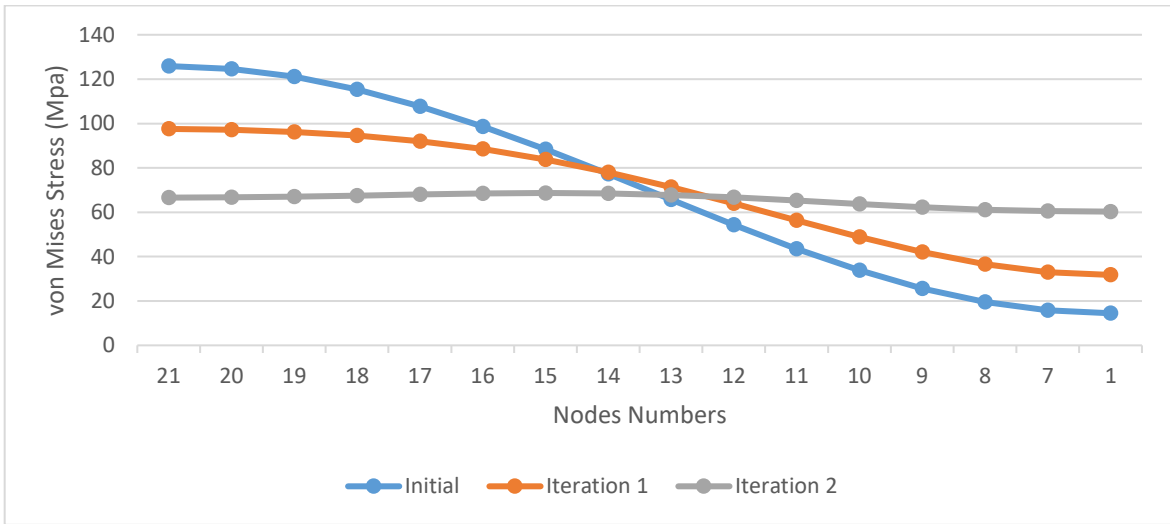


(c) Variation of ellipse axes ratio

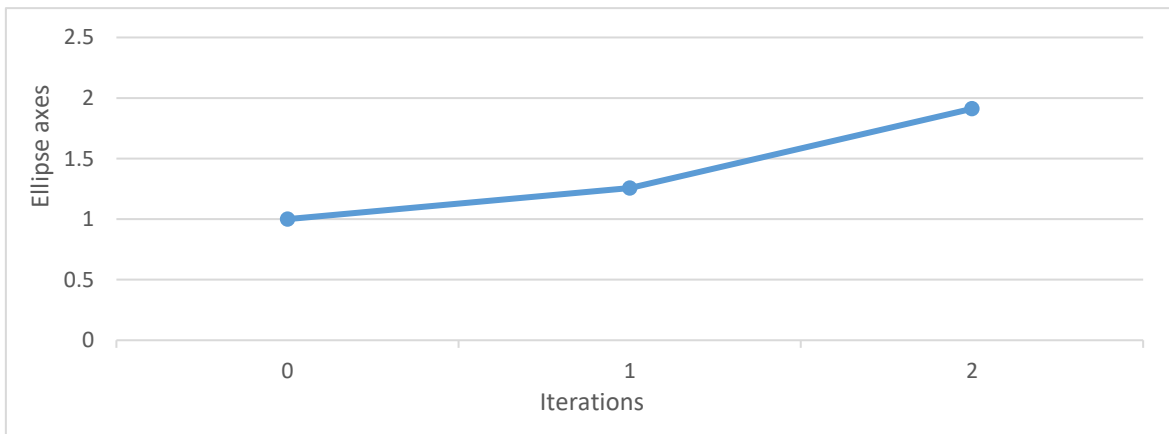
Figure 4.7: Optimization results of a plate with a hole ($D=10$ mm, $K = 500$, $\sigma_{ref} = 10$ MPa)



(a) von Mises stresses for first and last iterations: Iteration 1 (left), Iteration 3 (right)

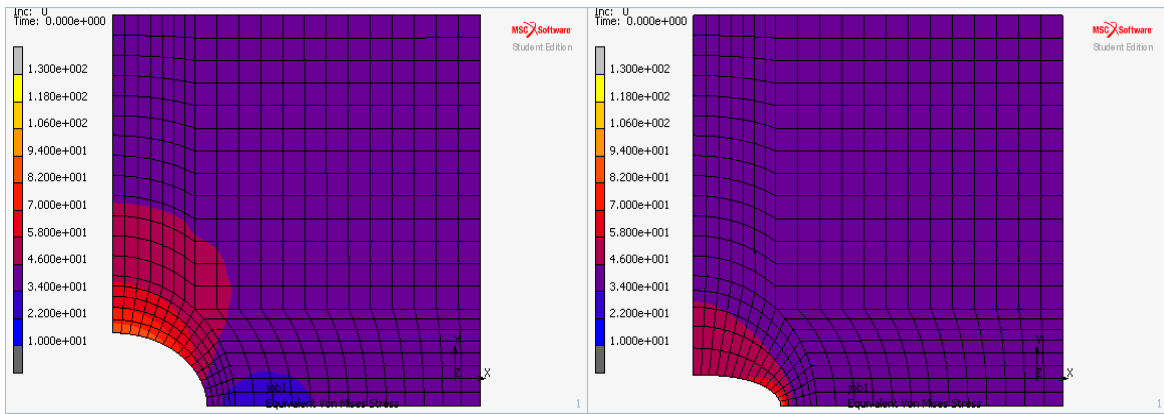


(b) Variation of von Mises stress distribution along the hole boundary

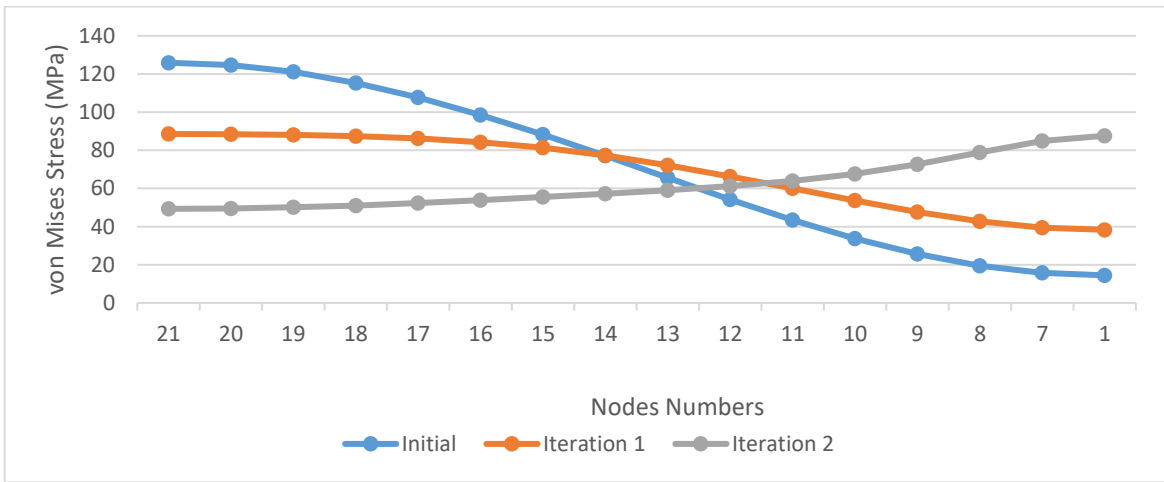


(c) Variation of ellipse axes ratio

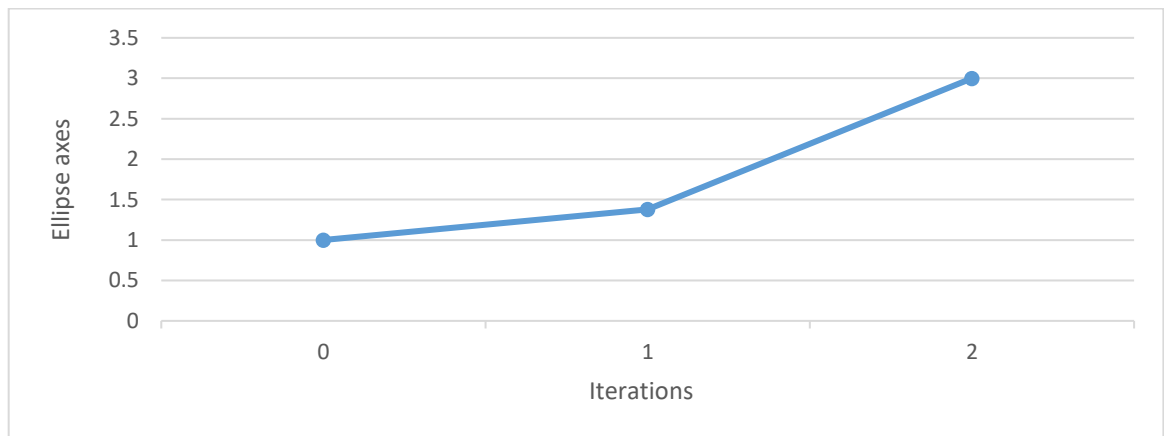
Figure 4.8: Optimization results of a plate with a hole ($D=10$ mm, $K = 750$, $\sigma_{ref} = 10$ MPa)



(a) von Mises stresses for first and last iterations: Iteration 1 (left), Iteration 2 (right)

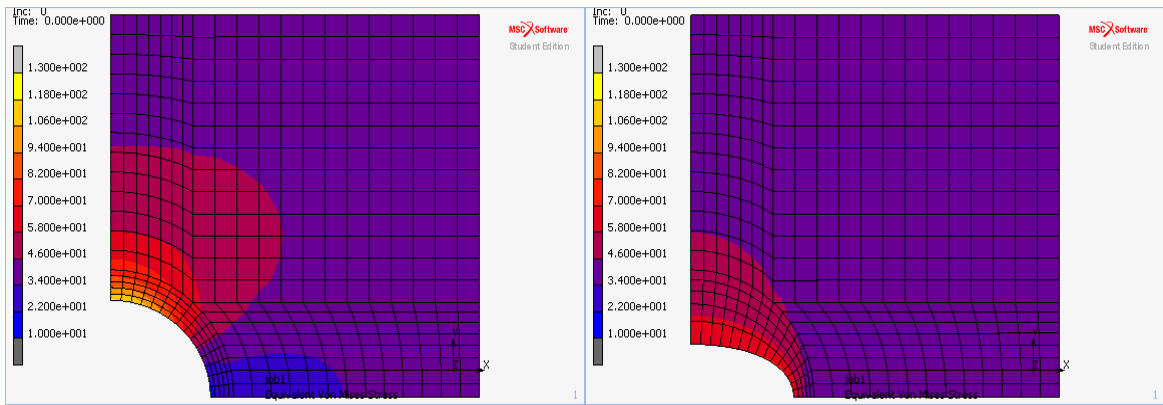


(b) Variation of von Mises stress distribution along the hole boundary

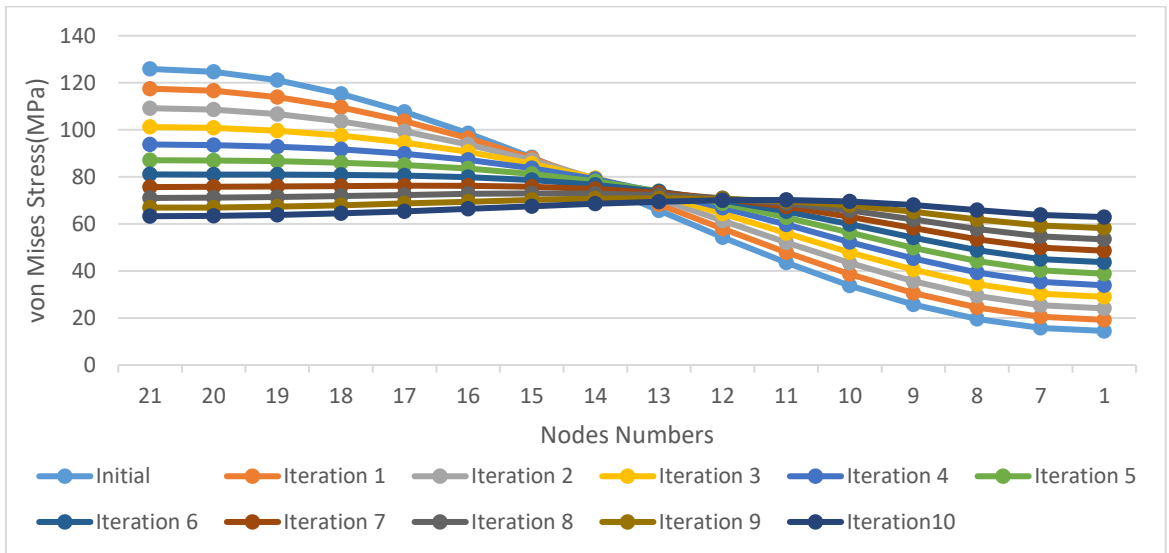


(c) Variation of ellipse axes ratio

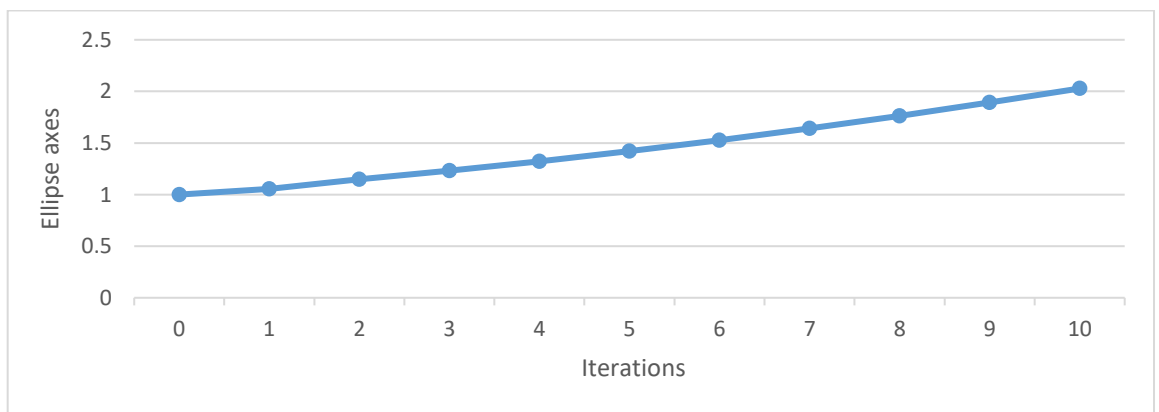
Figure 4.9: Optimization results of a plate with a hole ($D=10$ mm, $K=1000$, $\sigma_{ref} = 10$ MPa)



(a) von Mises stresses for first and last iterations: Iteration 1 (left), Iteration 10 (right)

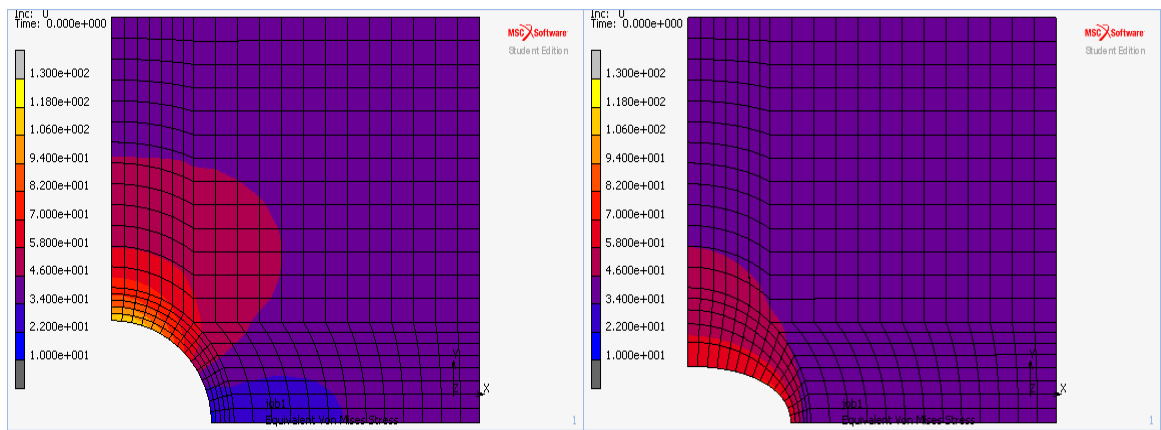


(b) Variation of von Mises stress distribution along the hole boundary

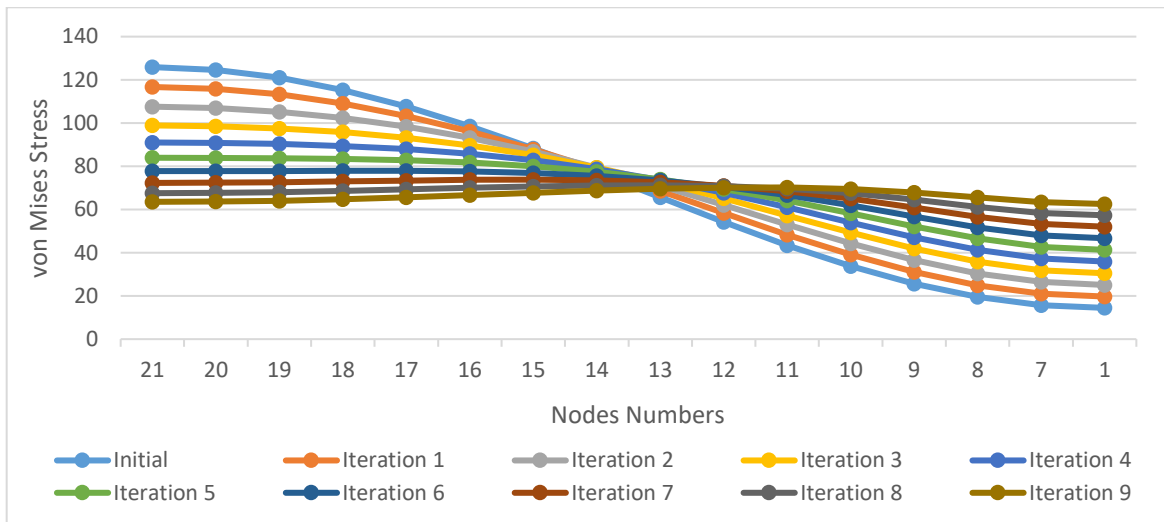


(c) Variation of ellipse axes ratio

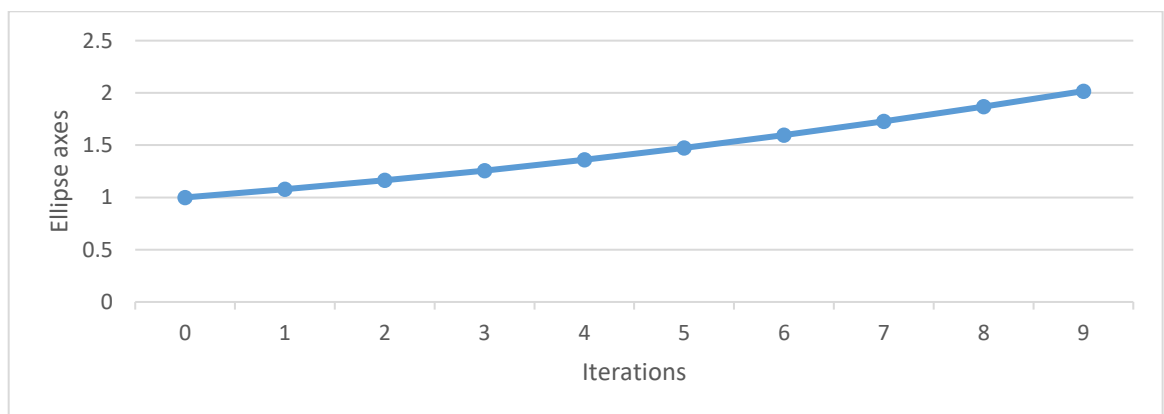
Figure 4.10: Optimization results of a plate with a hole ($D=10$ mm, $K=250$, $\sigma_{ref} = 40$ MPa)



(a) von Mises stresses for first and last iterations: Iteration 1 (left), Iteration 9 (right)

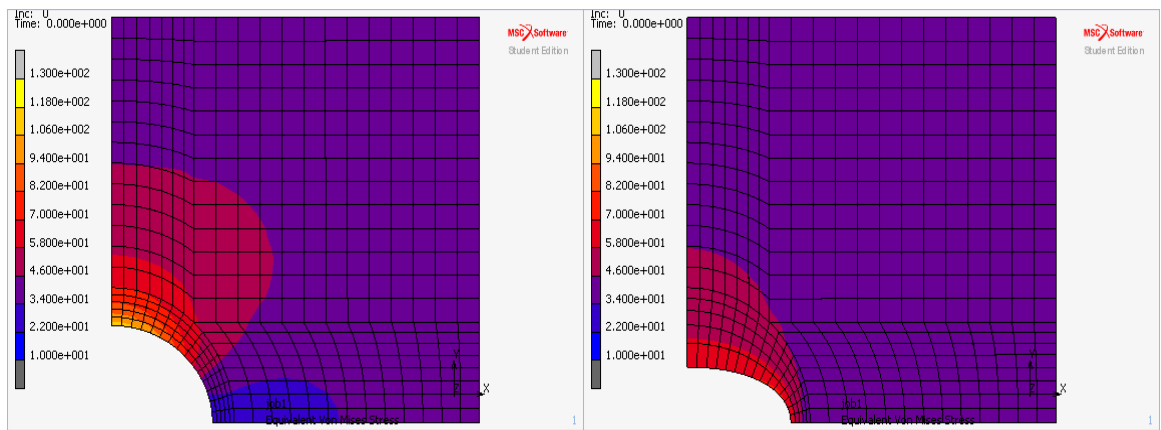


(b) Variation of von Mises stress distribution along the hole boundary

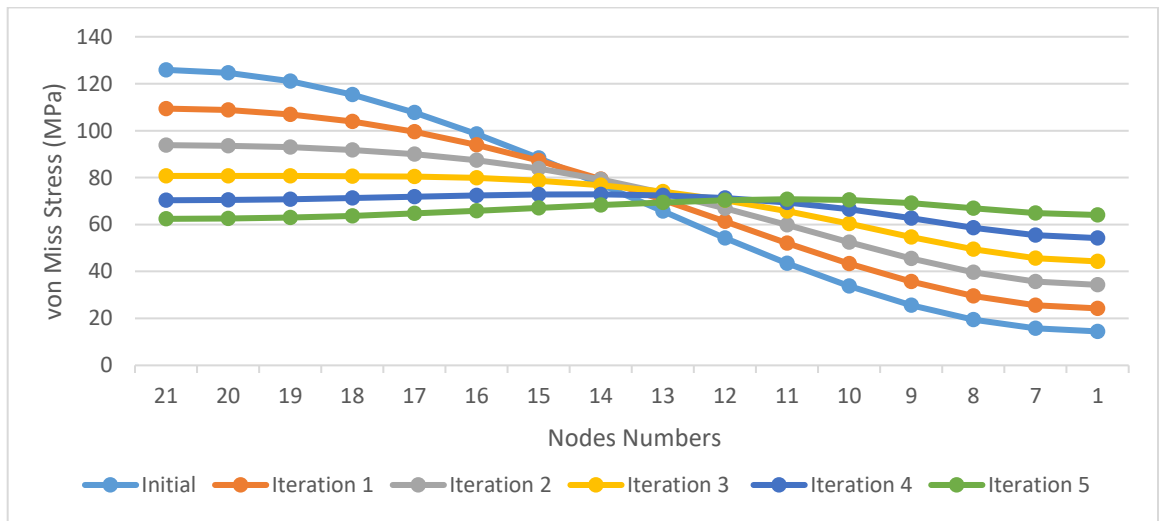


(c) Variation of ellipse axes ratio

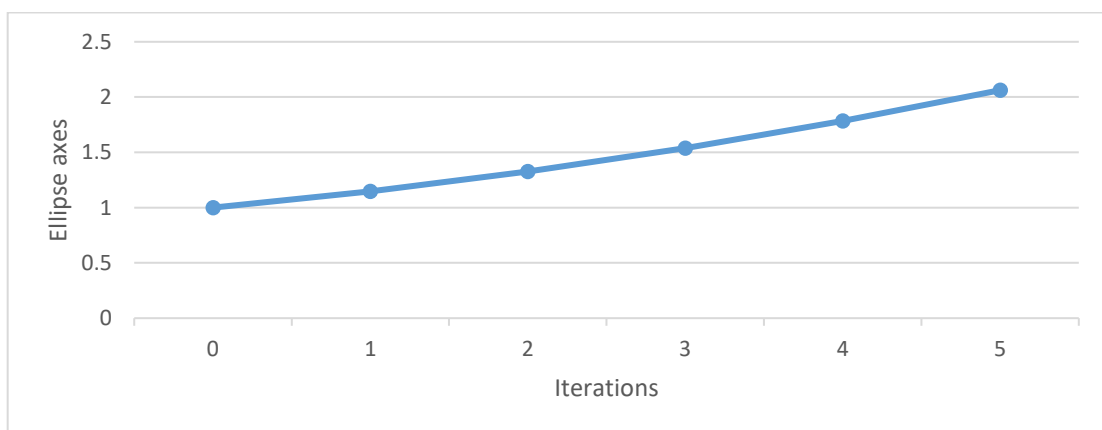
Figure 4.11: Optimization results of a plate with a hole ($D=10$ mm, $K=275$, $\sigma_{ref} = 40$ MPa)



(a) von Mises stresses for first and last iterations: Iteration 1 (left), Iteration 5 (right)

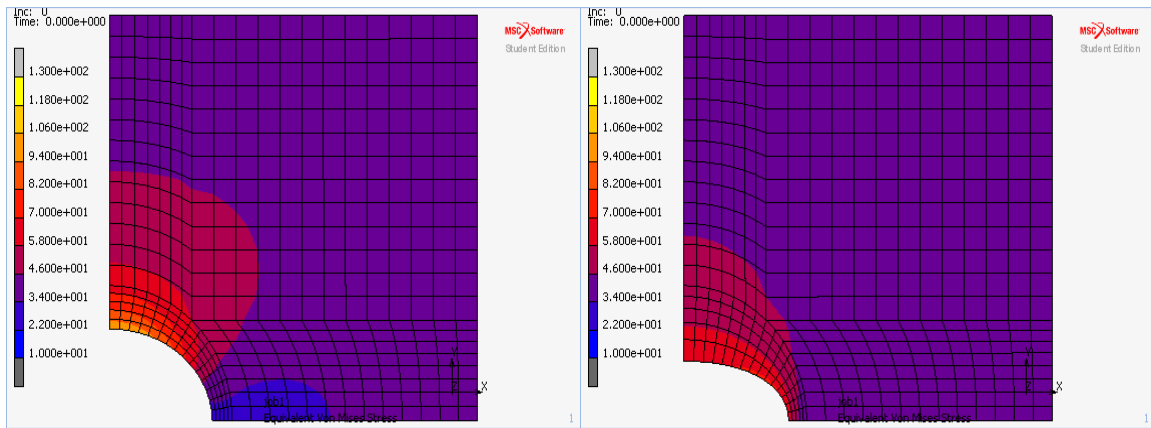


(b) Variation of von Mises stress distribution along the hole boundary

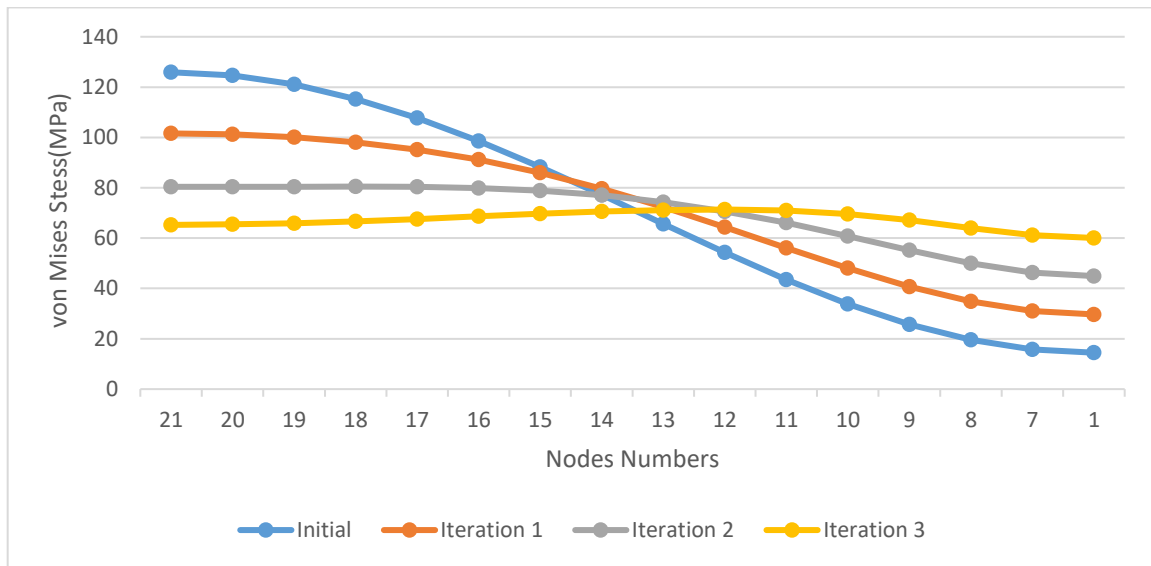


(c) Variation of ellipse axes ratio

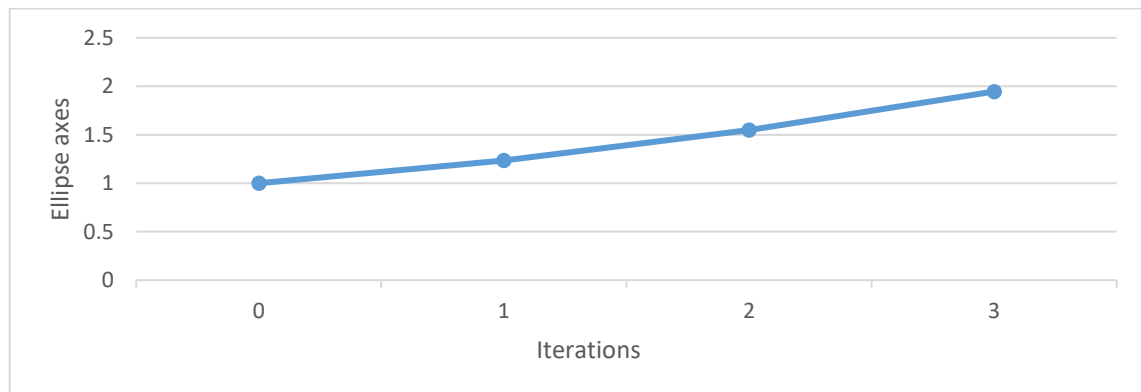
Figure 4.12: Optimization results of a plate with a hole ($D=10$ mm, $K=500$, $\sigma_{ref} = 40$ MPa)



(a) von Mises stresses for first and last iterations: Iteration 1 (left), Iteration 3 (right)

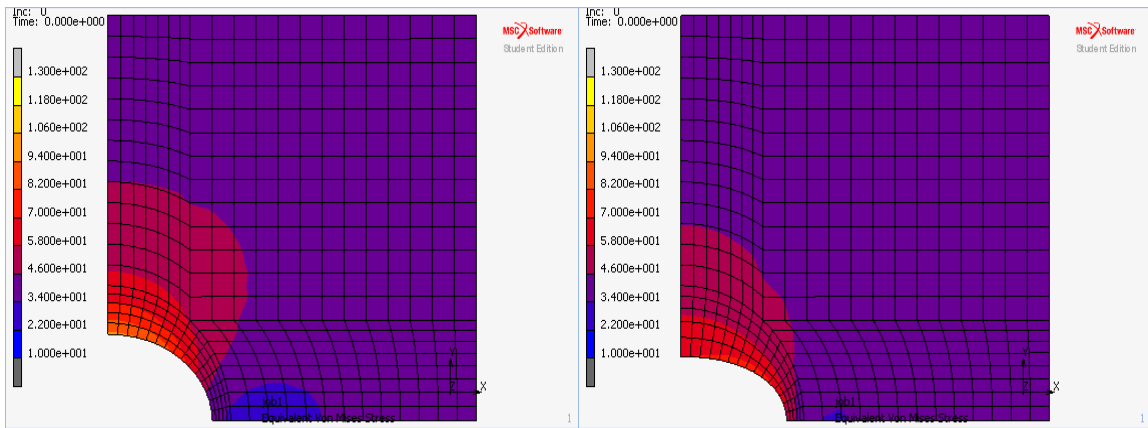


(b) Variation of von Mises stress distribution along the hole boundary

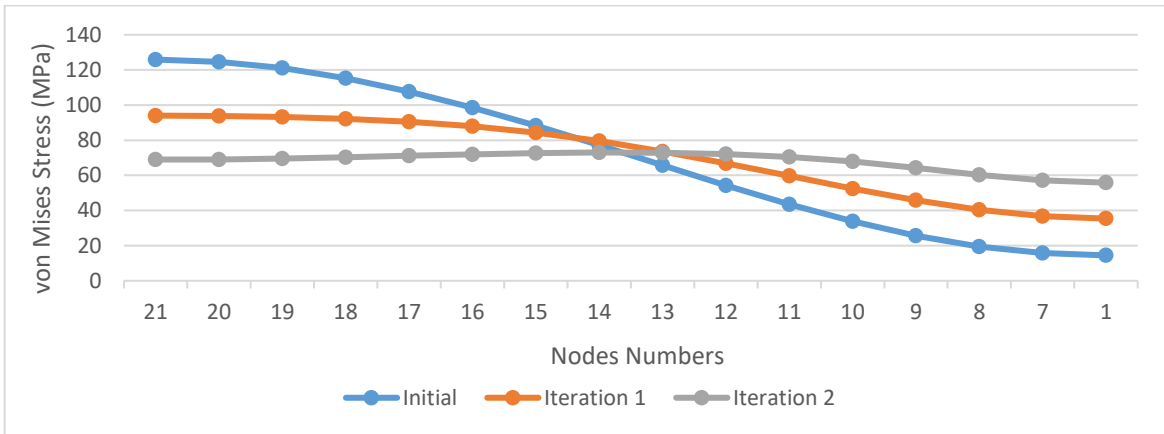


(c) Variation of ellipse axes ratio

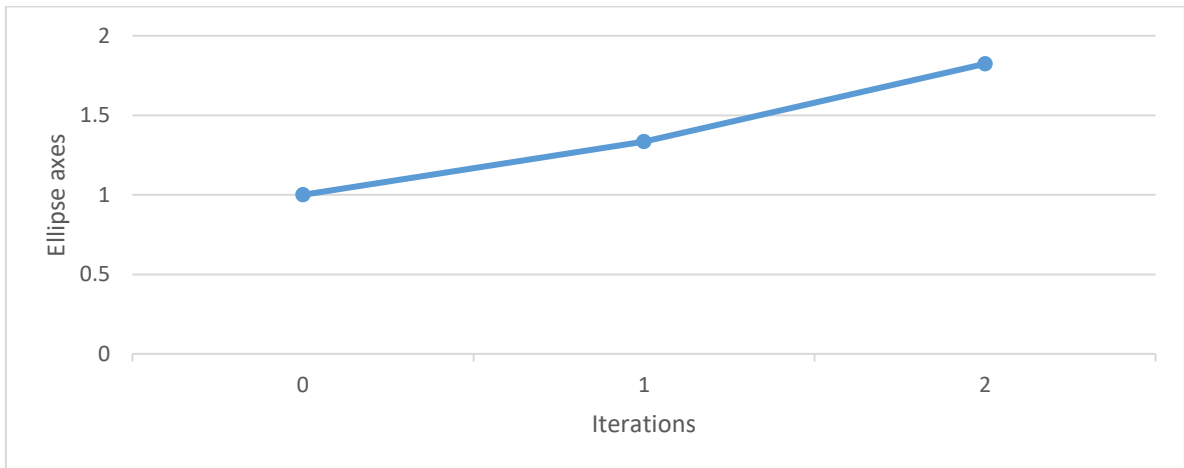
Figure 4.13: Optimization results of a plate with a hole ($D=10$ mm, $K=750$, $\sigma_{ref} = 40$ MPa)



(a) von Mises stresses for first and last iterations: Iteration 1 (left), Iteration 2 (right)

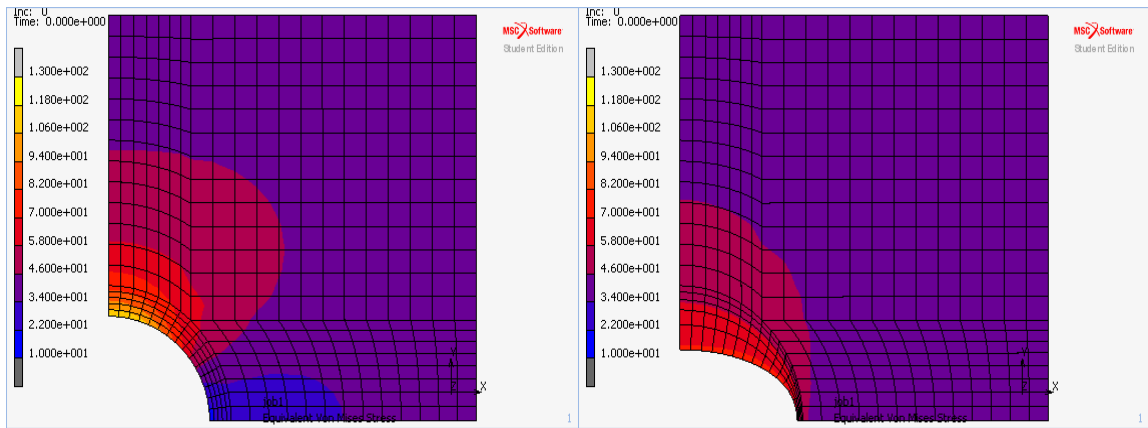


(b) Variation of von Mises stress distribution along the hole boundary

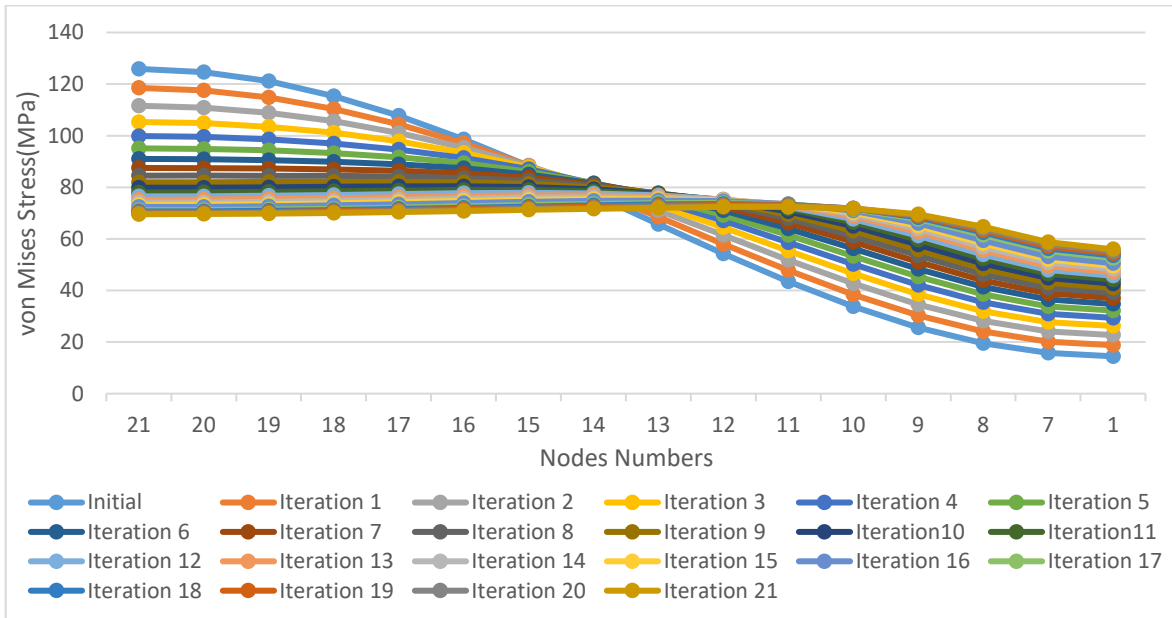


(c) Variation of ellipse axes ratio

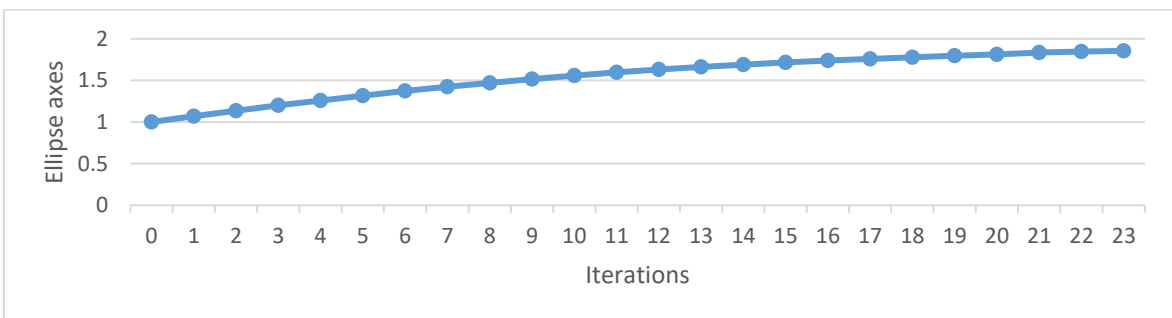
Figure 4.14: Optimization results of a plate with a hole ($D=10$ mm, $K=1000$, $\sigma_{ref}=40$ MPa)



(a) von Mises stresses for first and last iterations: Iteration 1 (left), Iteration 21 (right)

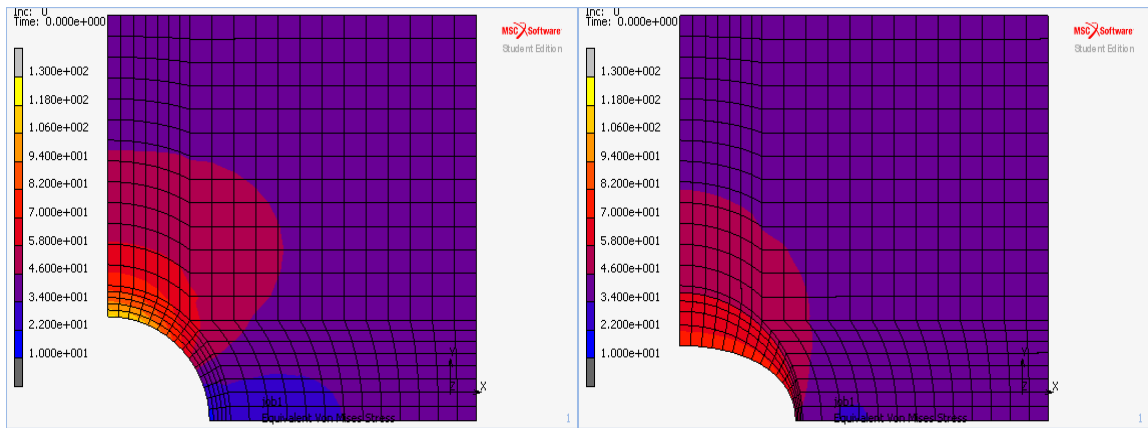


(b) Variation of von Mises stress distribution along the hole boundary

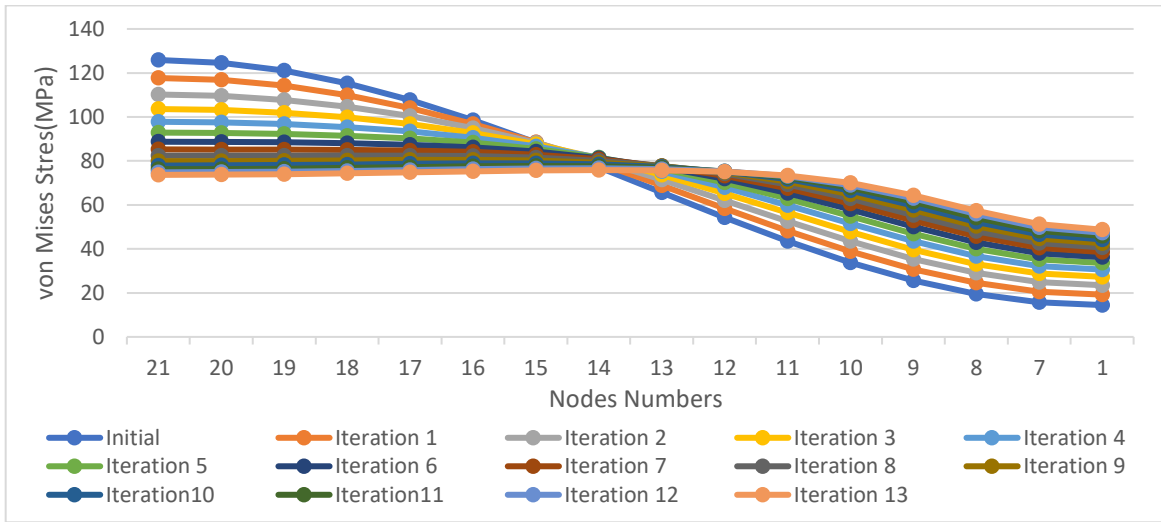


(c) Variation of ellipse axes ratio

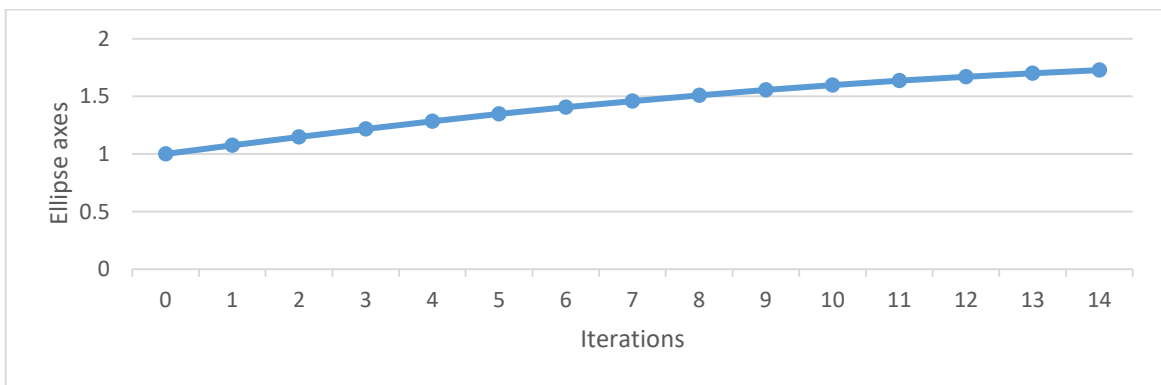
Figure 4.15: Optimization results of a plate with a hole ($D=10$ mm, $K=250$, $\sigma_{ref} = 60$ MPa)



(a) von Mises stresses for first and last iterations: Iteration 1 (left), Iteration 13 (right)

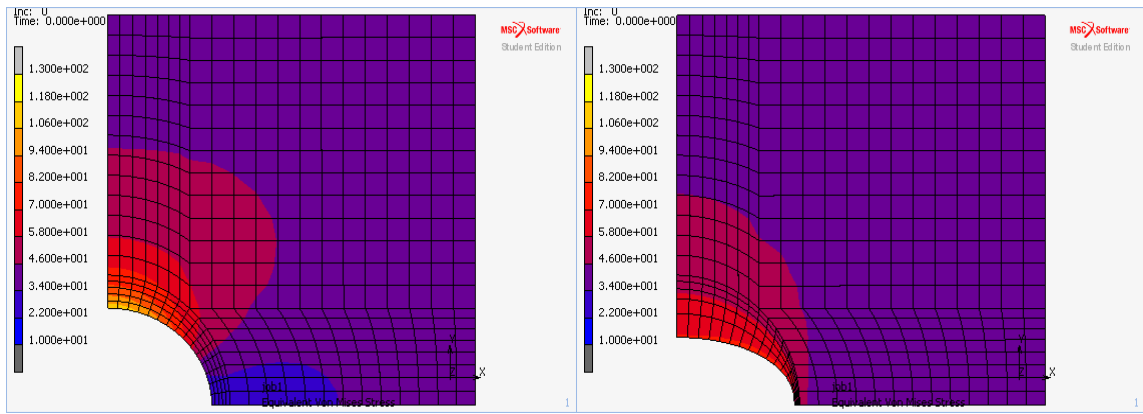


(b) Variation of von Mises stress distribution along the hole boundary

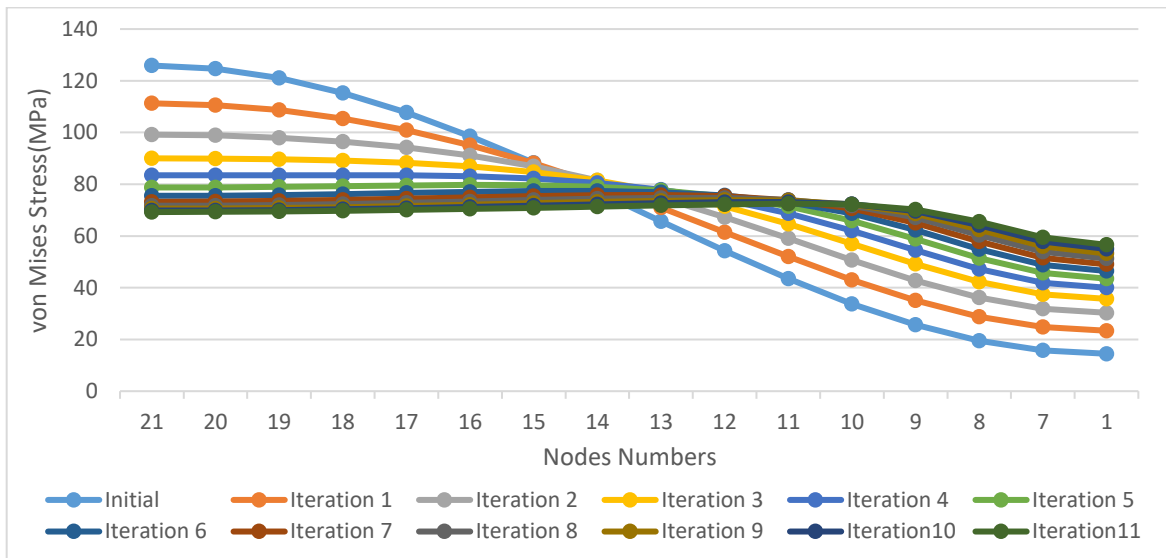


Variation of ellipse axes ratio

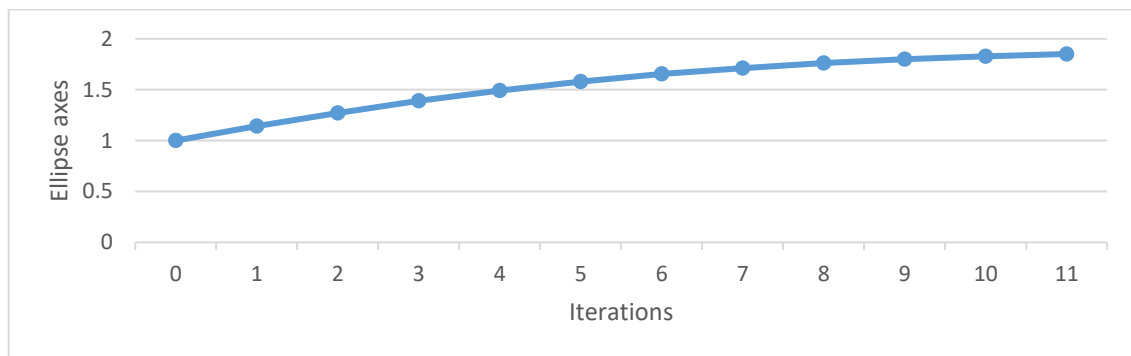
Figure 4.16: Optimization results of a plate with a hole ($D=10$ mm, $K=275$, $\sigma_{ref} = 60$ MPa)



(a) von Mises stresses for first and last iterations: Iteration 1 (left), Iteration 11 (right)

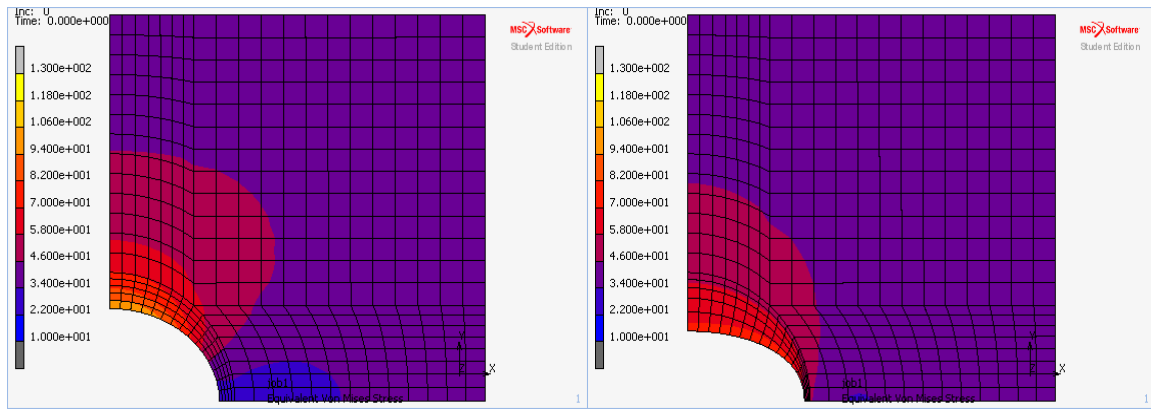


(b) Variation of von Mises stress distribution along the hole boundary

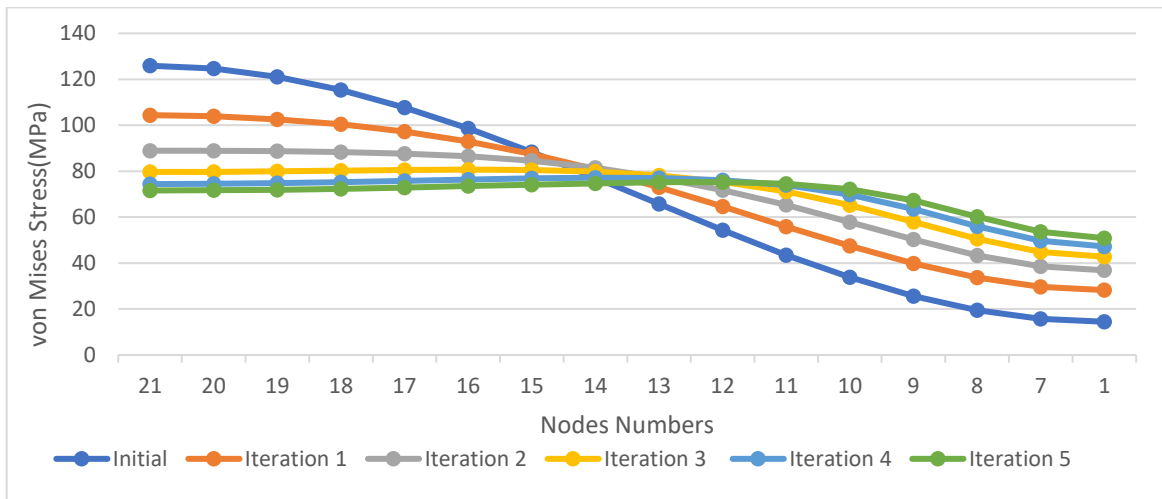


(c) Variation of ellipse axes ratio

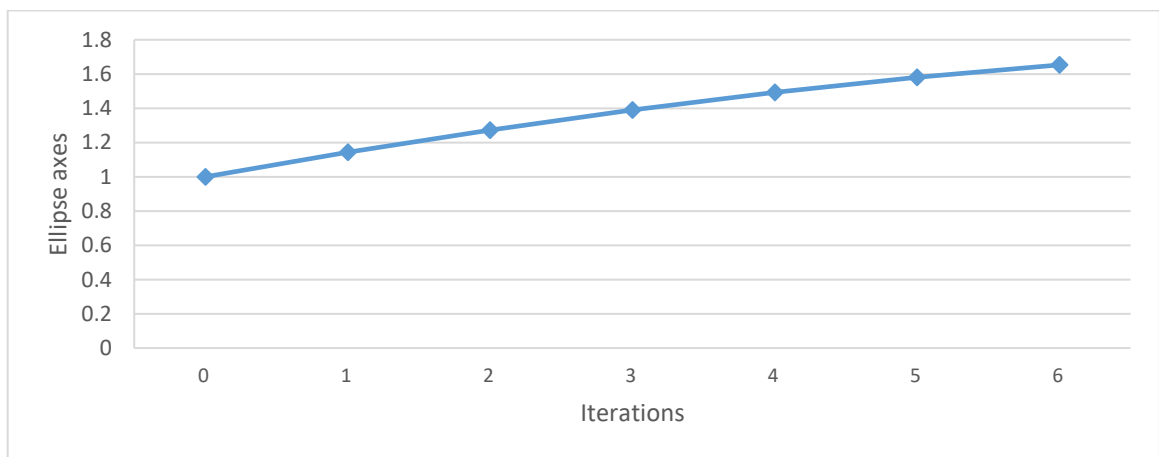
Figure 4.17: Optimization results of a plate with a hole ($D=10$ mm, $K=500$, $\sigma_{ref} = 60$ MPa)



(a) von Mises stresses for first and last iterations: Iteration 1 (left), Iteration 5 (right)

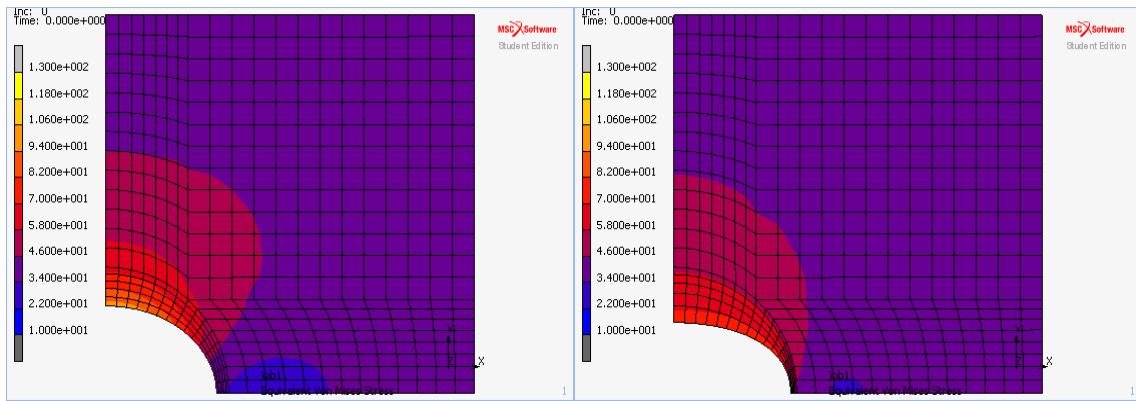


(b) Variation of von Mises stress distribution along the hole boundary

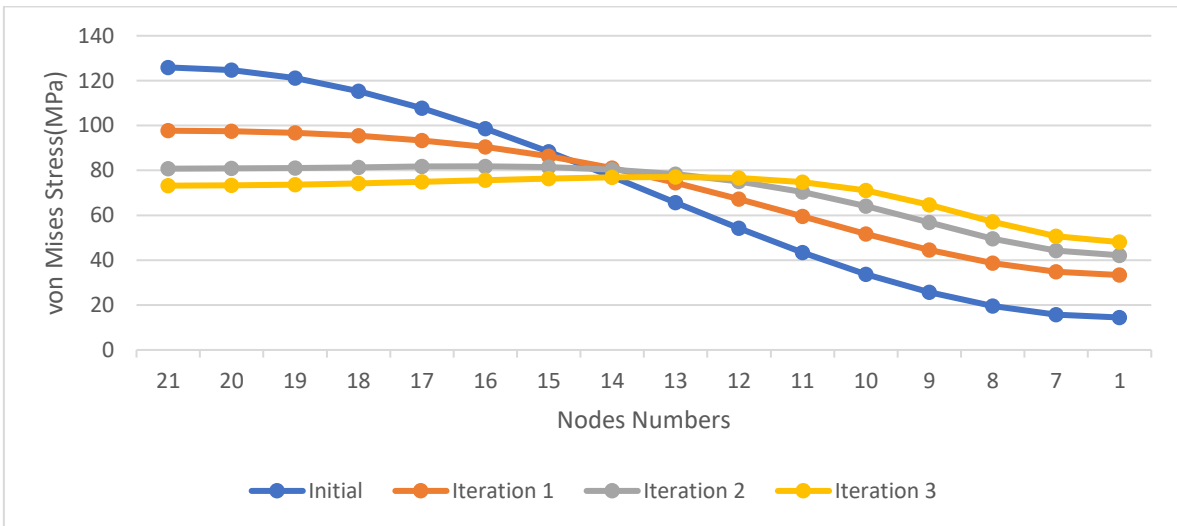


(c) Variation of ellipse axes ratio

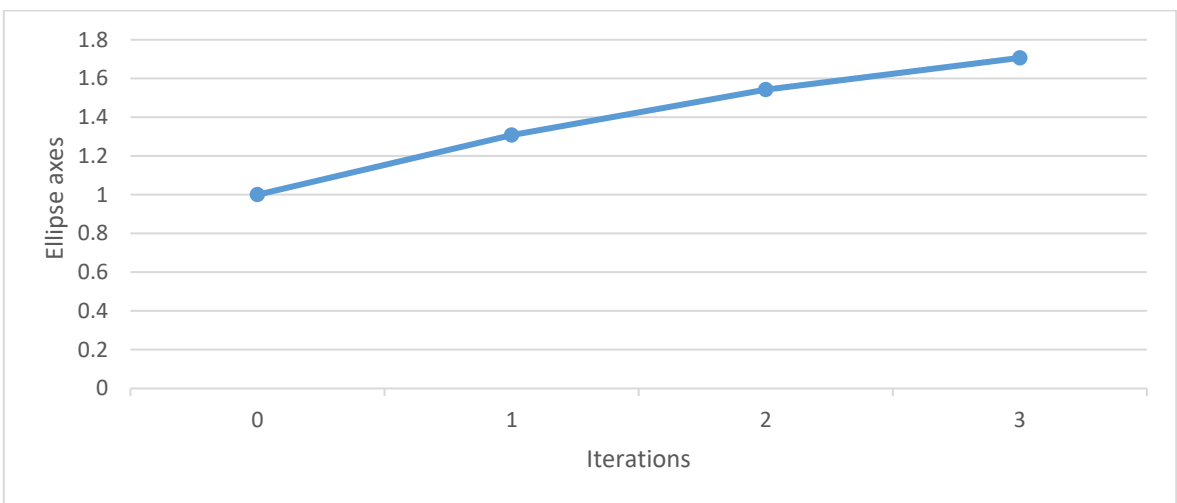
Figure 4.18: Optimization results of a plate with a hole ($D=10$ mm, $K=750$, $\sigma_{ref} = 60$ MPa)



(a) von Mises stresses for first and last iterations: Iteration 1 (left), Iteration 3 (right)



(b) Variation of von Mises stress distribution along the hole boundary



(c) Variation of ellipse axes ratio

Figure 4.19: Optimization results of a plate with a hole ($D=10$ mm, $K=1000$, $\sigma_{ref}=60$ MPa)

Table 4.2: Summary and comparison of results with domain thickness 10mm

σ_{ref}		Magnification factor k									
		250		275		500		750		1000	
		AY	ET	AY	ET	AY	ET	AY	ET	AY	ET
10	Iterations	6	7	6	4	3	4	2	--	2	--
	Max stress	65	67.2	69.22	67.2	67.02	69.2	68.69	--	87.62	--
	Ellipse axes ratio	2.05	2.03	1.99	2.1	1.97	1.91	1.91	--	2.9	--
40	Iterations	10	12	9	9	5	6	3	3	2	2
	Max stress	70.18	69.2	70.22	70	70.78	69.2	71.37	70	71.04	70.4
	Ellipse axes ratio	2.02	1.94	2.01	1.96	2.06	1.99	1.94	1.77	1.84	1.73
60	Iterations	21	19	13	13	11	8	5	5	3	4
	Max stress	71.14	71.6	72.15	71.2	71.31	70.8	71.98	70.8	70.27	71.6
	Ellipse axes ratio	1.85	1.97	1.82	1.94	1.85	1.94	1.90	2.00	1.80	1.99

AY: Ayoub Yahya, ET: Erman Tekkaya

4.2 Optimization of a Plate with a Hole with Domain Thickness 20 mm

The finite element models and the boundary conditions for stress and thermal analysis are shown in Figure 4.20 for domain thickness 20 mm. The von Mises stresses of stress analysis and total deflections of the thermal expansion analysis of the original shape can be seen in Figure 4.21. Similar to the analysis conducted for domain thickness 10 mm, the stress far away from the concentration zones is about 40 MPa. The maximum and minimum von Mises stresses were also around 130 MPa and 10 MPa respectively.

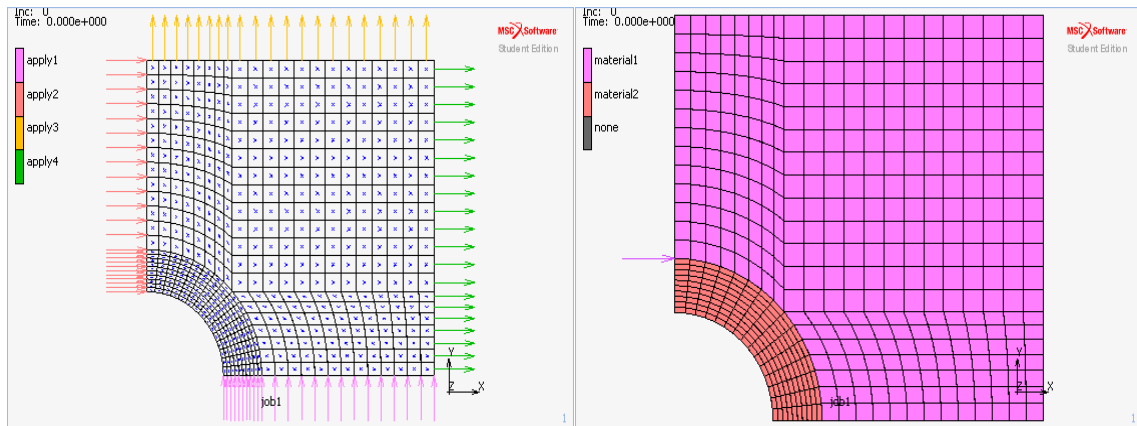


Figure 4.20: Finite element model for stress (left) and thermal (right) analysis (D=20mm)

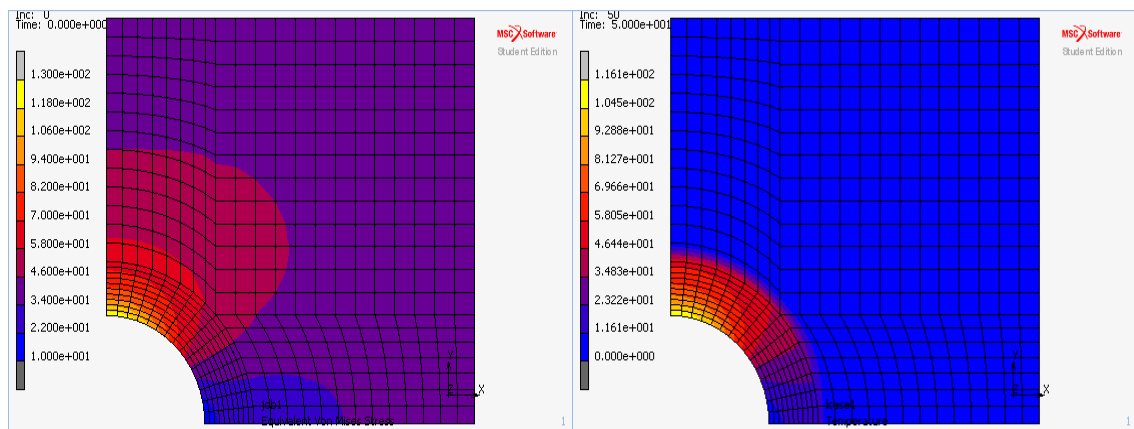
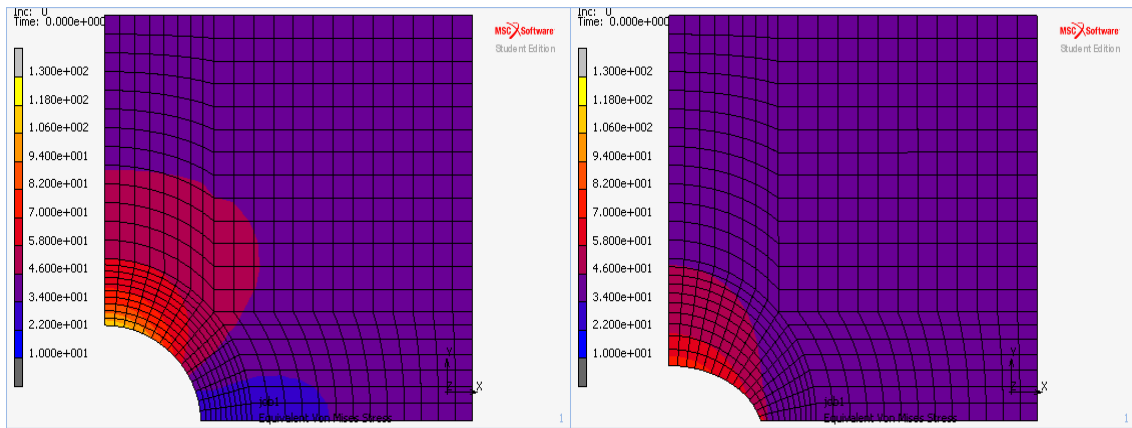
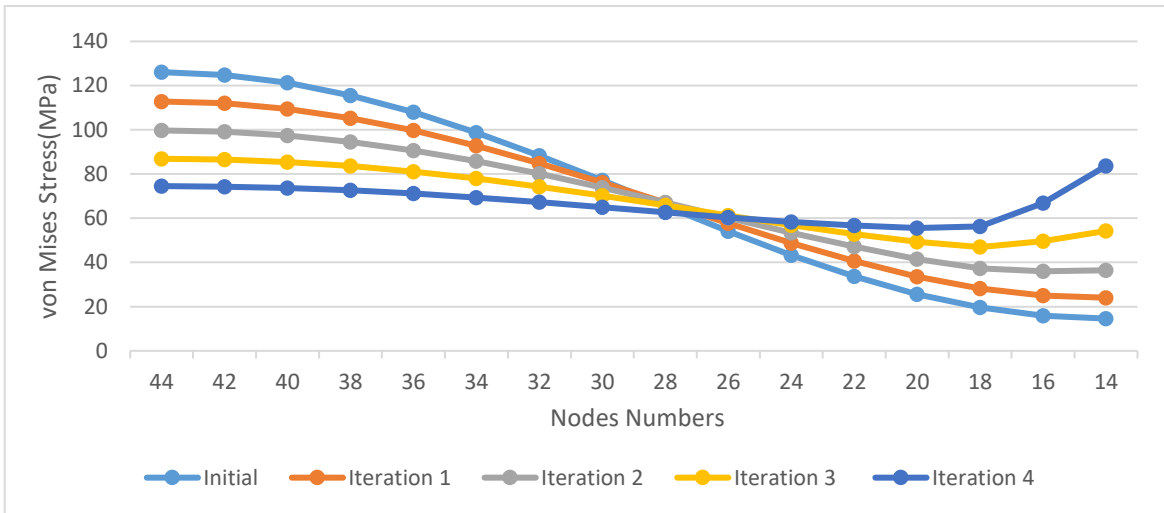


Figure 4.21: von Mises stress (left) and thermal deformations (right) of the original shape (D=20mm)

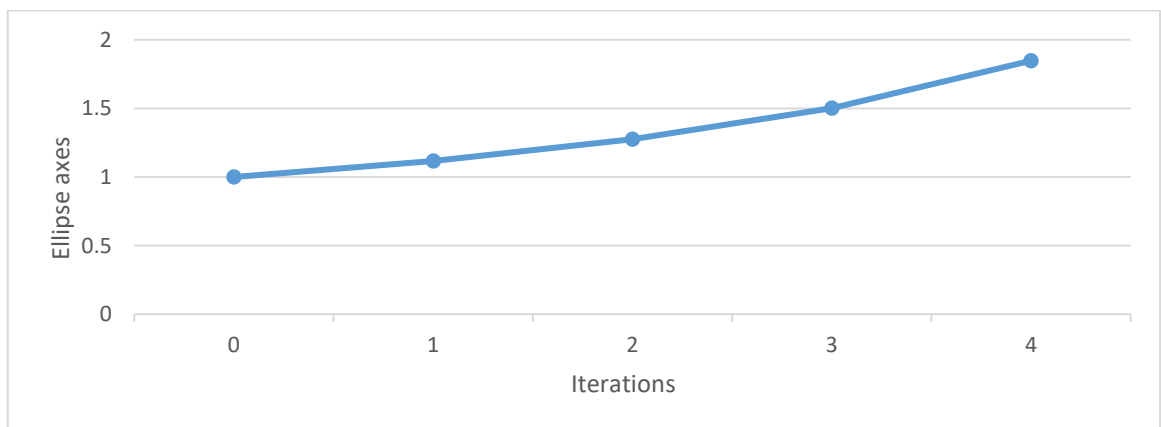
For domain thickness $D = 20$ mm, twelve optimization analyses were conducted including the combinations of reference stresses $\sigma_{ref} = 10, 40$ and 60 MPa and magnification factor $k = 250, 275, 500, 750$ and 1000 . The results obtained including (a) von Mises stress distributions of the plate after first and last iterations, (b) the change of von Mises stresses by iterations along the hole boundary, (c) the change of ellipse axes ratio by iterations are presented in Figures 4.22 to 4.33. A numerical dis-order was observed almost in all of the analyses towards the end of the iterations at the side of the ellipse on the x-axis. However, reasonable results were obtained, close to the results of domain thickness 10 mm, except reference stresses $\sigma_{ref} = 10$ MPa as given in Table 4.4.



(a) von Mises stresses for first and last iterations: Iteration 1 (left), Iteration 4 (right)

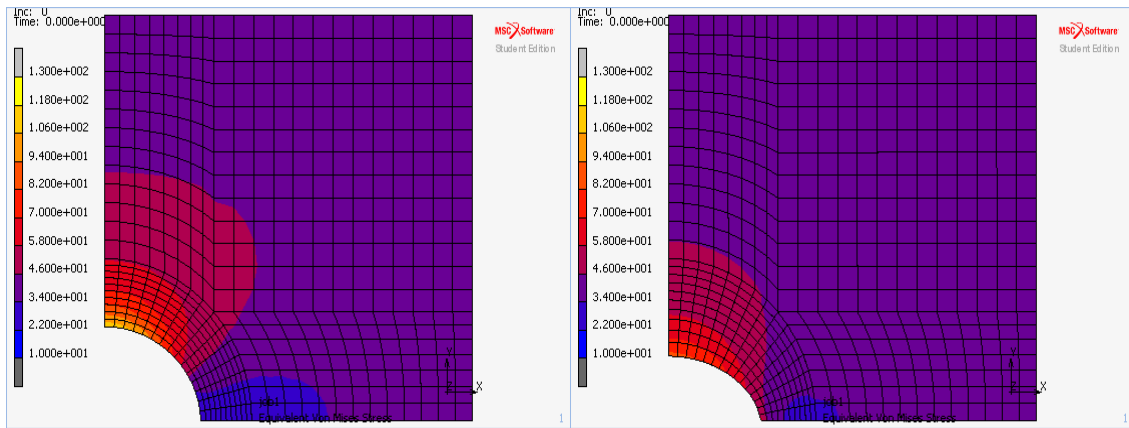


(b) Variation of von Mises stress distribution along the hole boundary

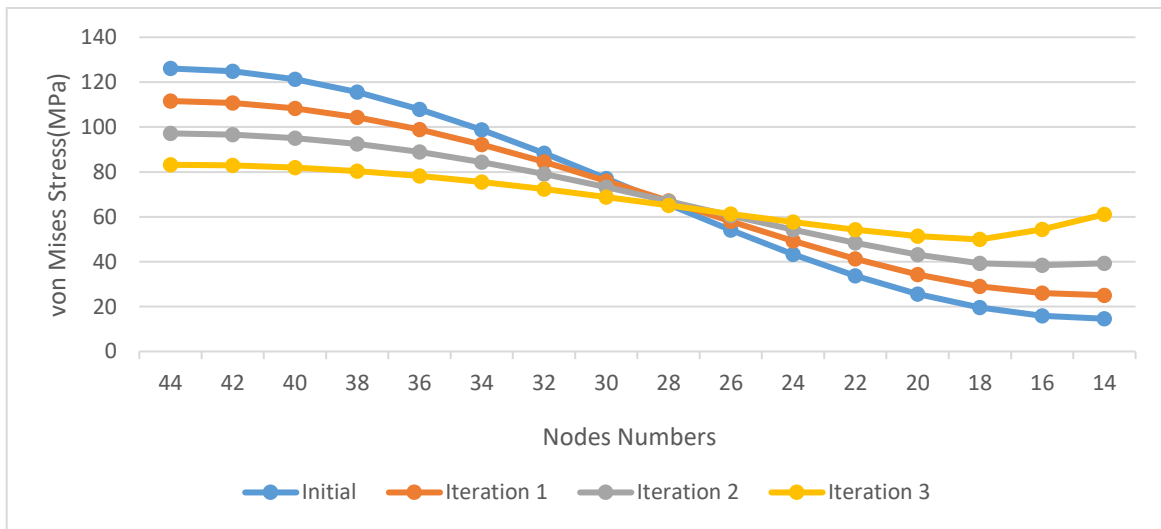


(c) Variation of ellipse axes ratio

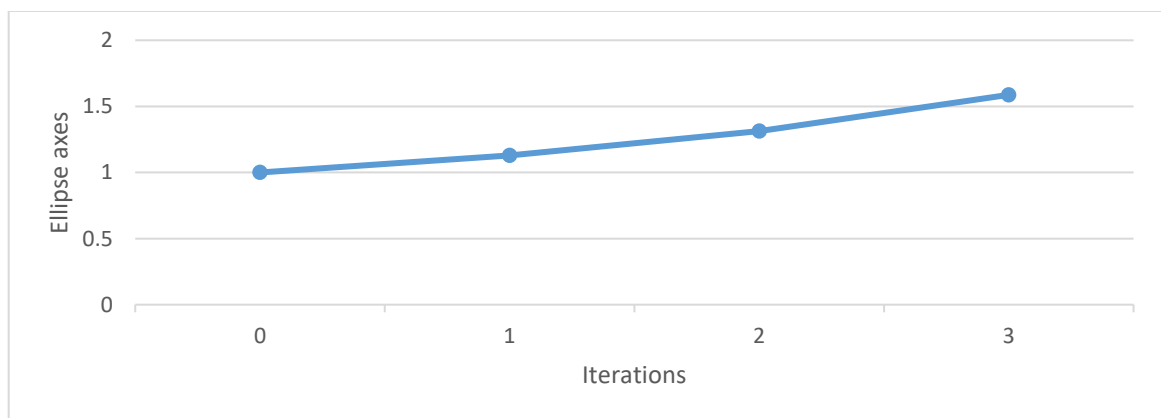
Figure 4.22: Optimization results of a plate with a hole ($D=20$ mm, $K=250$, $\sigma_{ref} = 10$ MPa)



(a) von Mises stresses for first and last iterations: Iteration 1 (left), Iteration 3 (right)

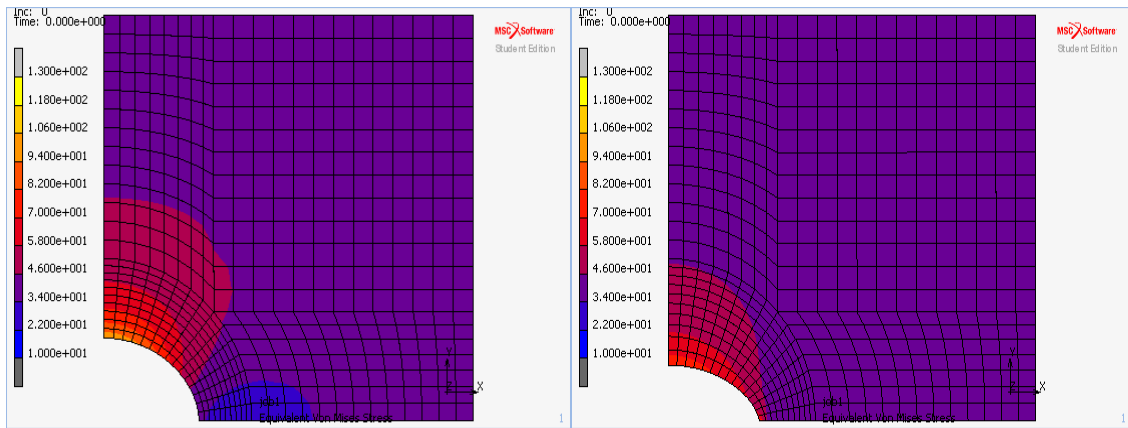


(b) Variation of von Mises stress distribution along the hole boundary

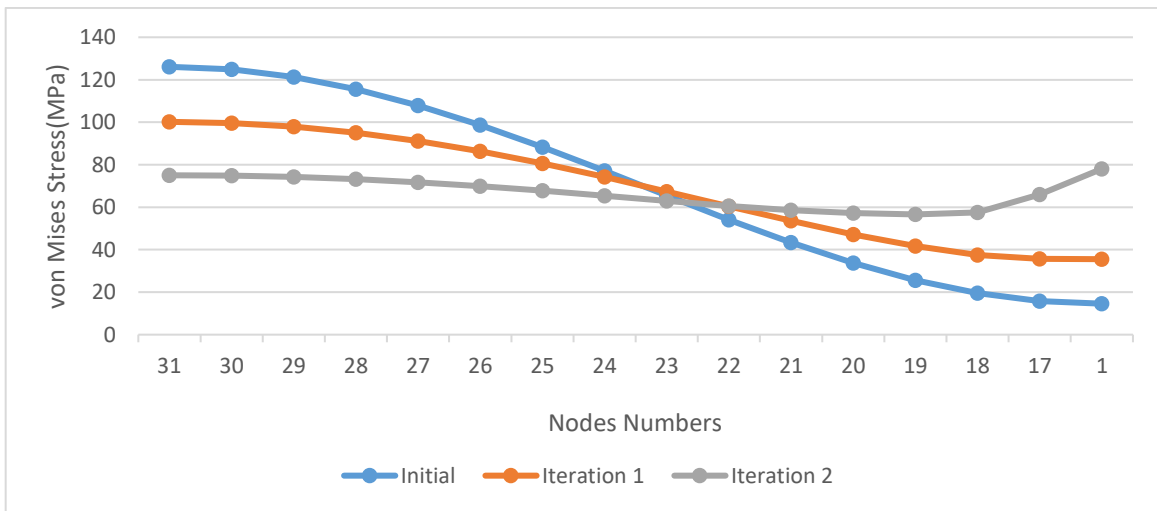


(c) Variation of ellipse axes ratio

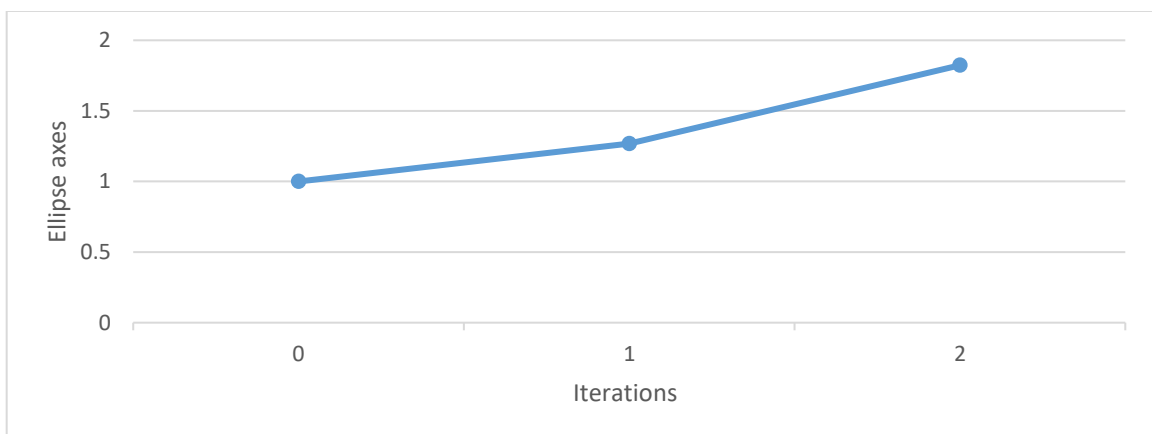
Figure 4.23: Optimization results of a plate with a hole ($D=20$ mm, $K=275$, $\sigma_{ref} = 10$ MPa)



(a) von Mises stresses for first and last iterations: Iteration 1 (left), Iteration 2 (right)

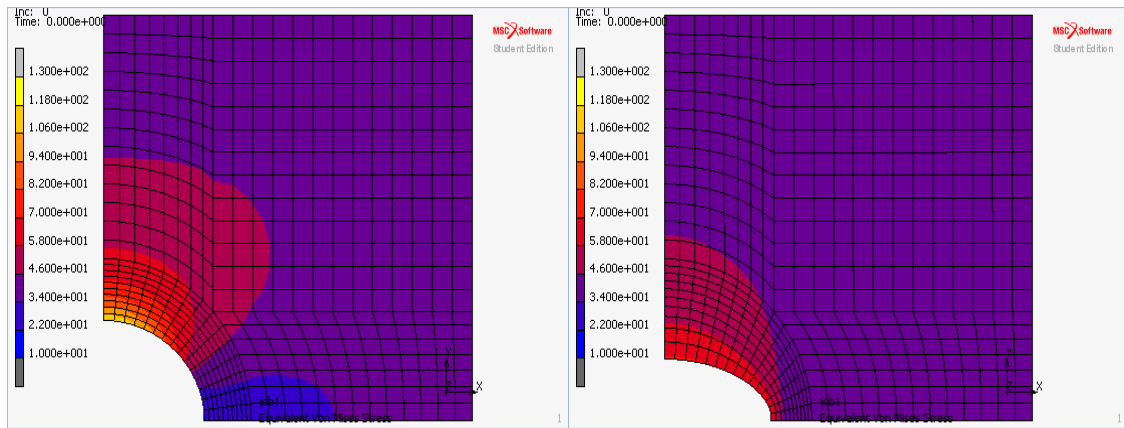


(b) Variation of von Mises stress distribution along the hole boundary

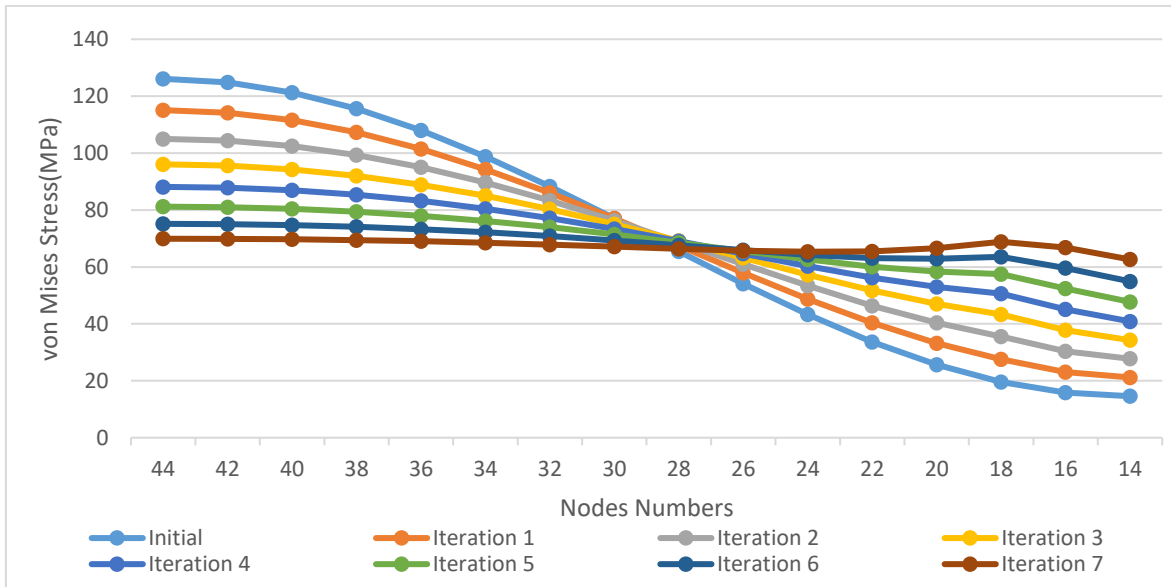


(c) Variation of ellipse axes ratio

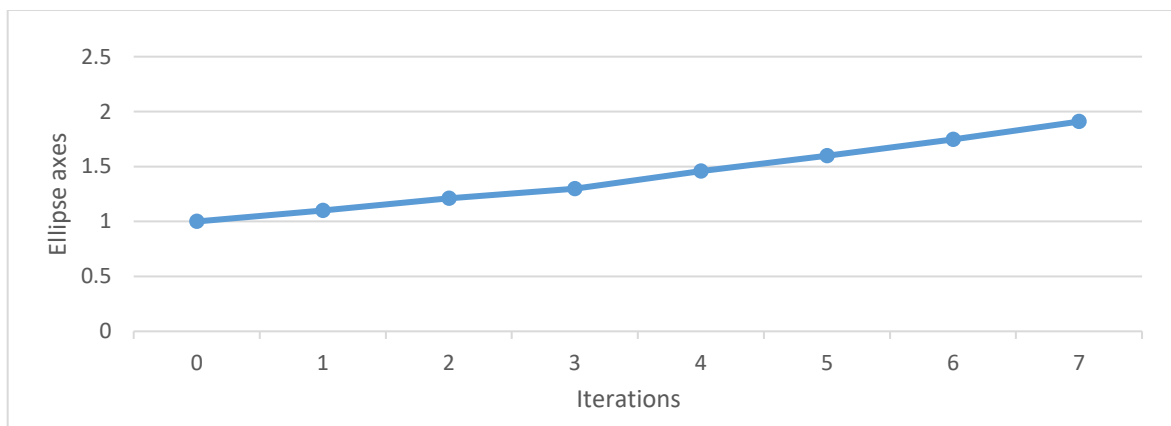
Figure 4.24: Optimization results of a plate with a hole ($D=20$ mm, $K=500$, $\sigma_{ref} = 10$ MPa)



(a) von Mises stresses for first and last iterations: Iteration 1 (left), Iteration 7 (right)

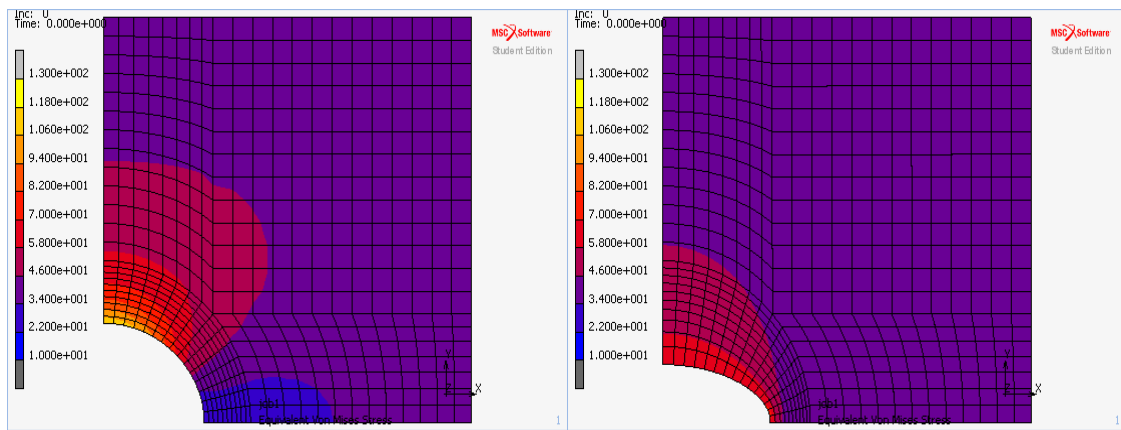


(b) Variation of von Mises stress distribution along the hole boundary

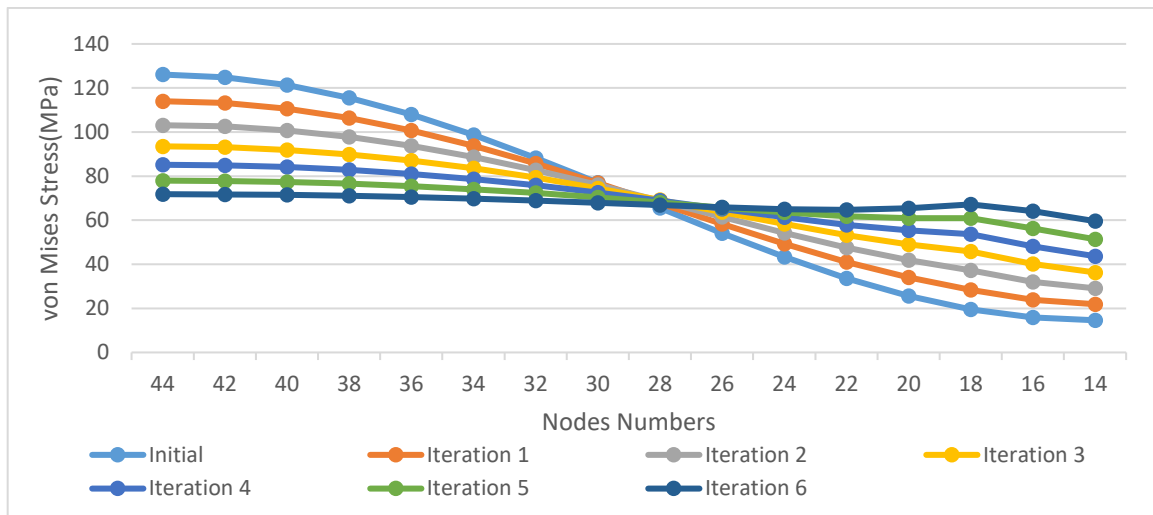


(c) Variation of ellipse axes ratio

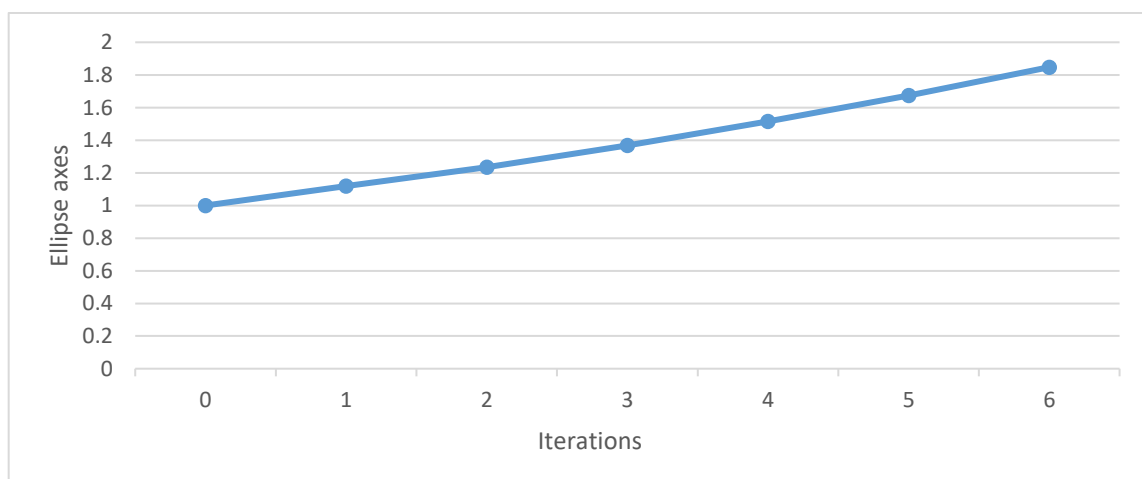
Figure 4.25: Optimization results of a plate with a hole ($D=20$ mm, $K=250$, $\sigma_{ref} = 40$ MPa)



(a) von Mises stresses for first and last iterations: Iteration 1 (left), Iteration 6 (right)

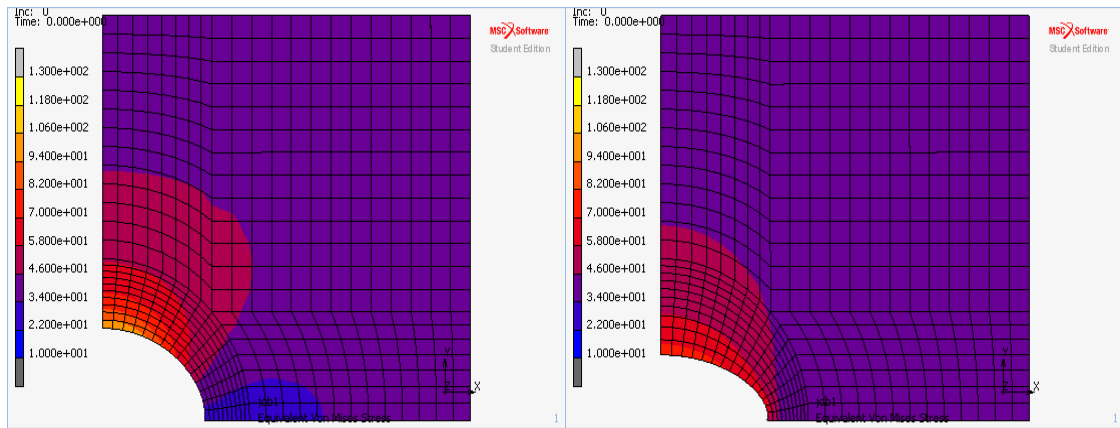


(b) Variation of von Mises stress distribution along the hole boundary

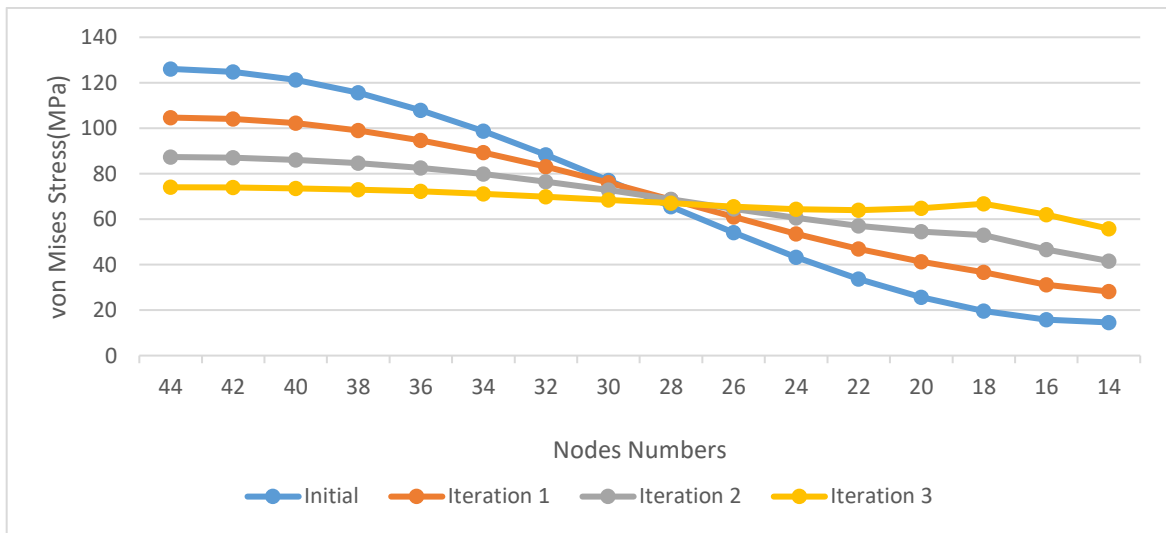


(c) Variation of ellipse axes ratio

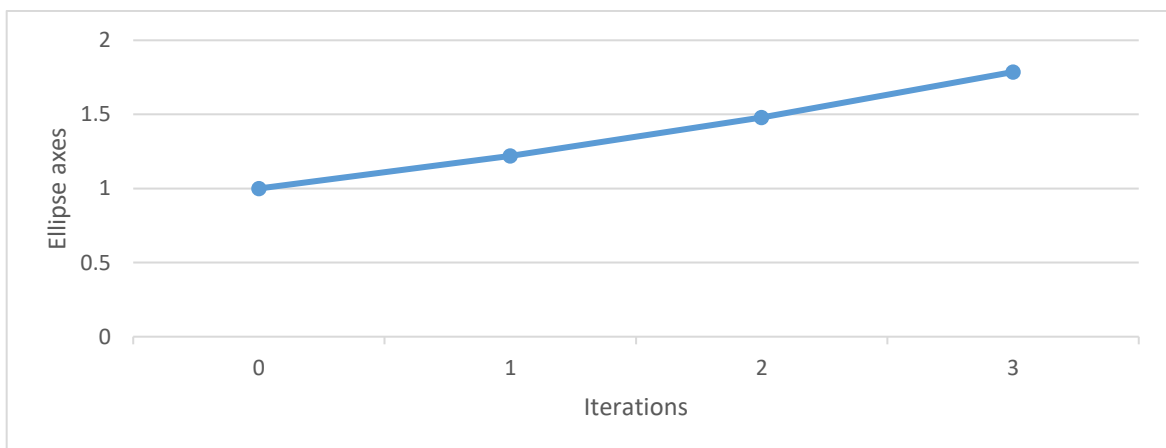
Figure 4.26: Optimization results of a plate with a hole ($D=20$ mm, $K=275$, $\sigma_{ref} = 40$ MPa)



(a) von Mises stresses for first and last iterations: Iteration 1 (left), Iteration 3 (right)

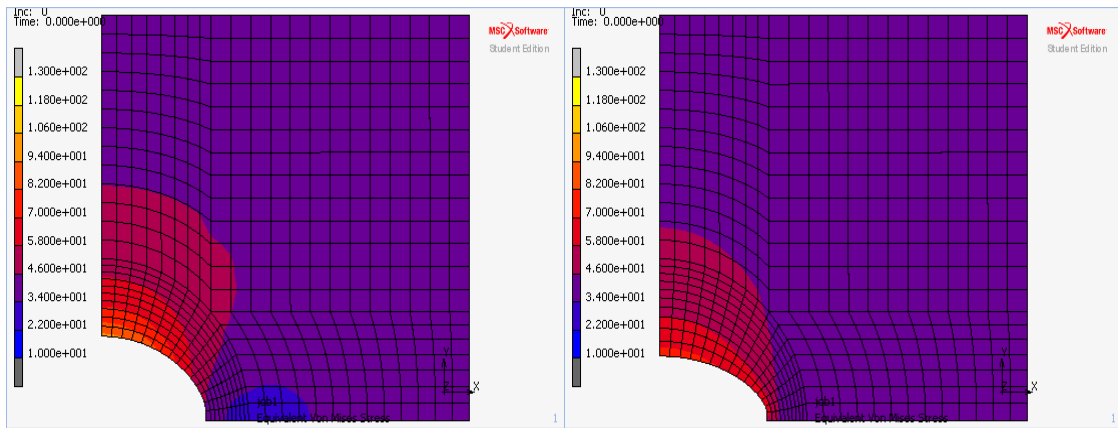


(b) Variation of von Mises stress distribution along the hole boundary

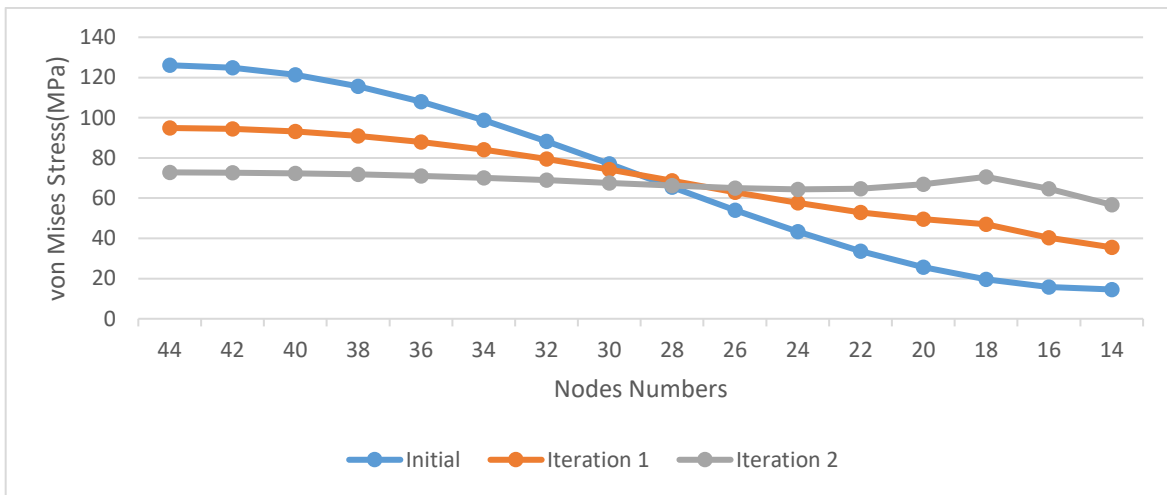


(c) Variation of ellipse axes ratio

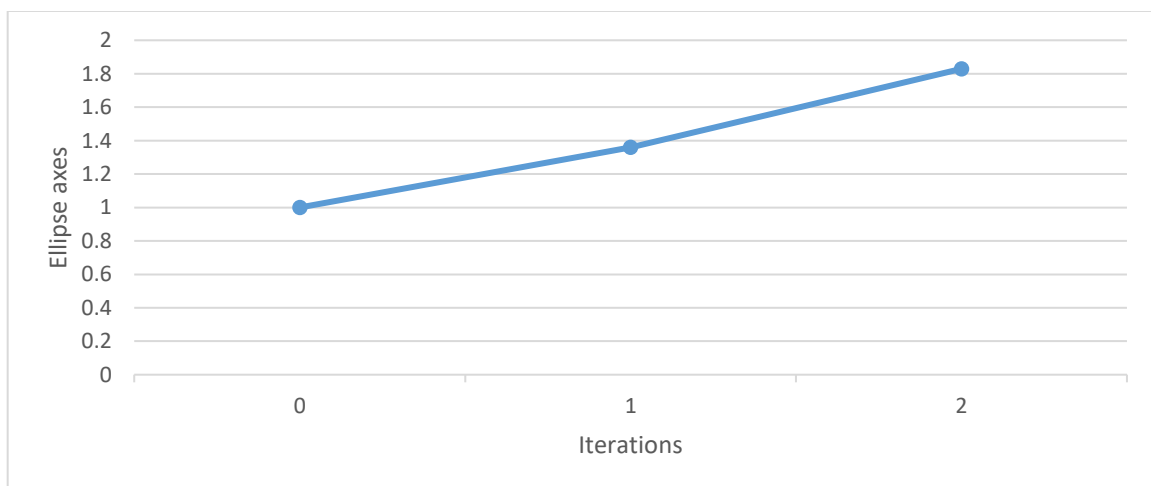
Figure 4.27: Optimization results of a plate with a hole ($D=20$ mm, $K=500$, $\sigma_{ref} = 40$ MPa)



(a) von Mises stresses for first and last iterations: Iteration 1 (left), Iteration 2 (right)

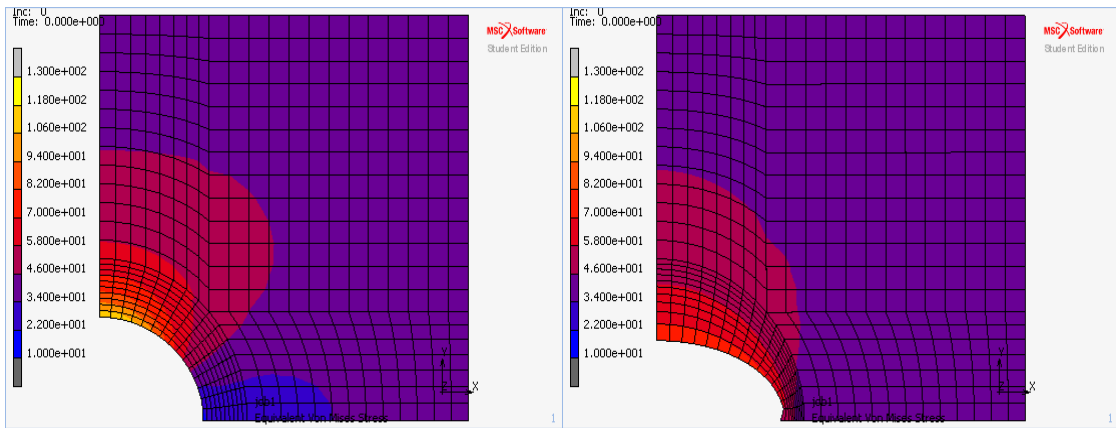


(b) Variation of von Mises stress distribution along the hole boundary

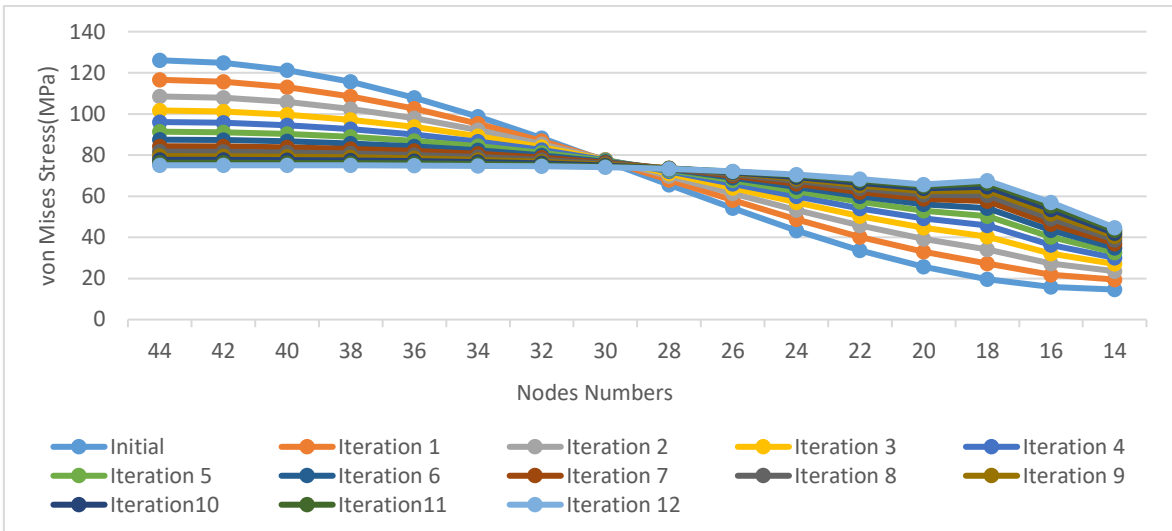


(c) Variation of ellipse axes ratio

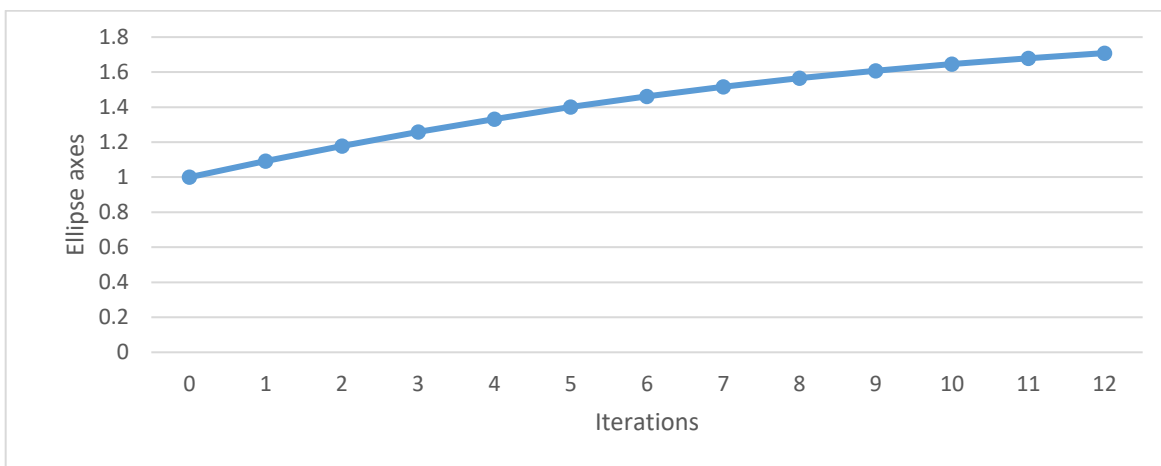
Figure 4.28: Optimization results of a plate with a hole ($D=20$ mm, $K=750$, $\sigma_{ref} = 40$ MPa)



(a) von Mises stresses for first and last iterations: Iteration 1 (left), Iteration 12 (right)

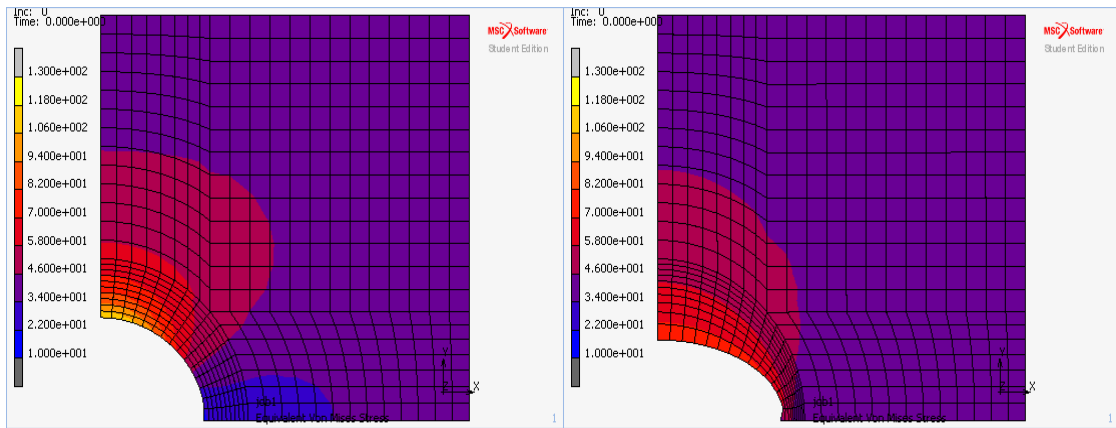


(b) Variation of von Mises stress distribution along the hole boundary

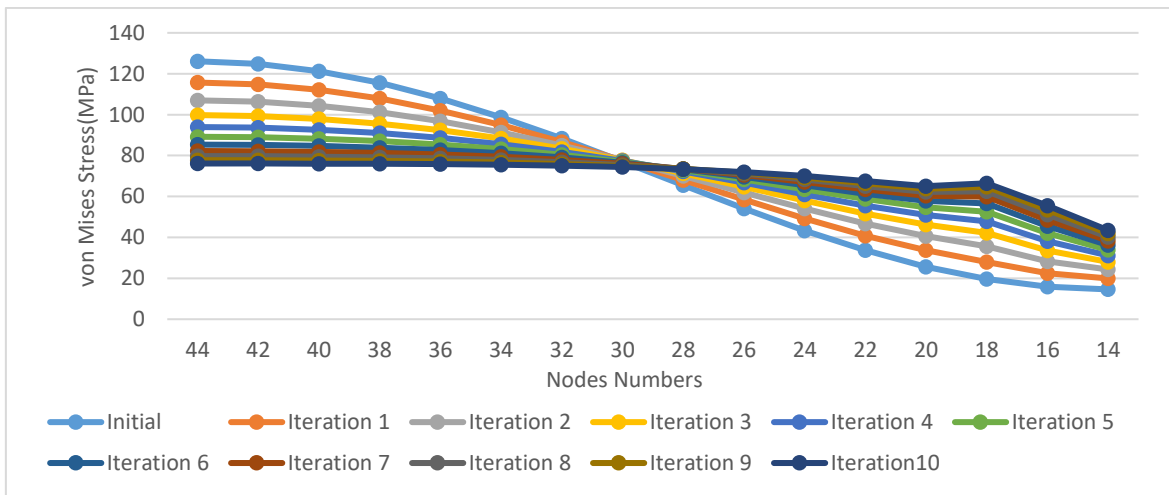


(c) Variation of ellipse axes ratio

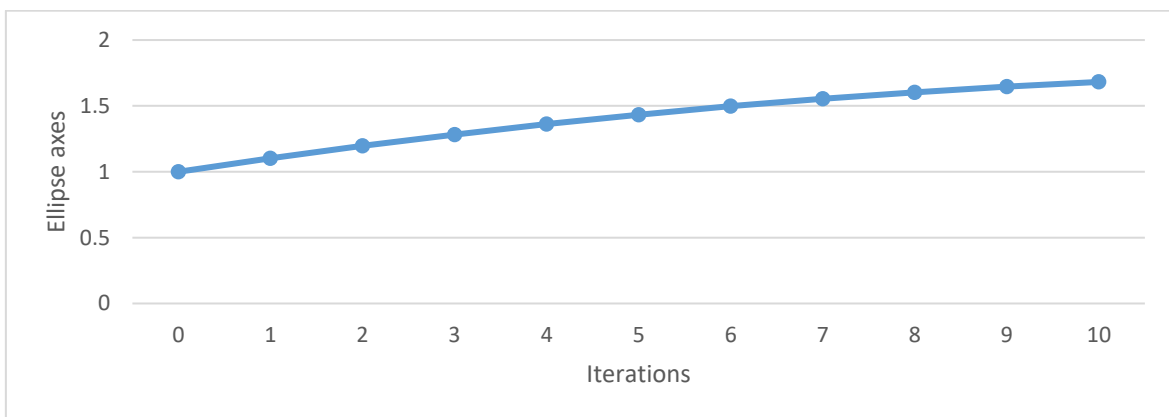
Figure 4.29: Optimization results of a plate with a hole ($D=20$ mm, $K=250$, $\sigma_{ref} = 60$ MPa)



(a) von Mises stresses for first and last iterations: Iteration 1 (left), Iteration 10 (right)

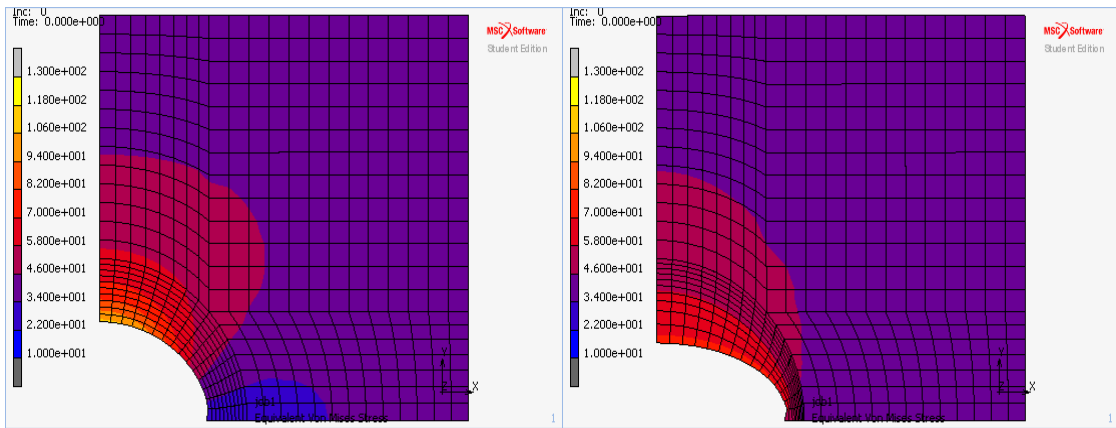


(b) Variation of von Mises stress distribution along the hole boundary

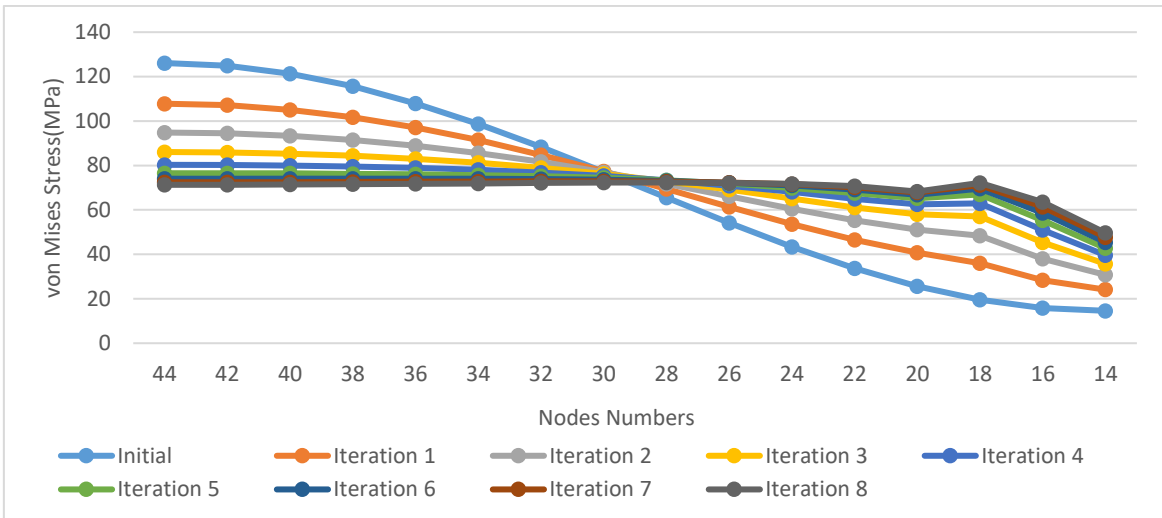


(c) Variation of ellipse axes ratio

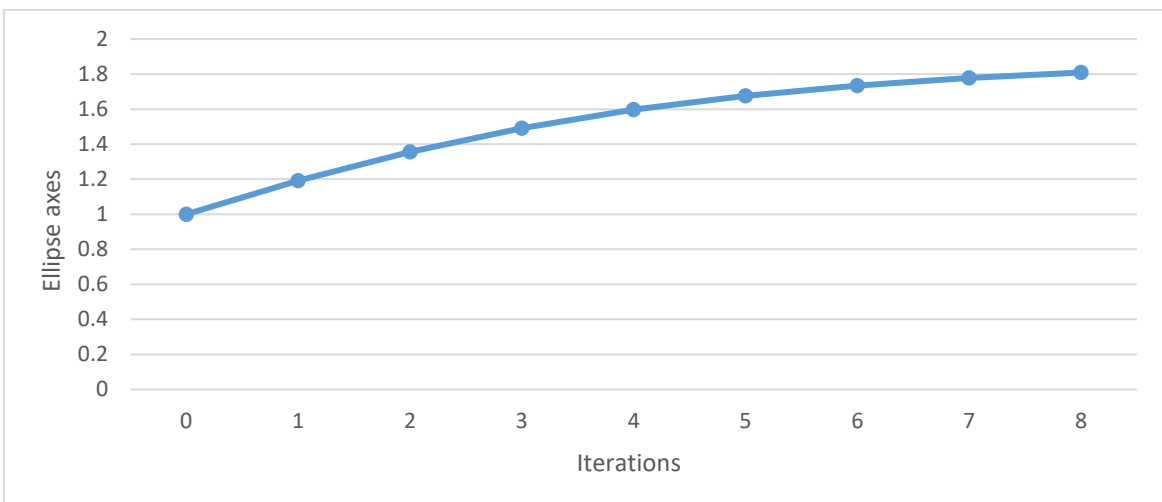
Figure 4.30: Optimization results of a plate with a hole ($D=20$ mm, $K=275$, $\sigma_{ref} = 60$ MPa)



(a) von Mises stresses for first and last iterations: Iteration 1 (left), Iteration 8 (right)

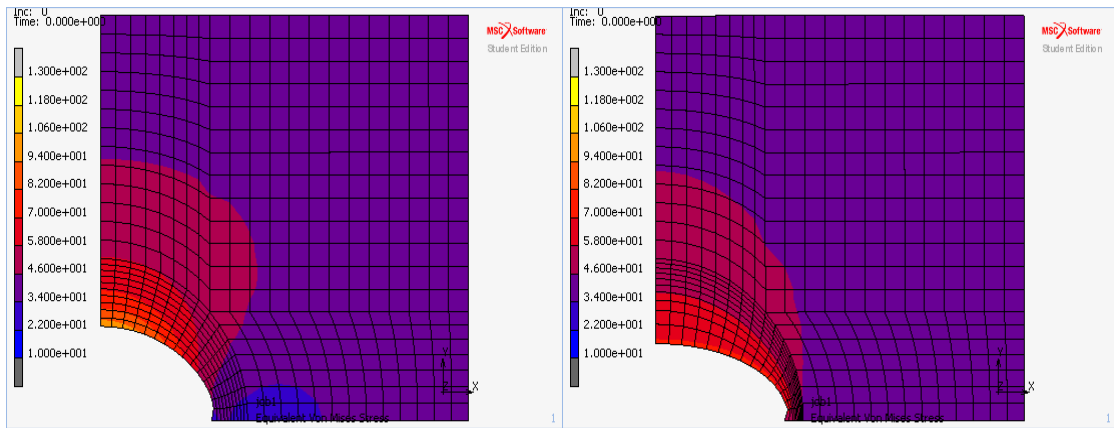


(b) Variation of von Mises stress distribution along the hole boundary

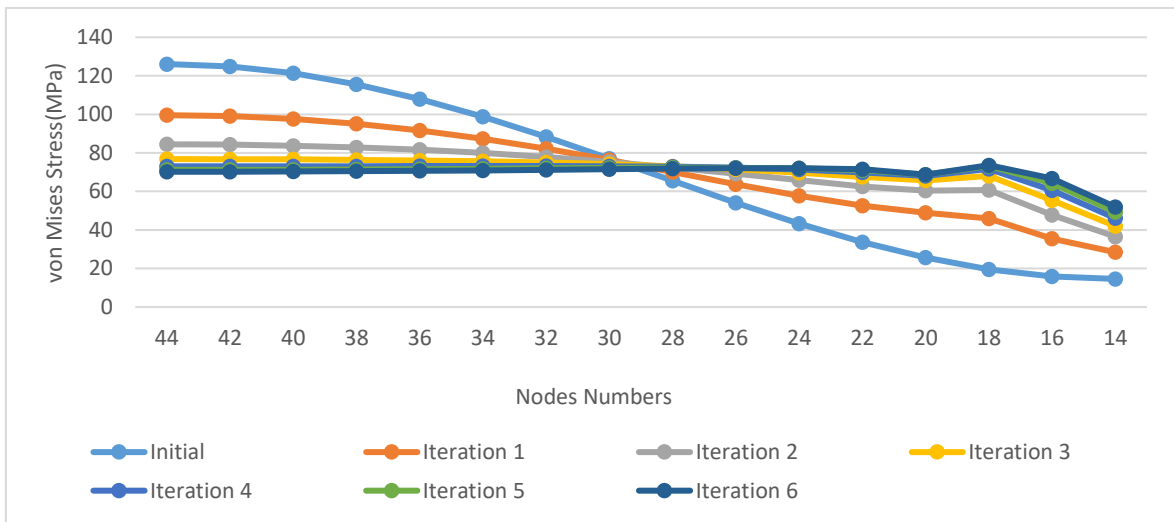


(c) Variation of ellipse axes ratio

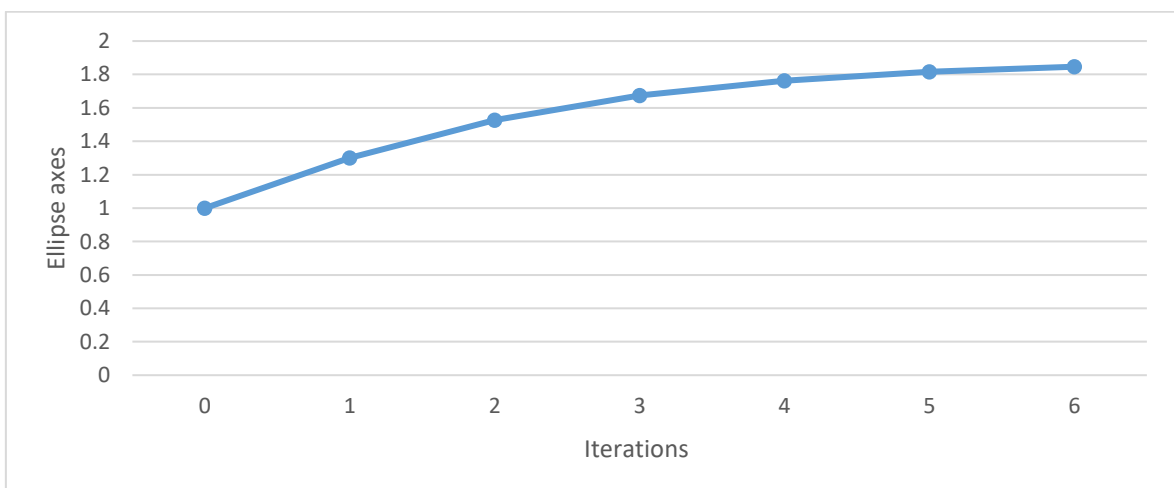
Figure 4.31: Optimization results of a plate with a hole ($D=20$ mm, $K=500$, $\sigma_{ref} = 60$ MPa)



(a) von Mises stresses for first and last iterations: Iteration 1 (left), Iteration 6 (right)

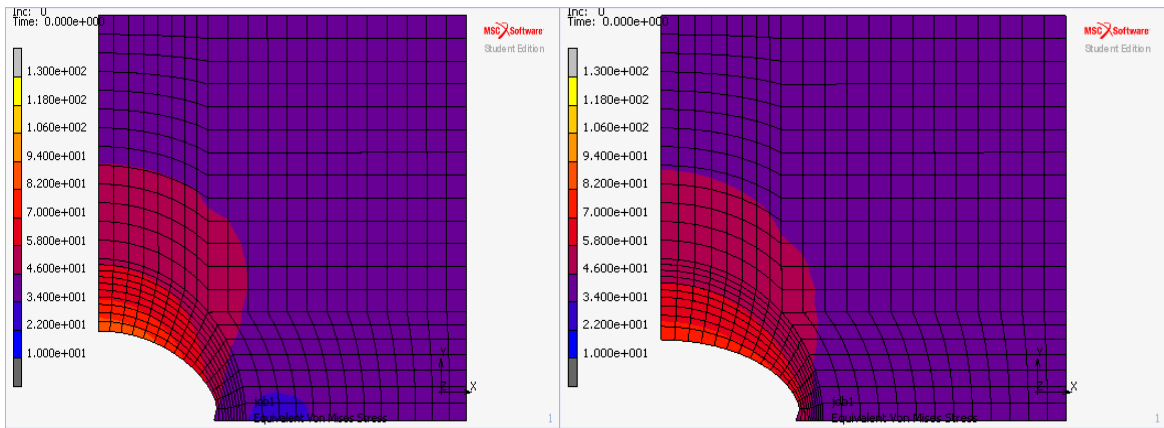


(b) Variation of von Mises stress distribution along the hole boundary

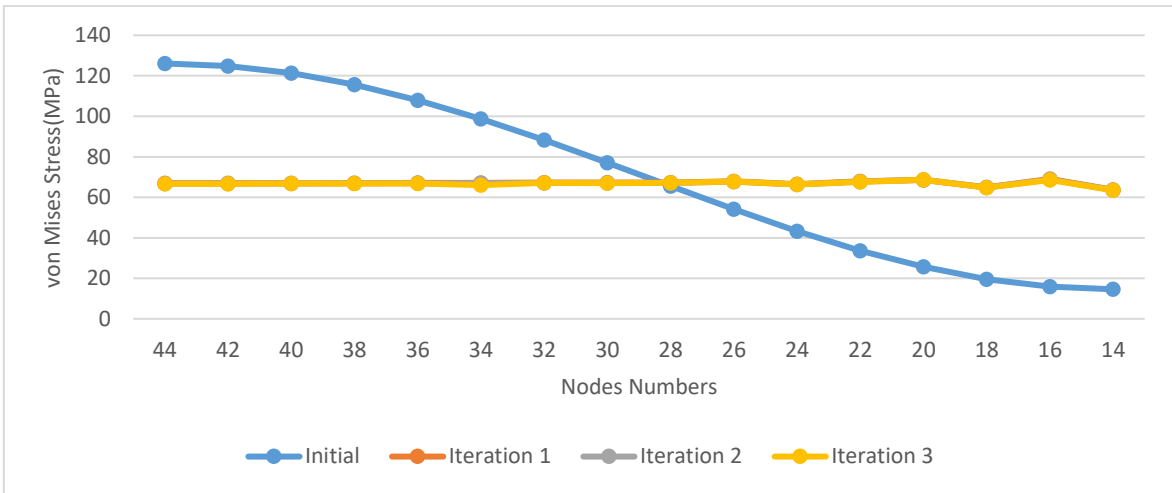


(c) Variation of ellipse axes ratio

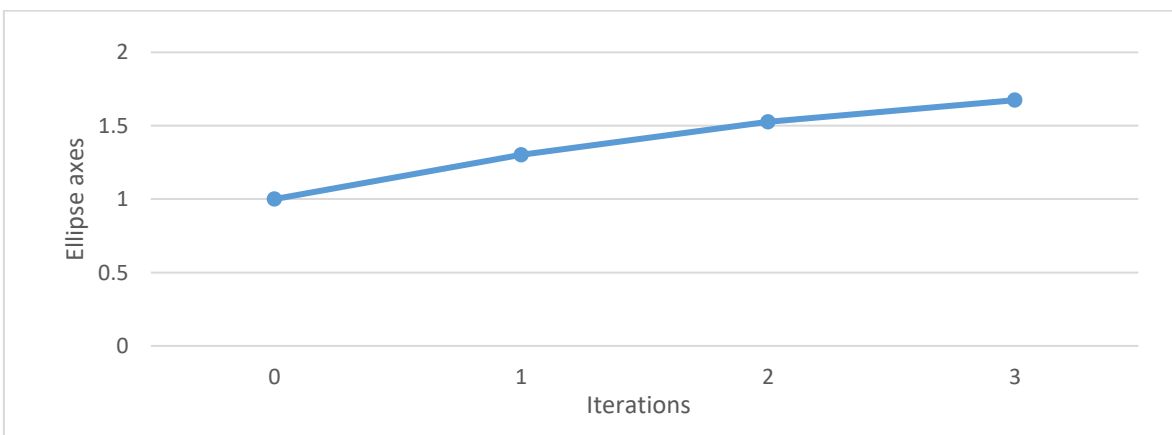
Figure 4.32: Optimization results of a plate with a hole ($D=20$ mm, $K=750$, $\sigma_{ref} = 60$ MPa)



(a) von Mises stresses for first and last iterations: Iteration 1 (left), Iteration 3 (right)



(b) Variation of von Mises stress distribution along the hole boundary



(c) Variation of ellipse axes ratio

Figure 4.33: Optimization results of a plate with a hole ($D=20$ mm, $K=1000$, $\sigma_{ref} = 60$ MPa)

Table 4.3: Summary of results with domain thickness 20mm

		Magnification factor k				
		250	275	500	750	1000
σ_{ref}		250	275	500	750	1000
10	Iterations	4	3	2	--	--
	Max stress	83.64	83.19	87.06	--	--
	Ellipse axes ratio	1.84	1.58	1.82	--	--
40	Iterations	7	6	3	2	--
	Max stress	69.92	71.82	74.04	72.82	--
	Ellipse axes ratio	1.90	1.84	1.78	1.82	--
60	Iterations	12	10	8	6	3
	Max stress	75.03	74.82	72.34	73.20	68.65
	Ellipse axes ratio	1.70	1.68	1.86	1.84	1.67

4.3 Optimization of a Plate with a Hole with Domain Thickness 30 mm

The finite element models and the boundary conditions for stress and thermal analysis are shown in Figure 4.34 for domain thickness 30 mm. The von Mises stresses of stress analysis and total deflections of the thermal expansion analysis of the original shape can be seen in Figure 4.35. Similar to the analysis conducted for domain thickness 10 mm, the stress far away from the concentration zones is about 40 MPa. The maximum and minimum von Mises stresses were also around 130 MPa and 10 MPa respectively.

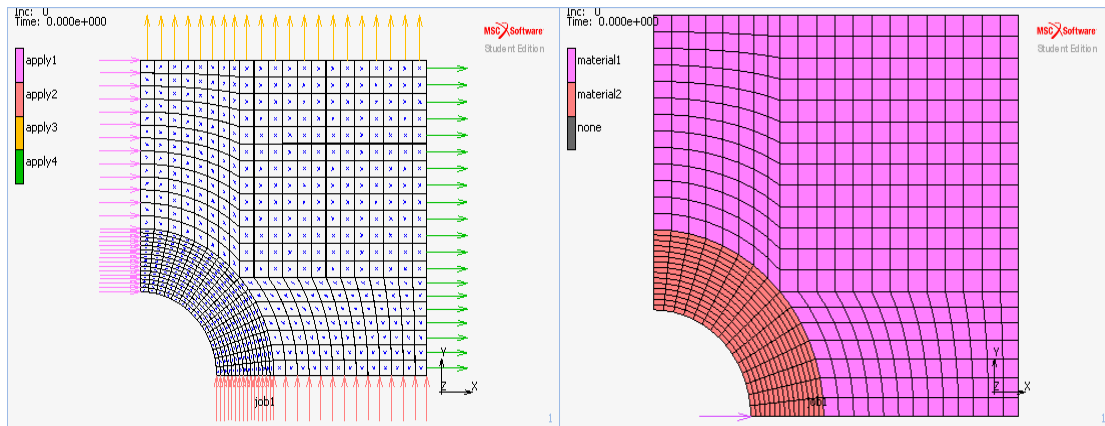


Figure 4.34: Finite element model for stress (left) and thermal (right) analysis (D=30mm)

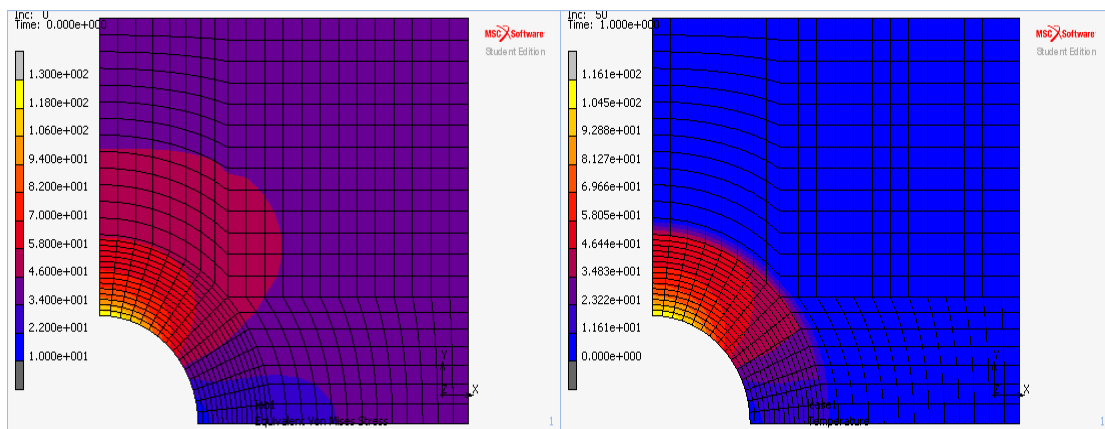
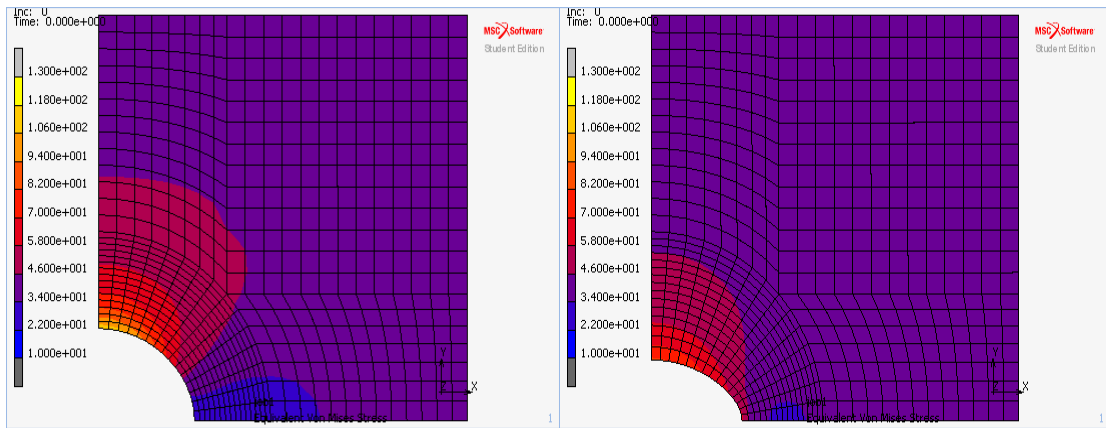
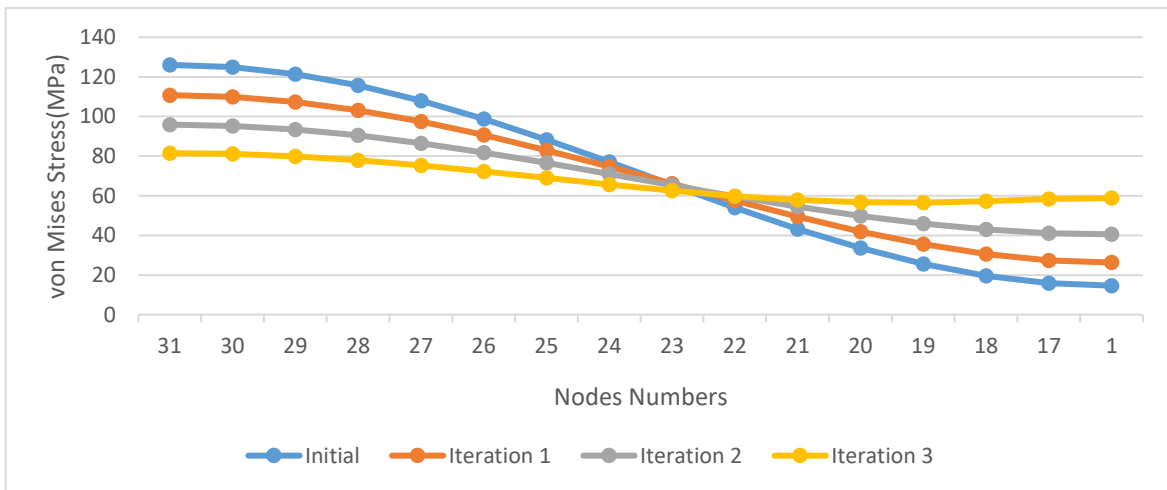


Figure 4.35: von Mises stresses (left) and thermal deformations (right) of the original shape (D=30mm)

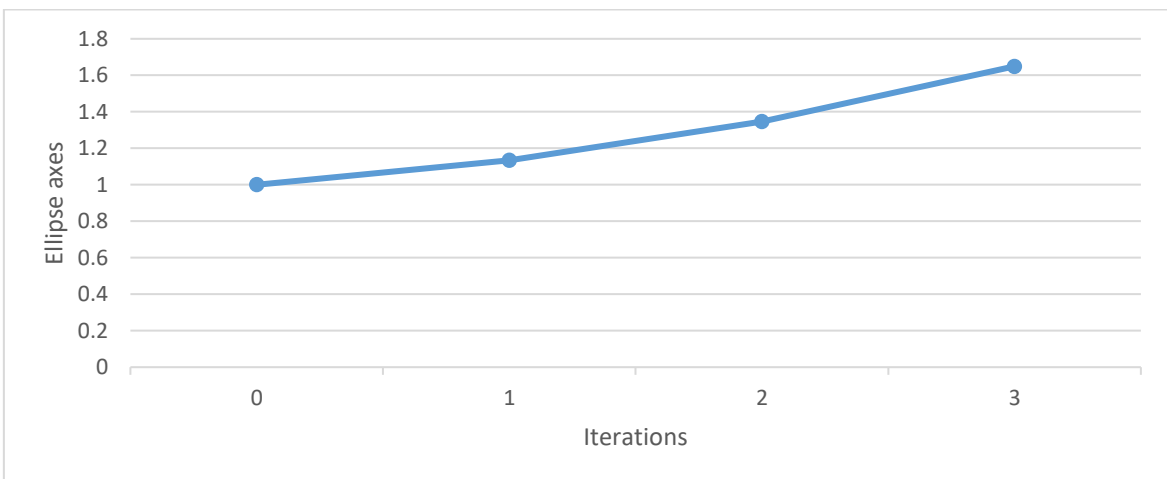
For domain thickness $D = 30$ mm, eleven optimization analyses were conducted including the combinations of reference stresses $\sigma_{ref} = 10, 40$ and 60 MPa and magnification factor $k = 250, 275, 500, 750$ and 1000 . The results obtained including (a) von Mises stress distributions of the plate after first and last iterations, (b) the change of von Mises stresses by iterations along the hole boundary, (c) the change of ellipse axes ratio by iterations are presented in Figures 4.36 to 4.46. No remarkable difference was observed from the previous domain 10 and 20 mm analyses results as given in Table 4.4.



(a) von Mises stresses for first and last iterations: Iteration 1 (left), Iteration 3 (right)

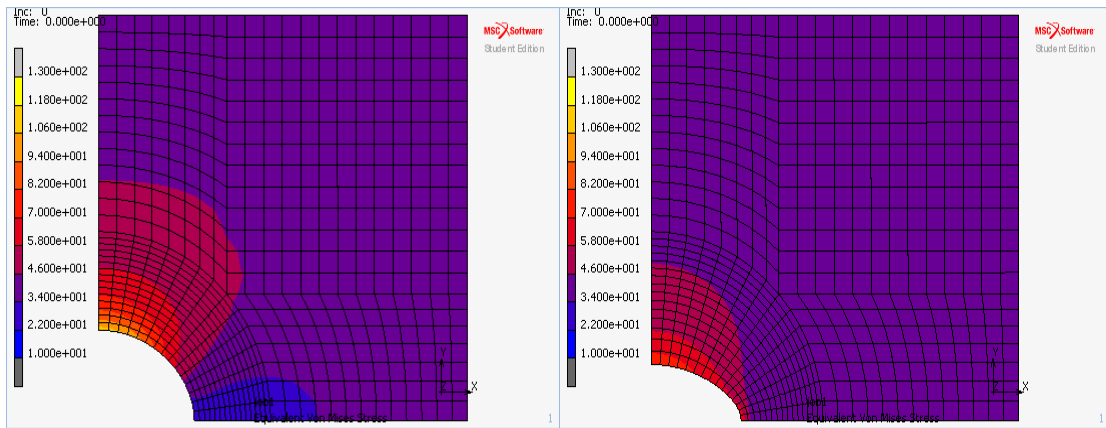


(b) Variation of von Mises stress distribution along the hole boundary

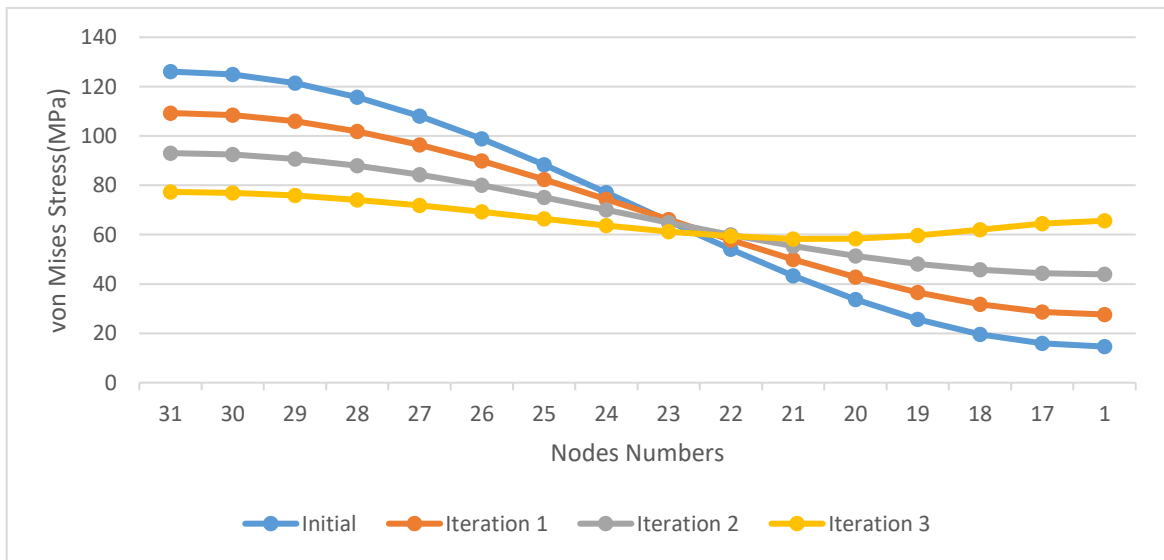


(c) Variation of ellipse axes ratio

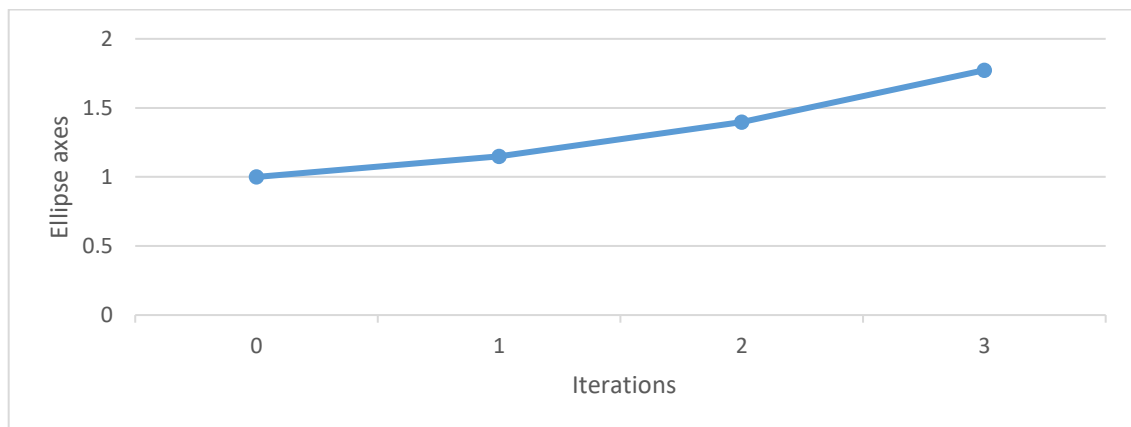
Figure 4.36: Optimization results of a plate with a hole ($D=30$ mm, $K=250$, $\sigma_{ref} = 10$ MPa)



(a) von Mises stresses for first and last iterations: Iteration 1 (left), Iteration 3 (right)

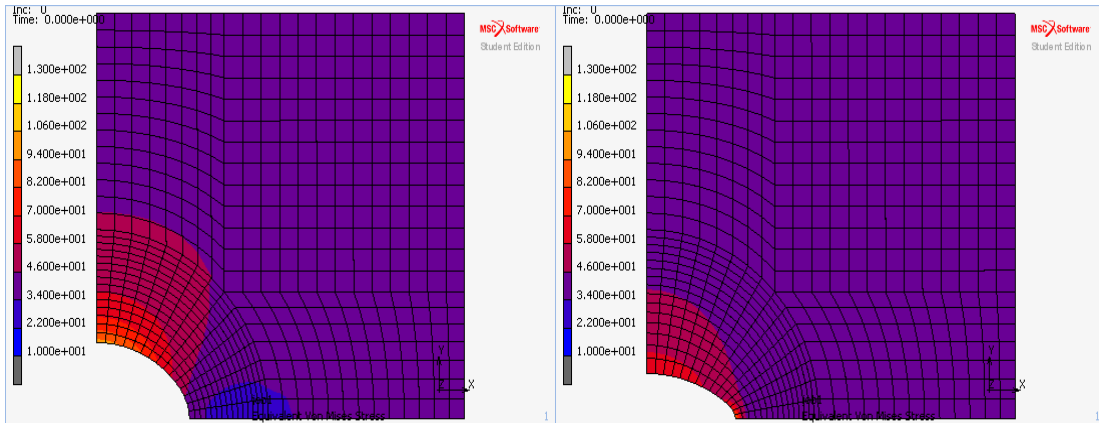


(b) Variation of von Mises stress distribution along the hole boundary

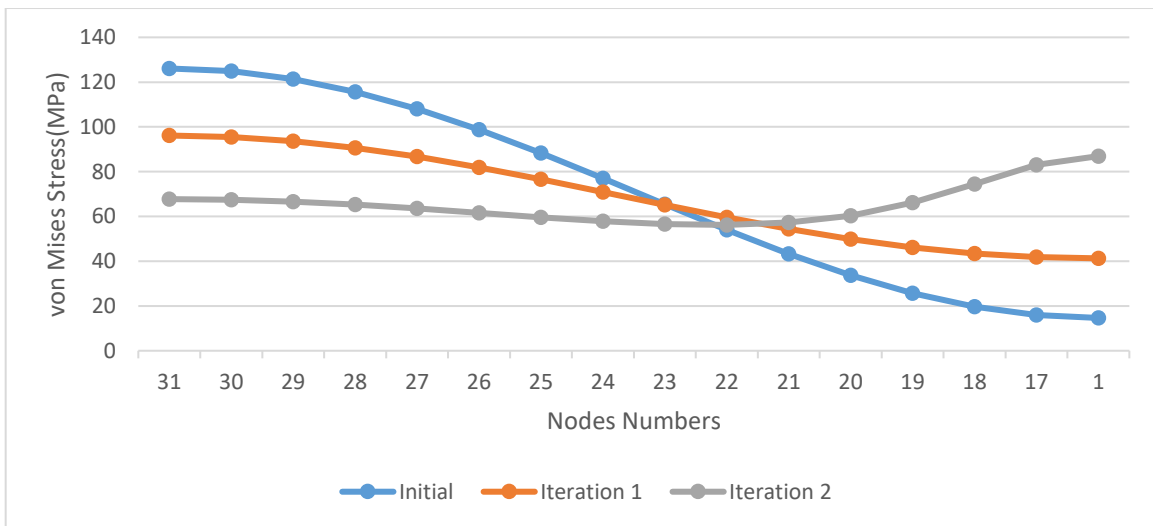


(c) Variation of ellipse axes ratio

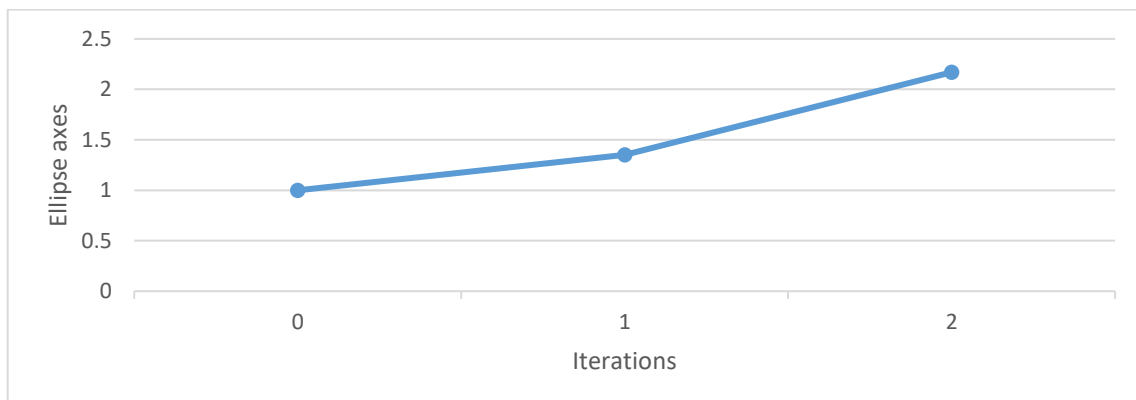
Figure 4.37: Optimization results of a plate with a hole ($D=30$ mm, $K=275$, $\sigma_{ref} = 10$ MPa)



(a) von Mises stresses for first and last iterations: Iteration 1 (left), Iteration 2 (right)

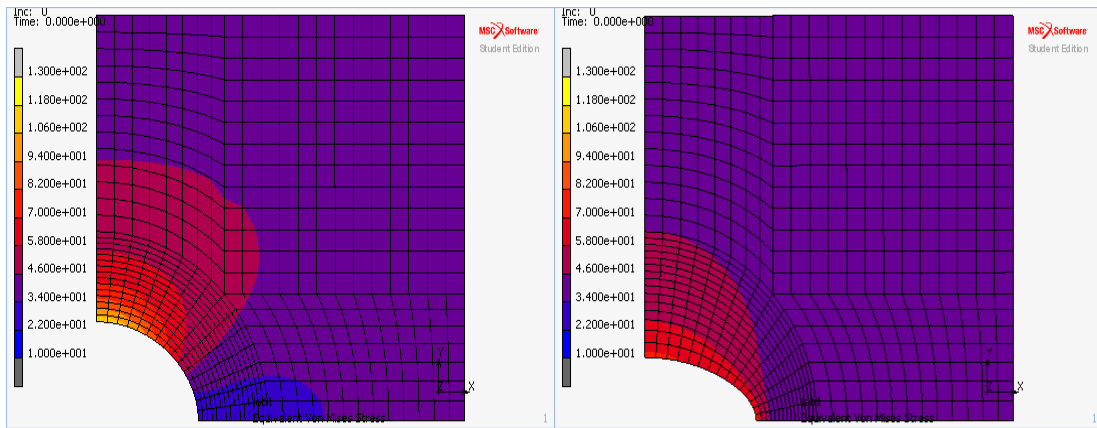


(b) Variation of von Mises stress distribution along the hole boundary

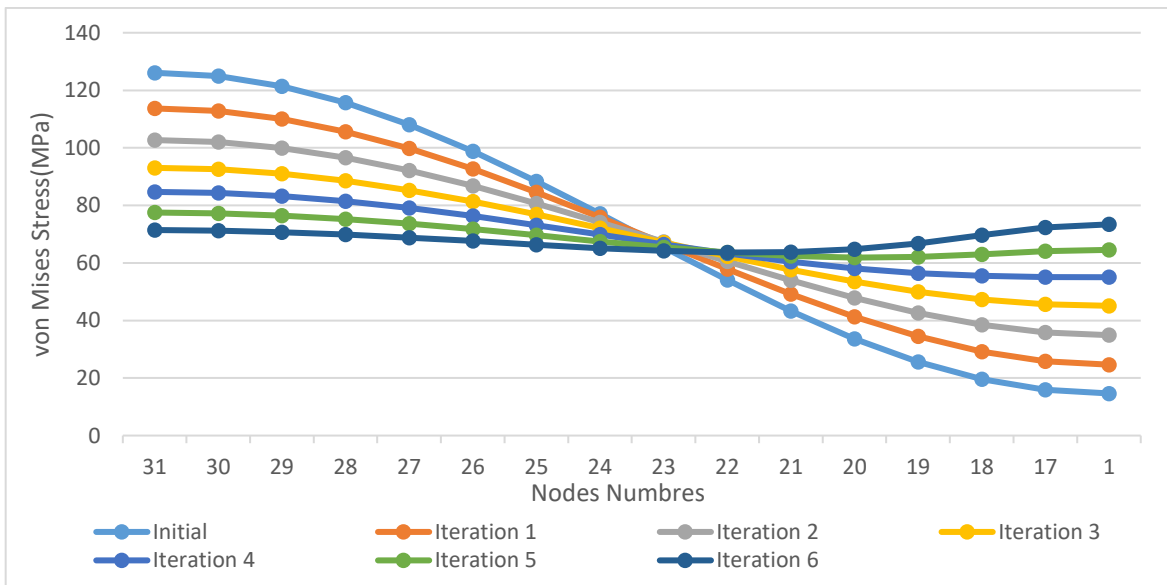


(c) Variation of ellipse axes ratio

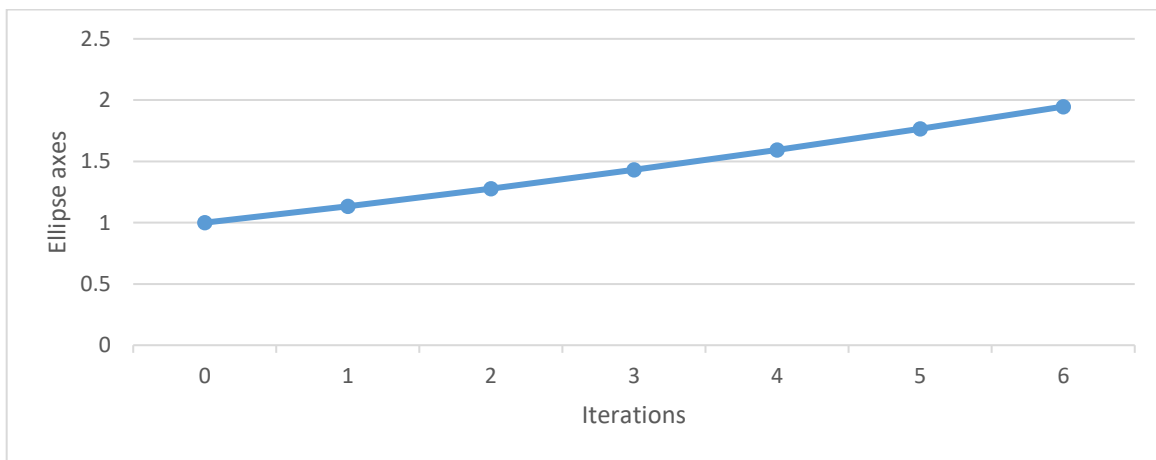
Figure 4.38: Optimization results of a plate with a hole ($D=30$ mm, $K=500$, $\sigma_{ref} = 10$ MPa)



(a) von Mises stresses for first and last iterations: Iteration 1 (left), Iteration 6 (right)

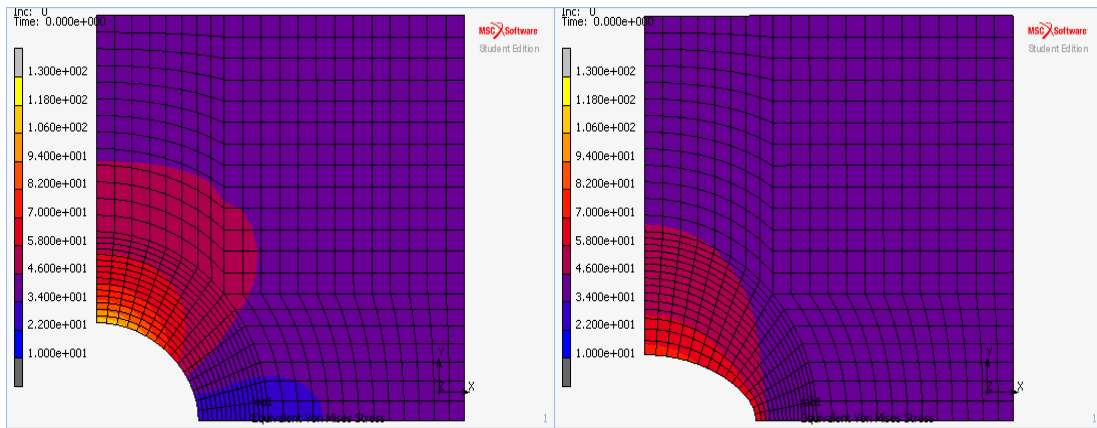


(b) Variation of von Mises stress distribution along the hole boundary

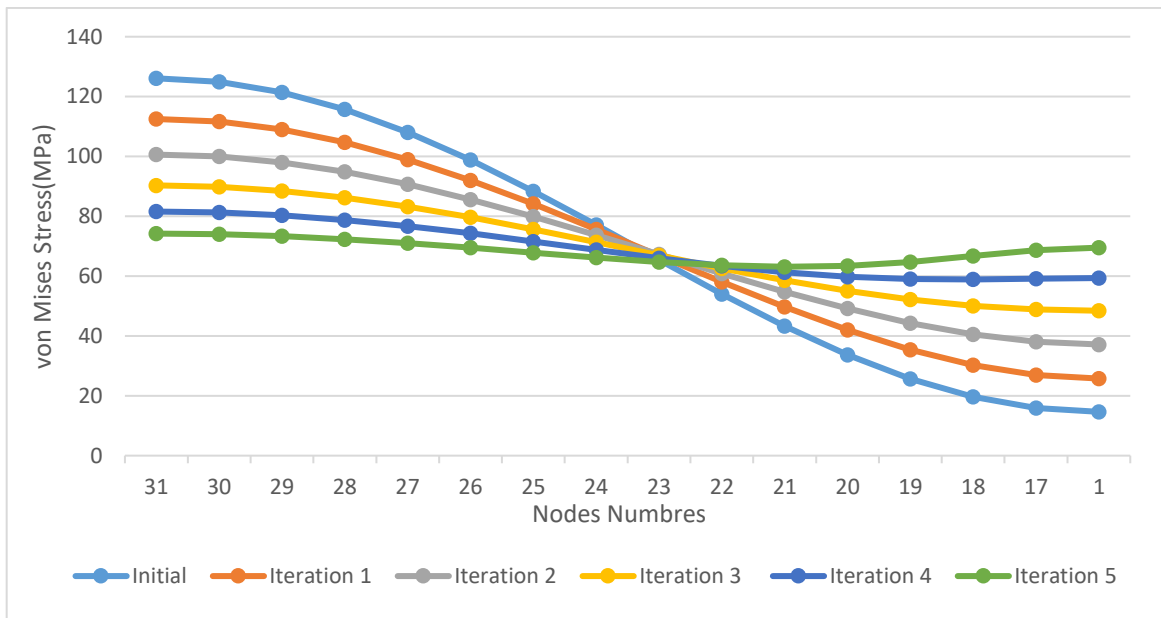


(c) Variation of ellipse axes ratio

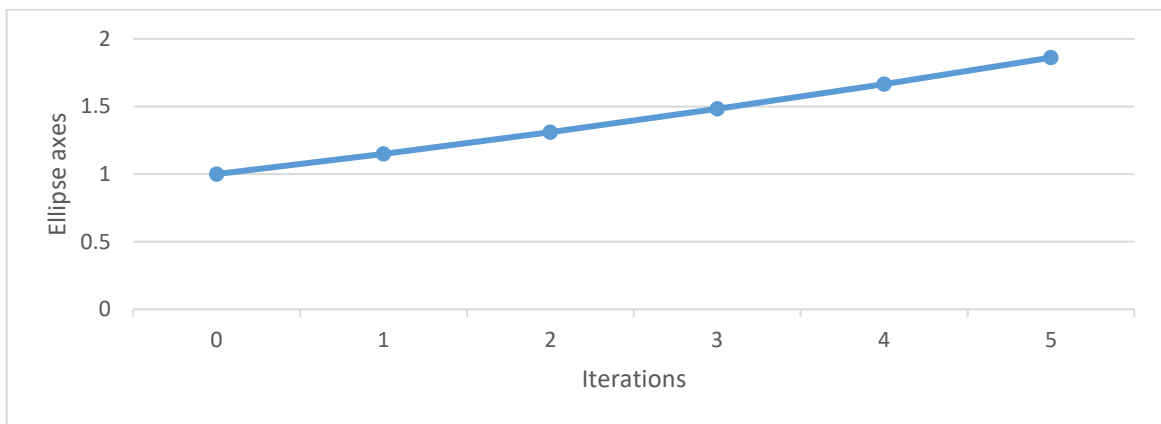
Figure 4.39: Optimization results of a plate with a hole ($D=30$ mm, $K=250$, $\sigma_{ref} = 40$ MPa)



(a) von Mises stresses for first and last iterations: Iteration 1 (left), Iteration 5 (right)

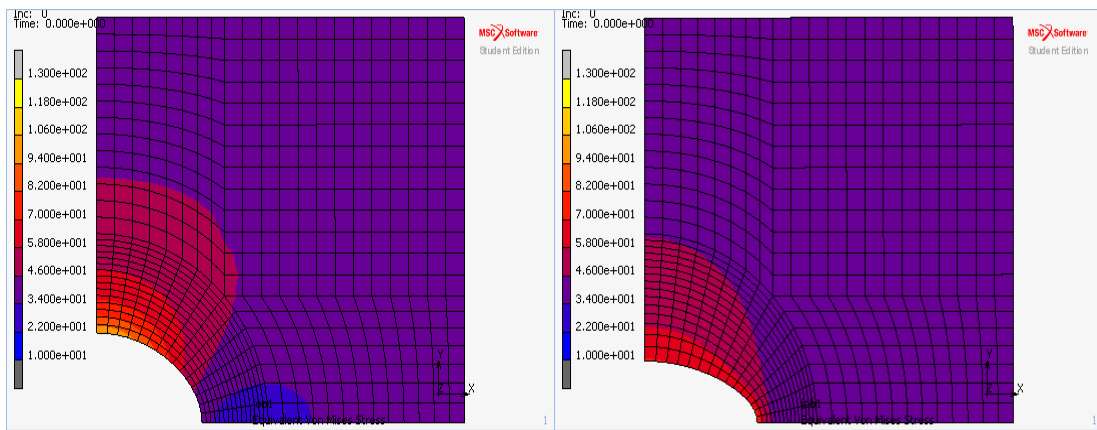


(b) Variation of von Mises stress distribution along the hole boundary

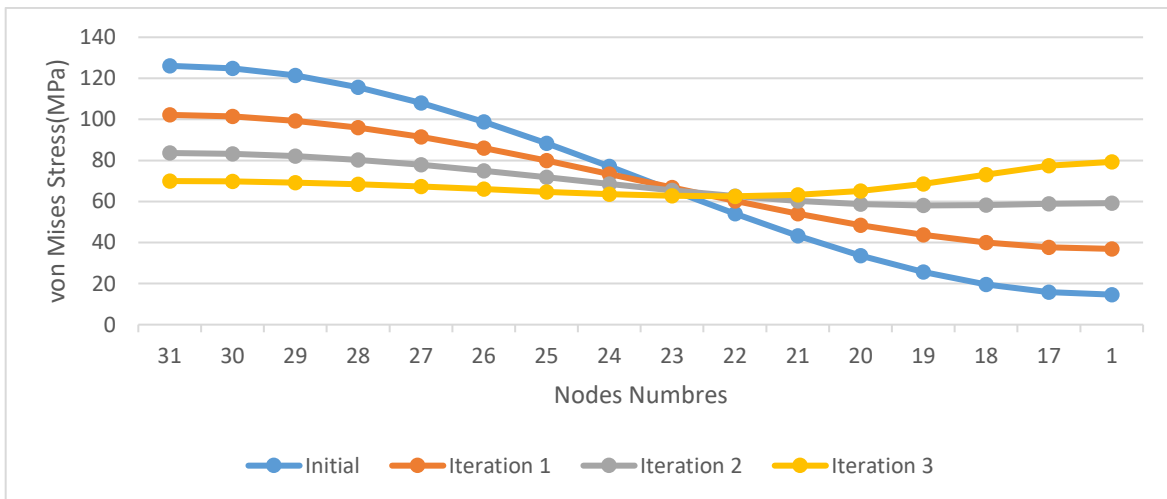


(c) Variation of ellipse axes ratio

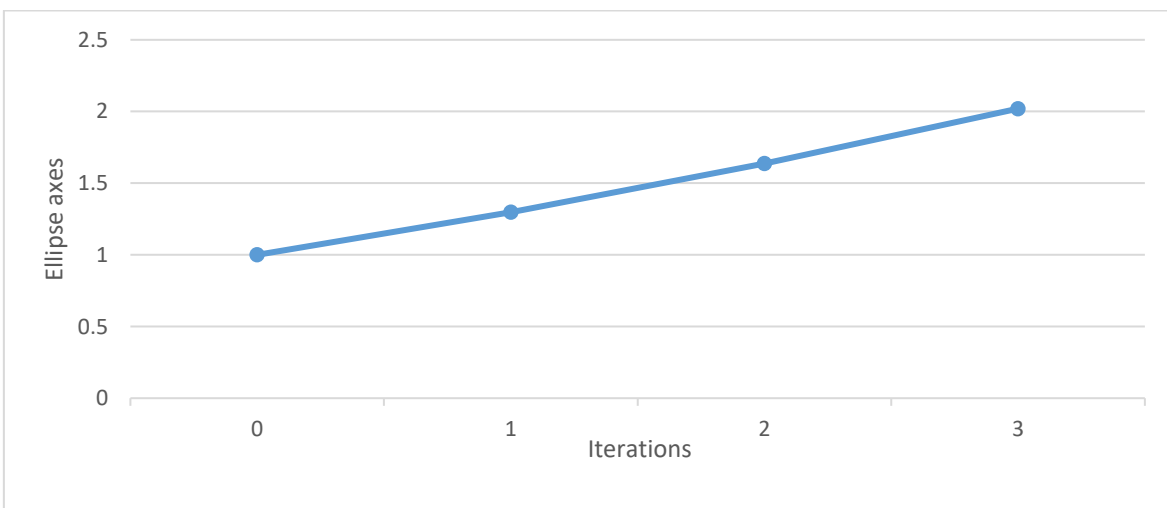
Figure 4.40: Optimization results of a plate with a hole ($D=30$ mm, $K=275$, $\sigma_{ref} = 40$ MPa)



(a) von Mises stresses for first and last iterations: Iteration 1 (left), Iteration 3 (right)

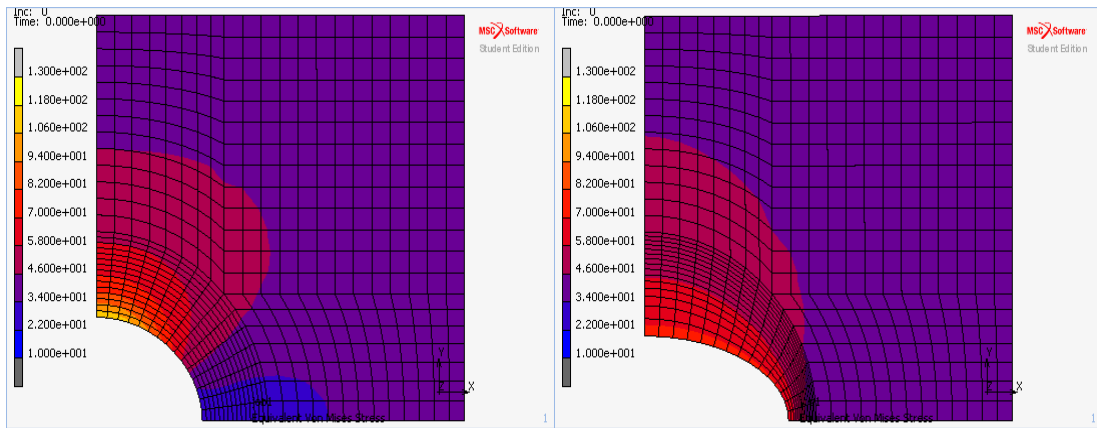


(b) Variation of von Mises stress distribution along the hole boundary

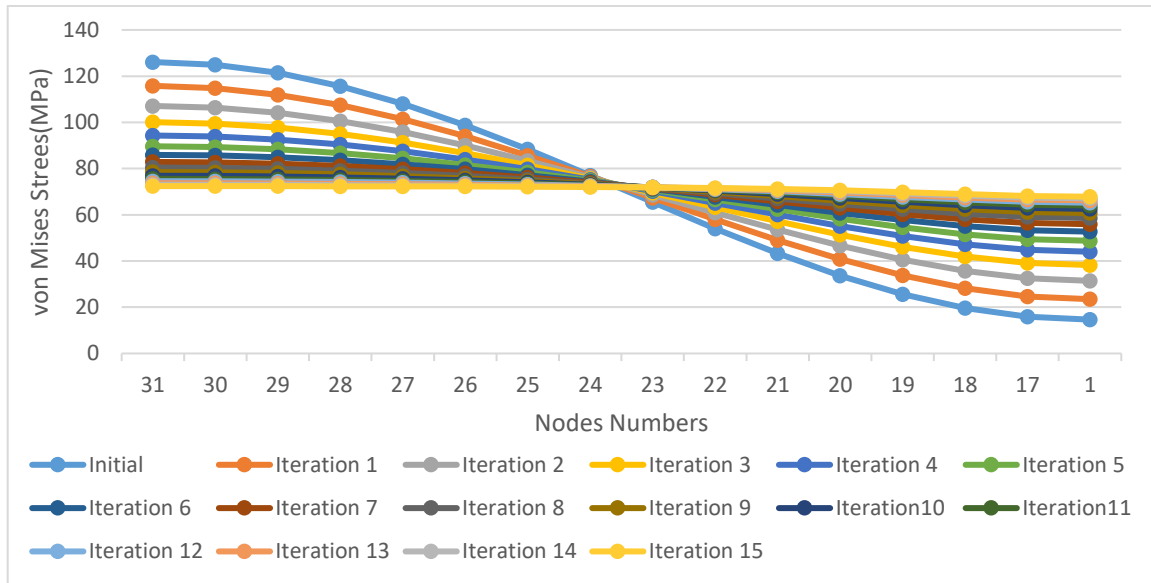


(c) Variation of ellipse axes ratio

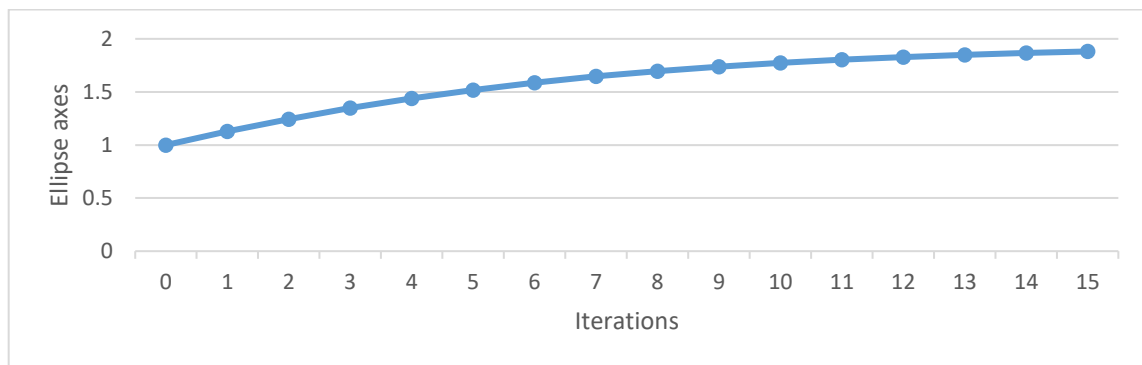
Figure 4.41: Optimization results of a plate with a hole ($D=30$ mm, $K=500$, $\sigma_{ref} = 40$ MPa)



(a) von Mises stresses for first and last iterations: Iteration 1 (left), Iteration 15 (right)

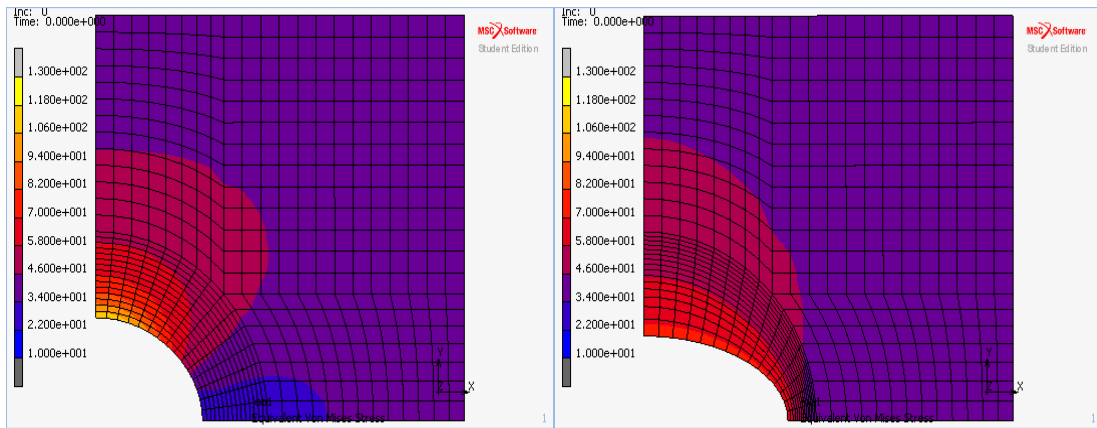


(b) Variation of von Mises stress distribution along the hole boundary

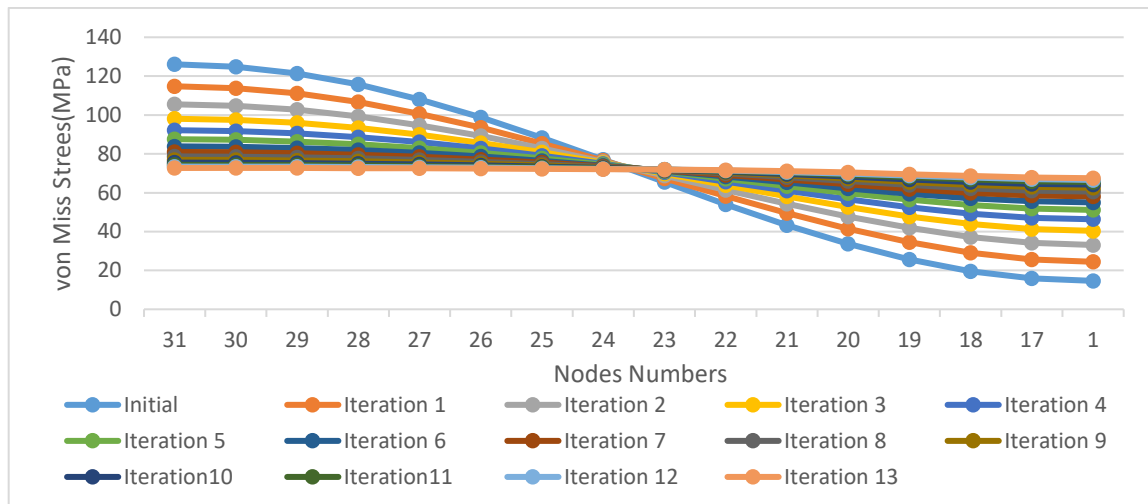


(c) Variation of ellipse axes ratio

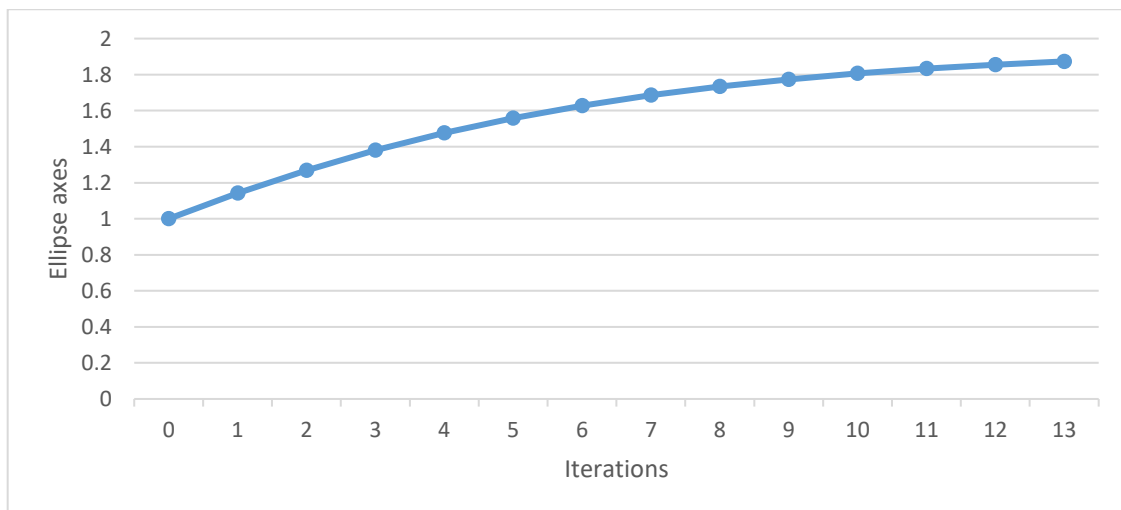
Figure 4.42: Optimization results of a plate with a hole ($D=30$ mm, $K=250$, $\sigma_{ref} = 60$ MPa)



(a) von Mises stresses for first and last iterations: Iteration 1 (left), Iteration 13 (right)

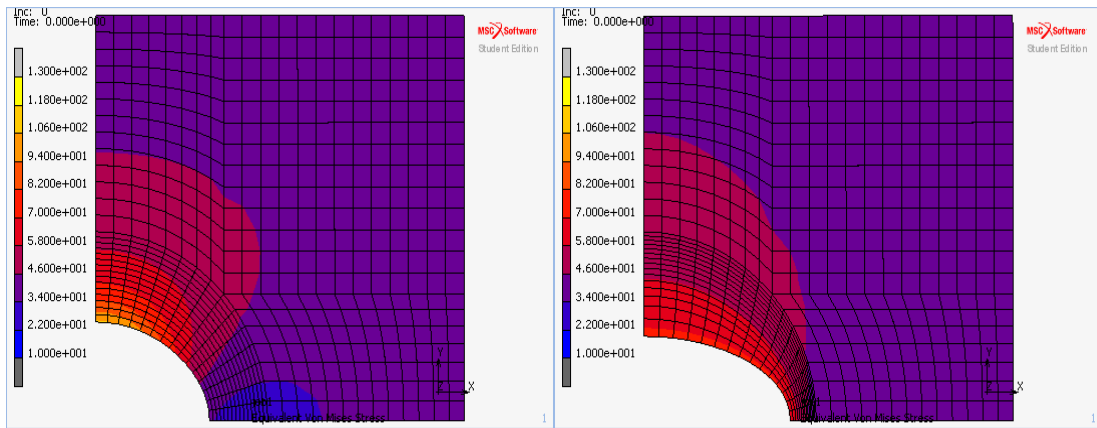


(b) Variation of von Mises stress distribution along the hole boundary

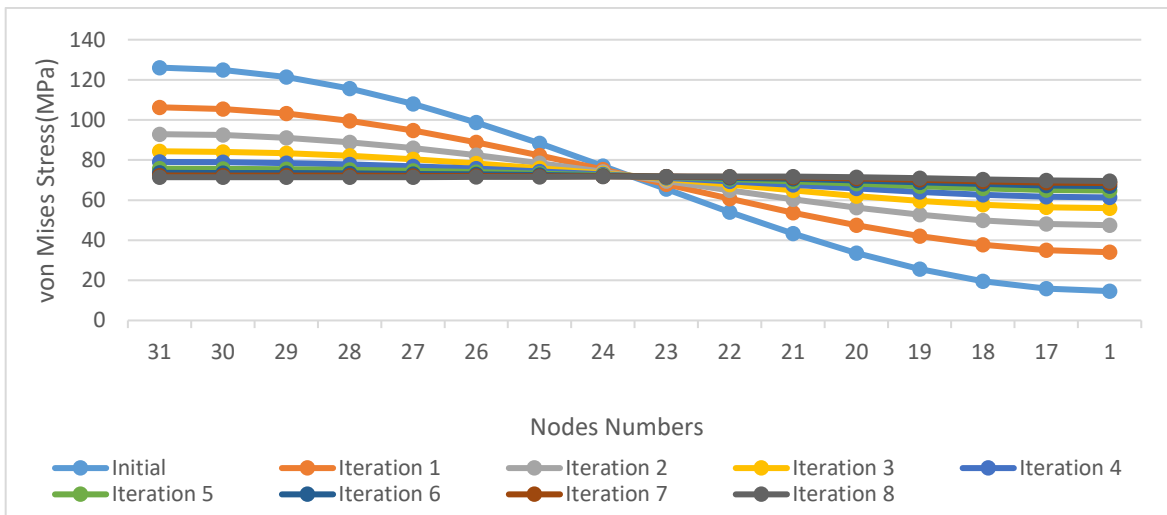


(c) Variation of ellipse axes ratio

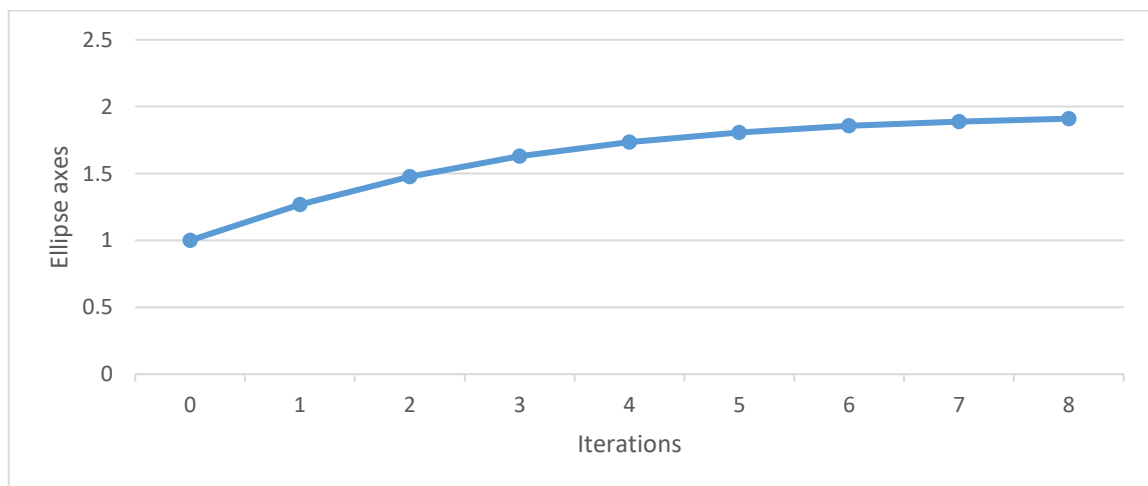
Figure 4.43: Optimization results of a plate with a hole ($D=30$ mm, $K=275$, $\sigma_{ref} = 60$ MPa)



(a) von Mises stresses for first and last iterations: Iteration 1 (left), Iteration 8 (right)

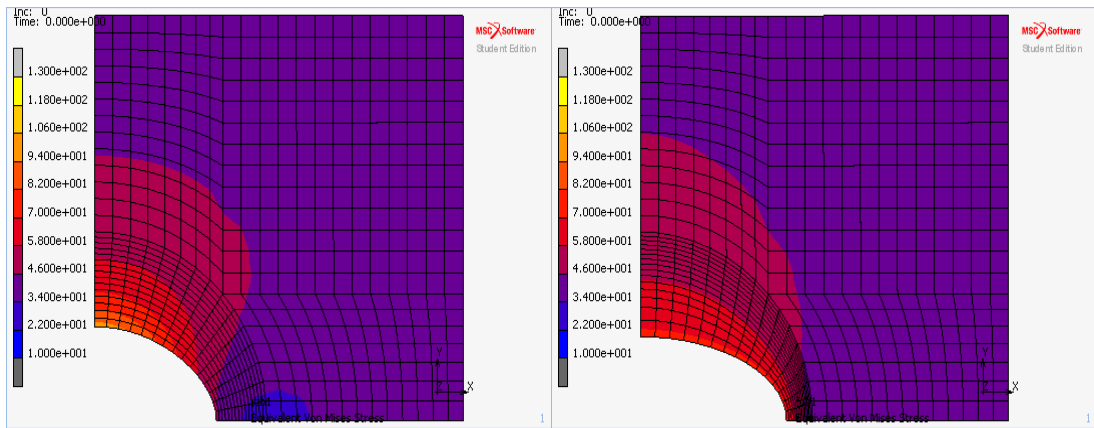


(b) Variation of von Mises stress distribution along the hole boundary

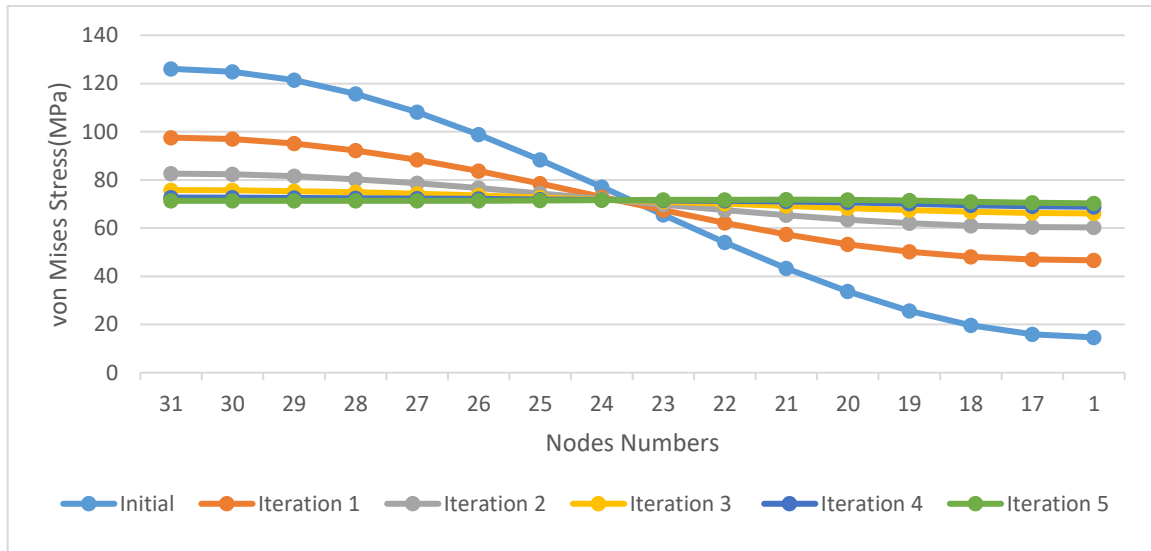


(c) Variation of ellipse axes ratio

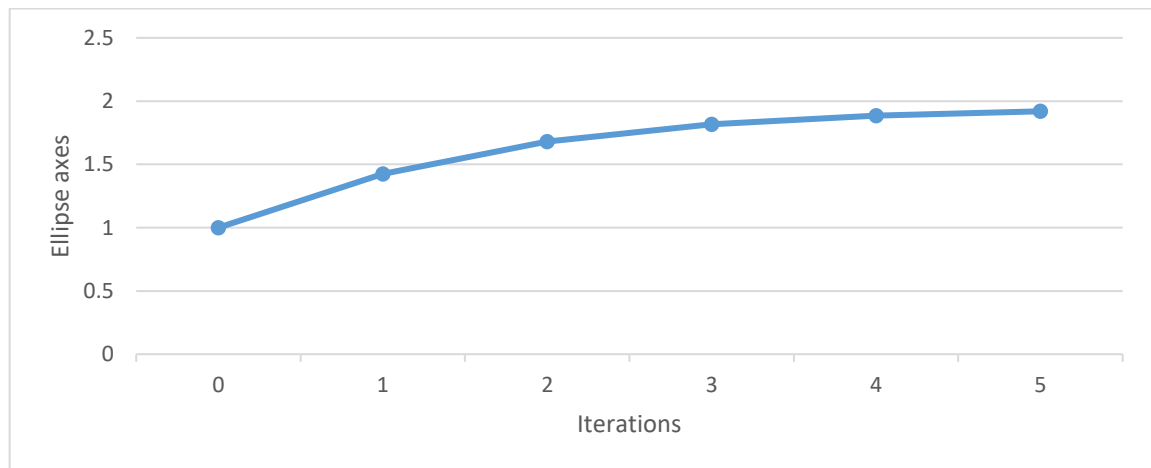
Figure 4.44: Optimization results of a plate with a hole ($D=30$ mm, $K=500$, $\sigma_{ref} = 60$ MPa)



(a) von Mises stresses for first and last iterations: Iteration 1 (left), Iteration 5 (right)

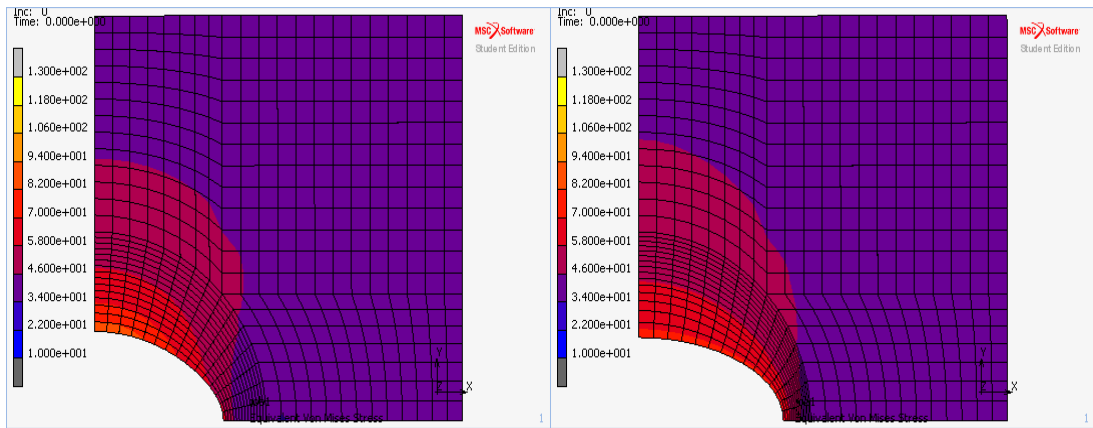


(b) Variation of von Mises stress distribution along the hole boundary

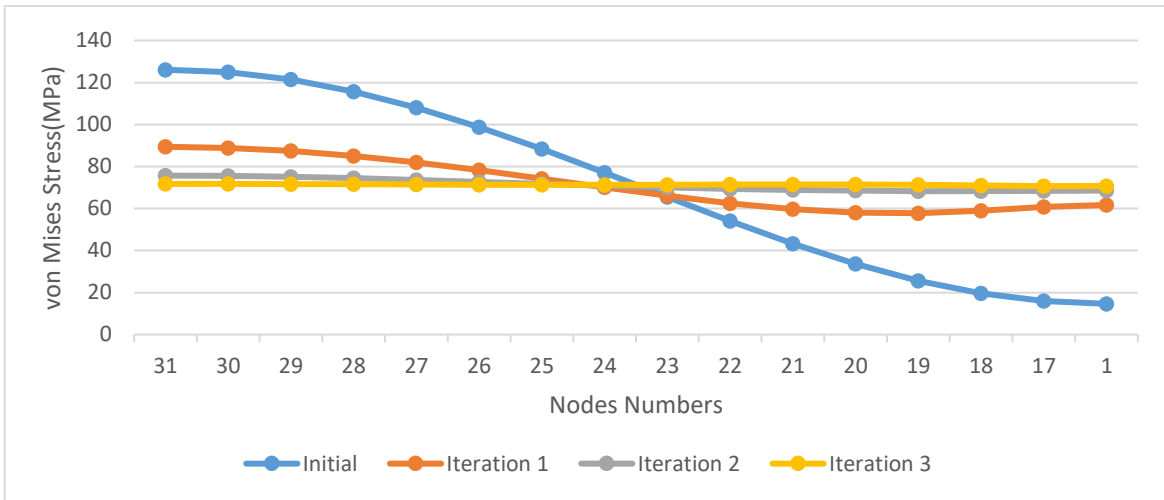


(c) Variation of ellipse axes ratio

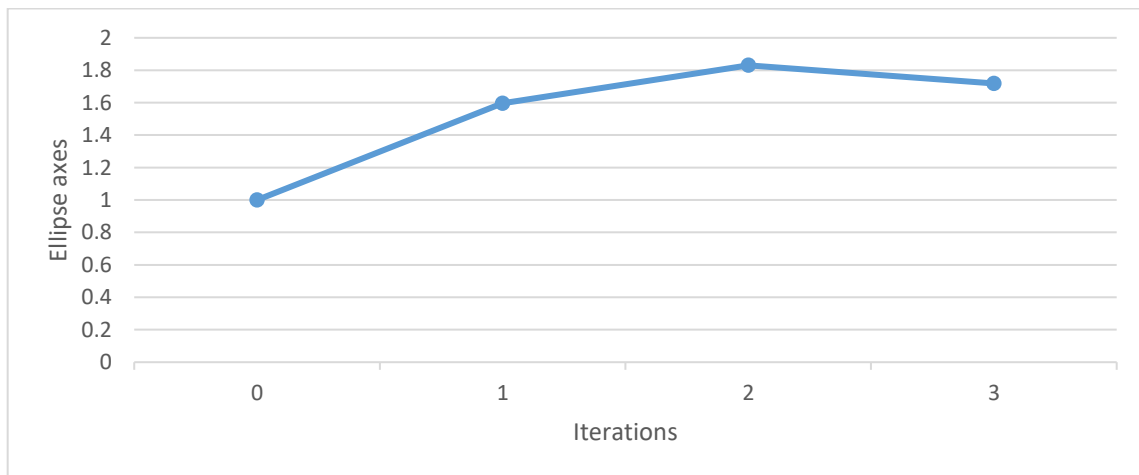
Figure 4.45: Optimization results of a plate with a hole ($D=30$ mm, $K=750$, $\sigma_{ref} = 60$ MPa)



(a) von Mises stresses for first and last iterations: Iteration 1 (left), Iteration 3 (right)



(b) Variation of von Mises stress distribution along the hole boundary



(c) Variation of ellipse axes ratio

Figure 4.46: Optimization results of a plate with a hole ($D=30$ mm, $K=1000$, $\sigma_{ref}=60$ MPa)

Table 4.4: Summary of results with domain thickness 30mm

		Magnification factor k				
		250	275	500	750	1000
σ_{ref}		250	275	500	750	1000
10	Iterations	3	3	2	--	--
	Max stress	81.53	77.33	86.93	--	--
	Ellipse axes ratio	1.64	1.77	2.17	--	--
40	Iterations	6	5	3	--	--
	Max stress	73.41	74.2	79.3	--	--
	Ellipse axes ratio	1.94	1.86	2.01	--	--
60	Iterations	15	13	8	5	3
	Max stress	72.42	72.75	71.78	71.88	70.71
	Ellipse axes ratio	1.64	1.77	1.91	1.91	1.80

4.4 Optimization of a Plate with a Hole with Domain Thickness 40 mm

The finite element models and the boundary conditions for stress and thermal analysis are shown in Figure 4.47 for domain thickness 40 mm. The von Mises stresses of stress analysis and total deflections of the thermal expansion analysis of the original shape can be seen in Figure 4.48. Similar to the analysis conducted for domain thickness 10 mm, the stress far away from the concentration zones is about 40 MPa. The maximum and minimum von Mises stresses were also around 130 MPa and 10 MPa respectively.

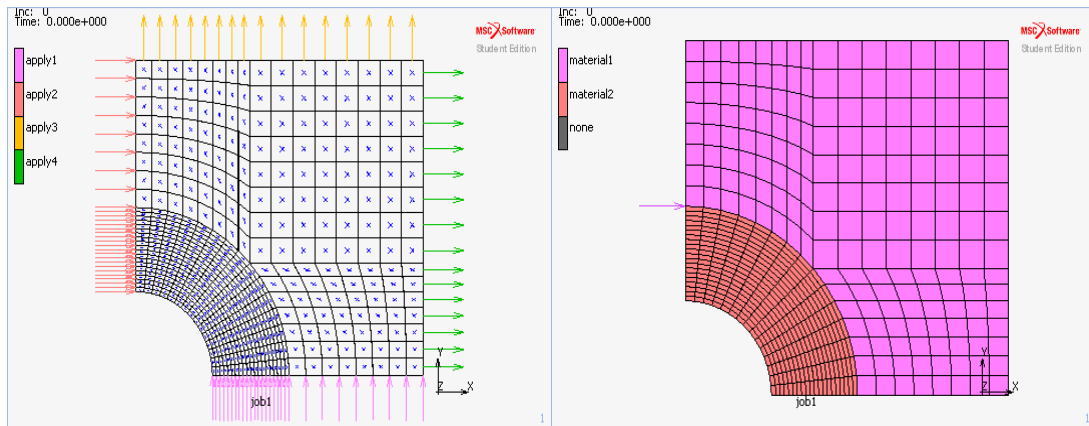


Figure 4.47: Finite element model for stress (left) and thermal (right) analysis (D=40mm)

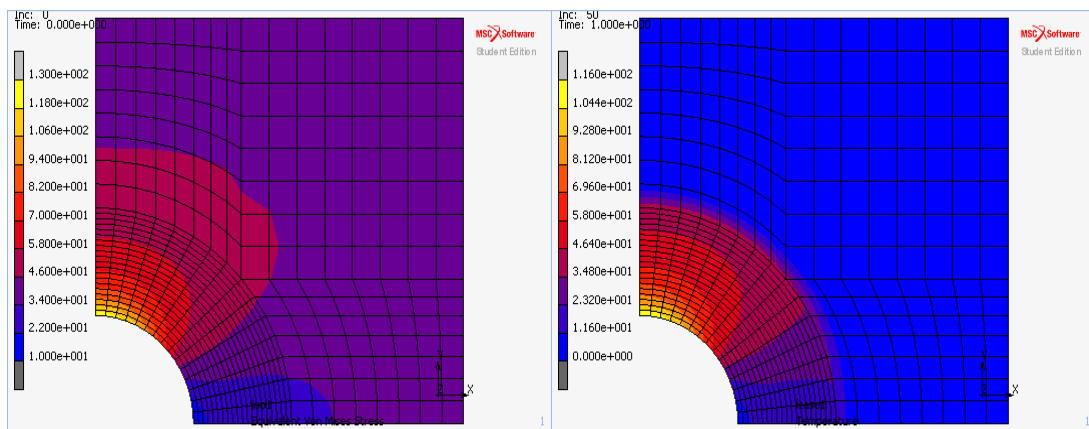
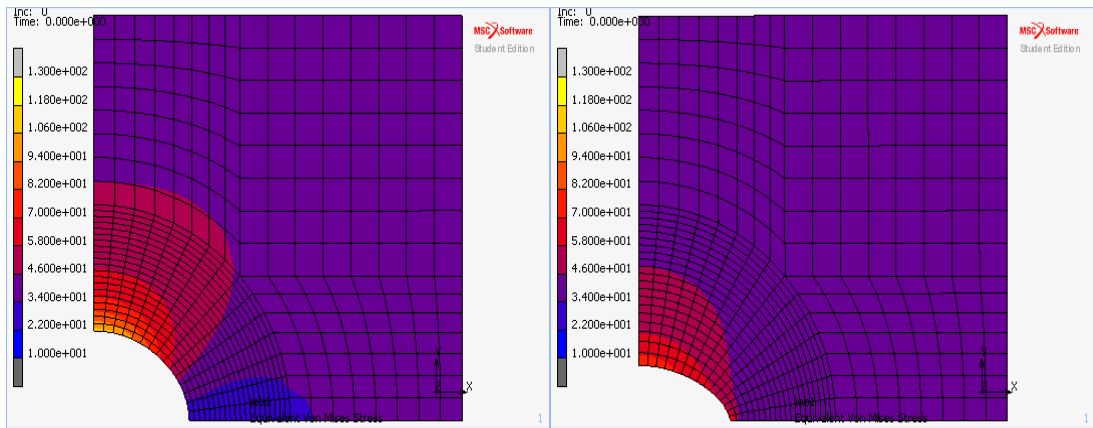
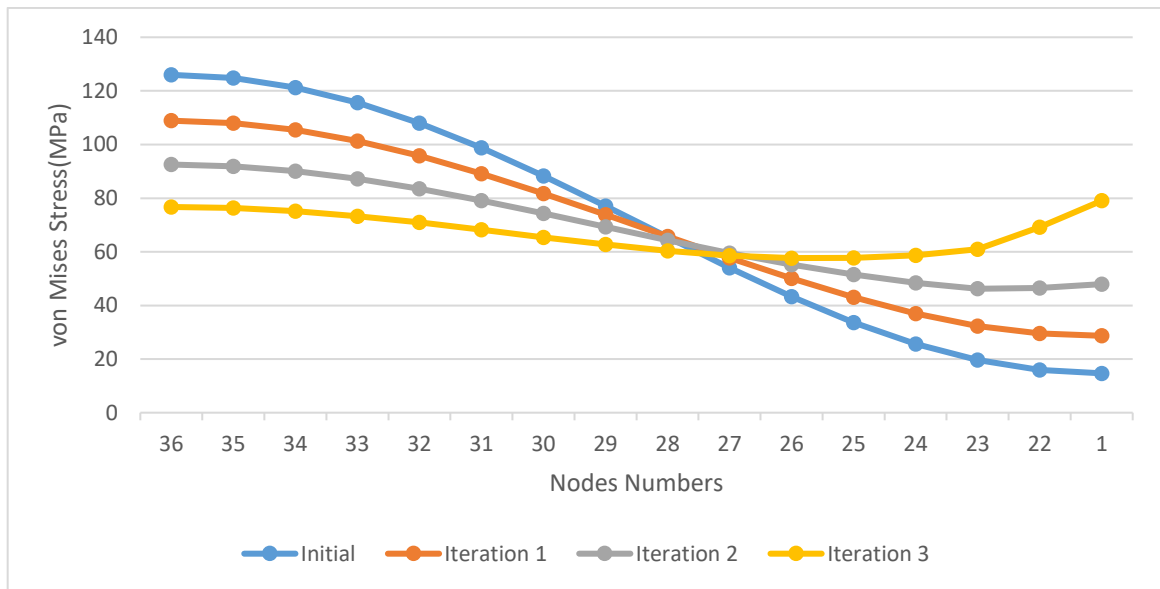


Figure 4.48: von Mises stresses (left) and thermal deformations (right) of the original shape (D =40mm)

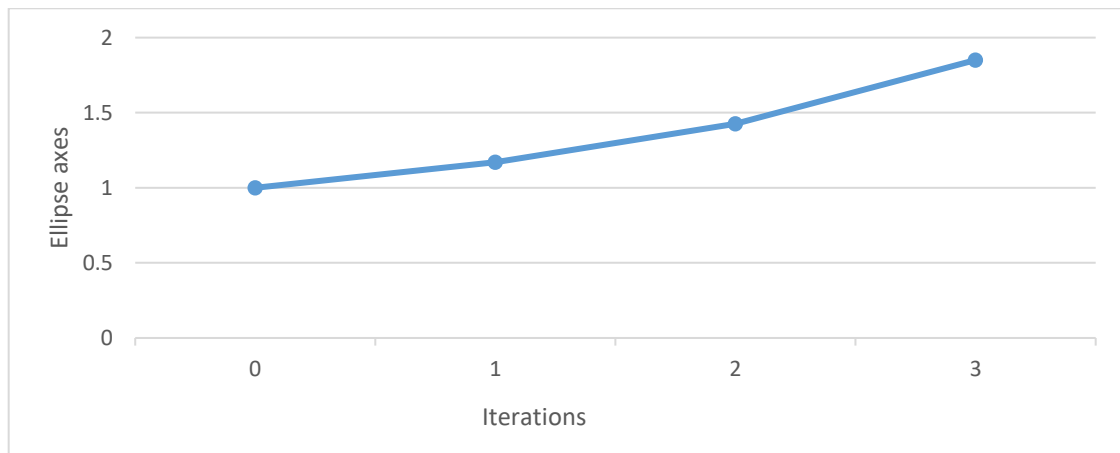
For domain thickness $D = 40$ mm, nine optimization analyses were conducted including the combinations of reference stresses $\sigma_{ref} = 10, 40$ and 60 MPa and magnification factor $k = 100, 200, 250, 275$ and 500 . The results obtained are given in Figures 4.49 to 4.57. The results, summarized in Table 4.5, showed that $\sigma_{ref} = 40$ MPa with magnification factors around 200 and 250 were trustable for further investigations. In the following section the method was extended to optimization of the geometry modeled by automatic mesh generation.



(a) von Mises stresses for first and last iterations: Iteration 1 (left), Iteration 3 (right)

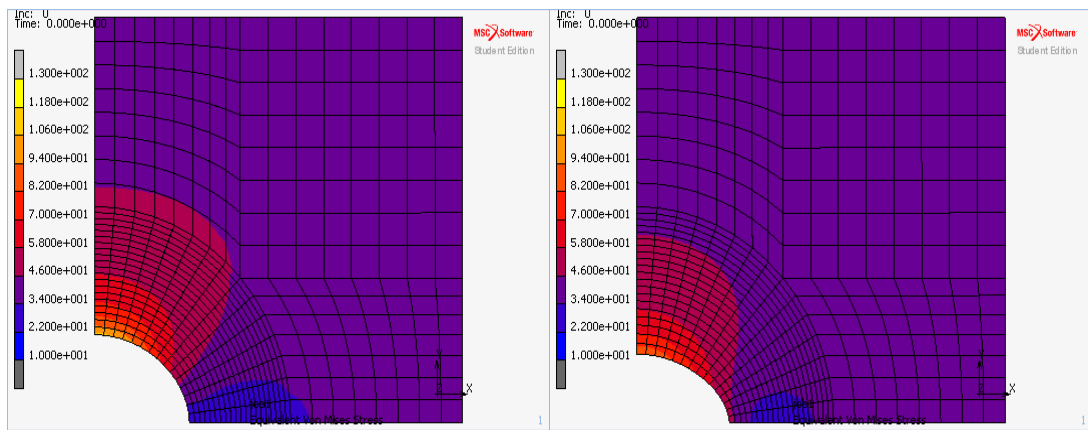


(b) Variation of von Mises stress distribution along the hole boundary

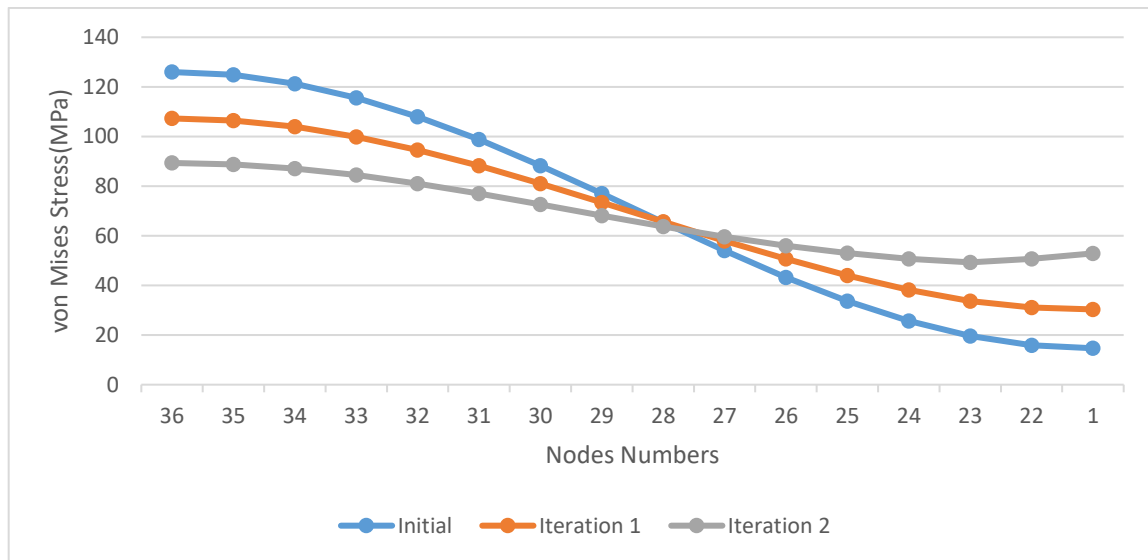


(c) Variation of ellipse axes ratio

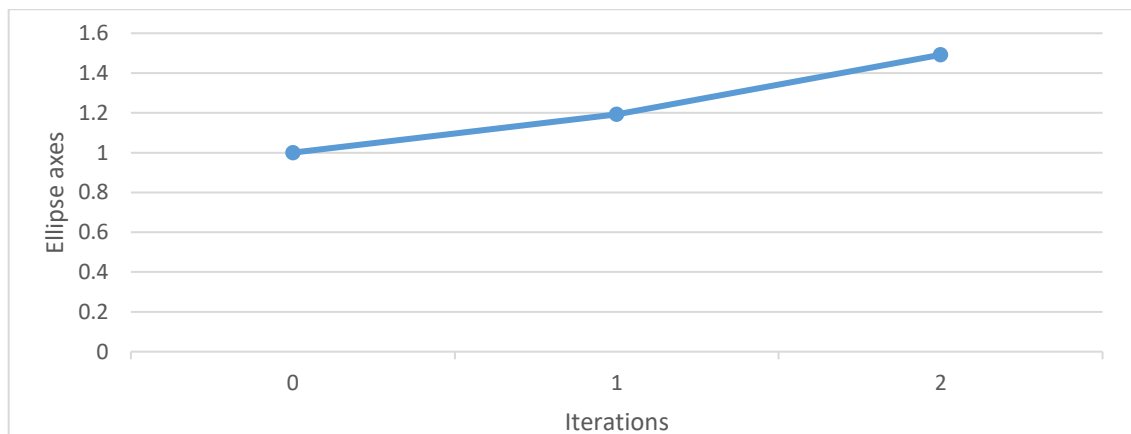
Figure 4.49: Optimization results of a plate with a hole ($D=40$ mm, $K=250$, $\sigma_{ref}=10$ MPa)



(a) von Mises stresses for first and last iterations: Iteration 1 (left), Iteration 2 (right)

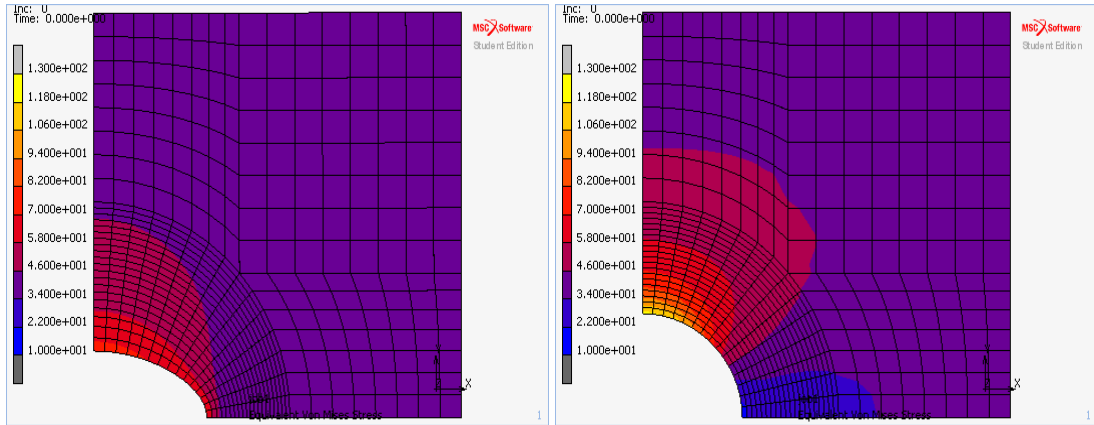


(b) Variation of von Mises stress distribution along the hole boundary

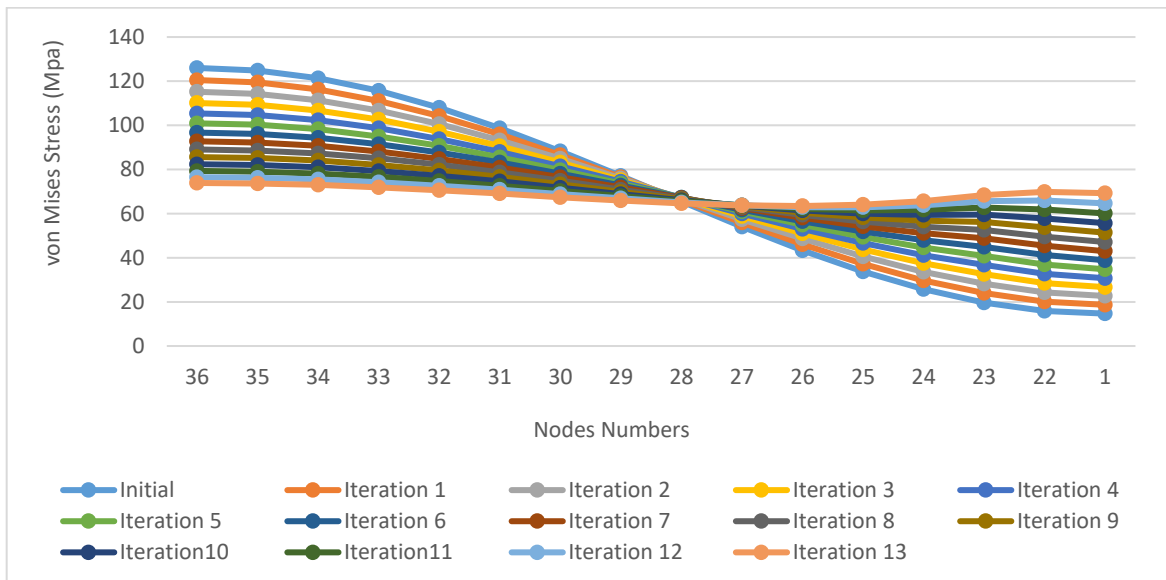


(c) Variation of ellipse axes ratio

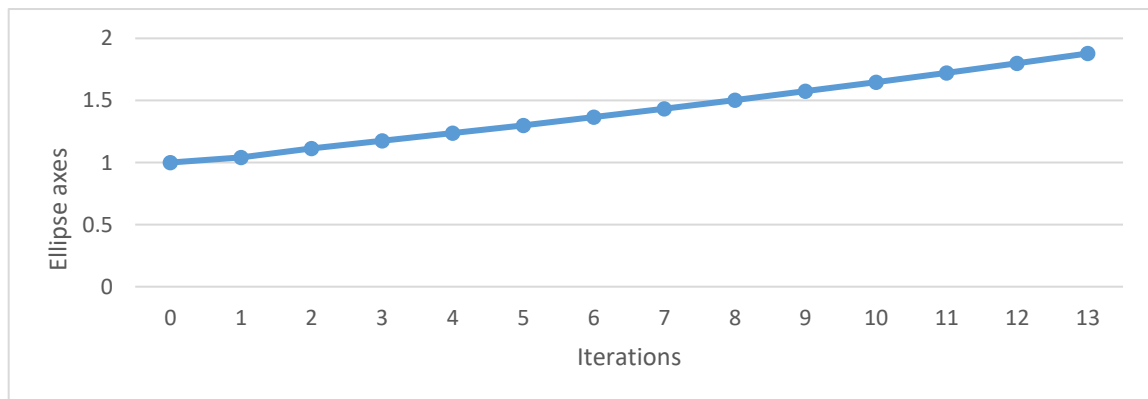
Figure 4.50: Optimization results of a plate with a hole ($D=40$ mm, $K=275$, $\sigma_{ref}=10$ MPa)



(a) von Mises stresses for first and last iterations: Iteration 1 (left), Iteration 13 (right)

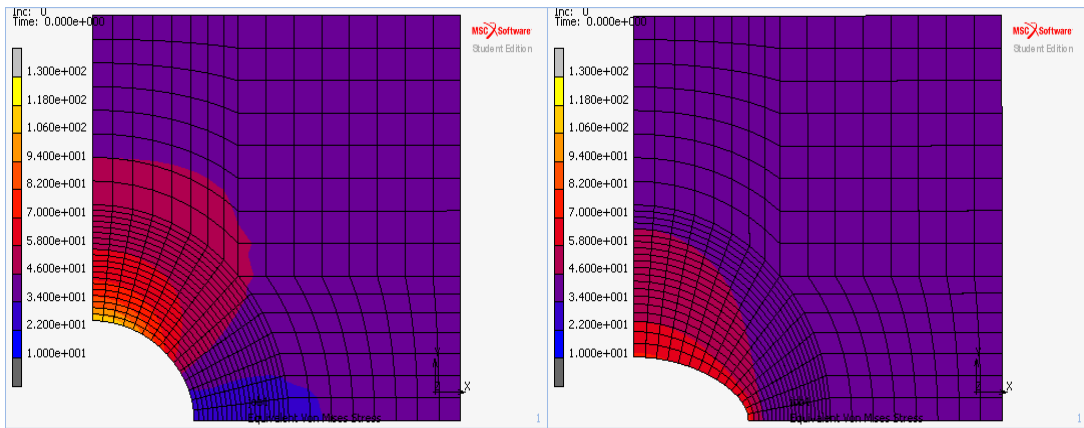


(b) Variation of von Mises stress distribution along the hole boundary

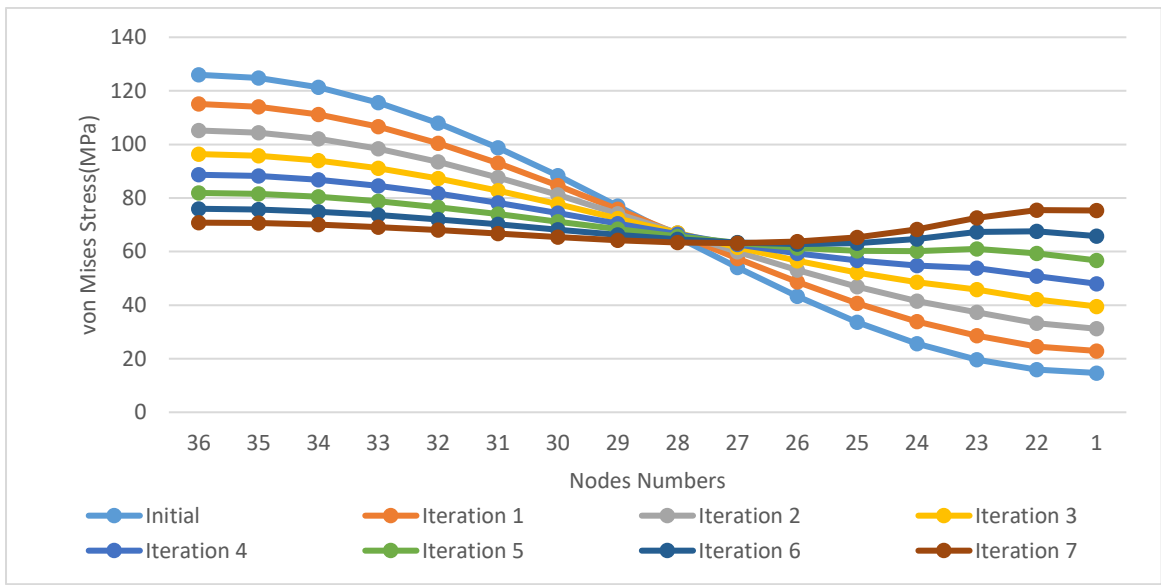


(c) Variation of ellipse axes ratio

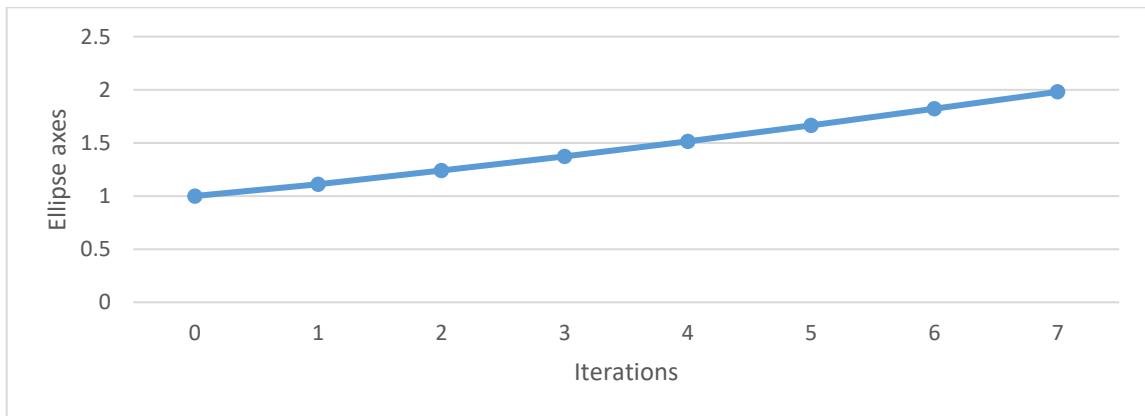
Figure 4.51: Optimization results of a plate with a hole ($D=40$ mm, $K=100$, $\sigma_{ref} = 40$ MPa)



(a) von Mises stresses for first and last iterations: Iteration 1 (left), Iteration 7 (right)

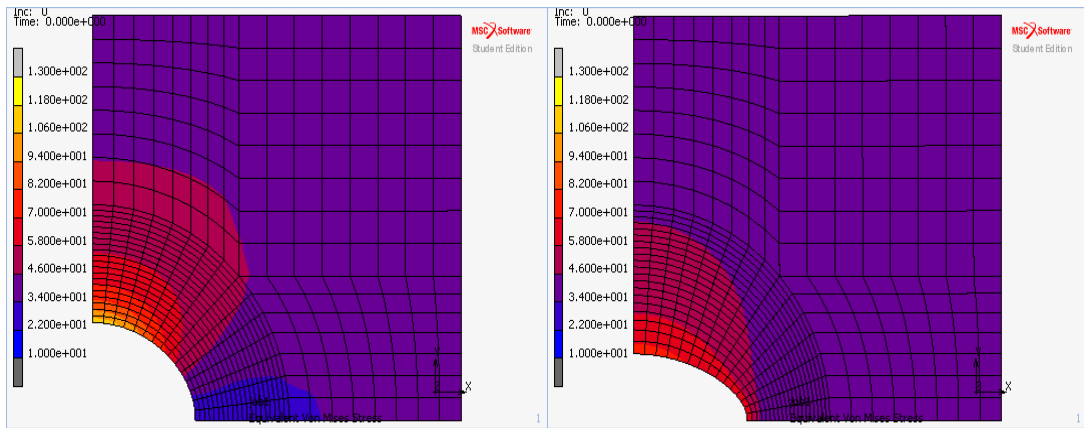


(b) Variation of von Mises stress distribution along the hole boundary

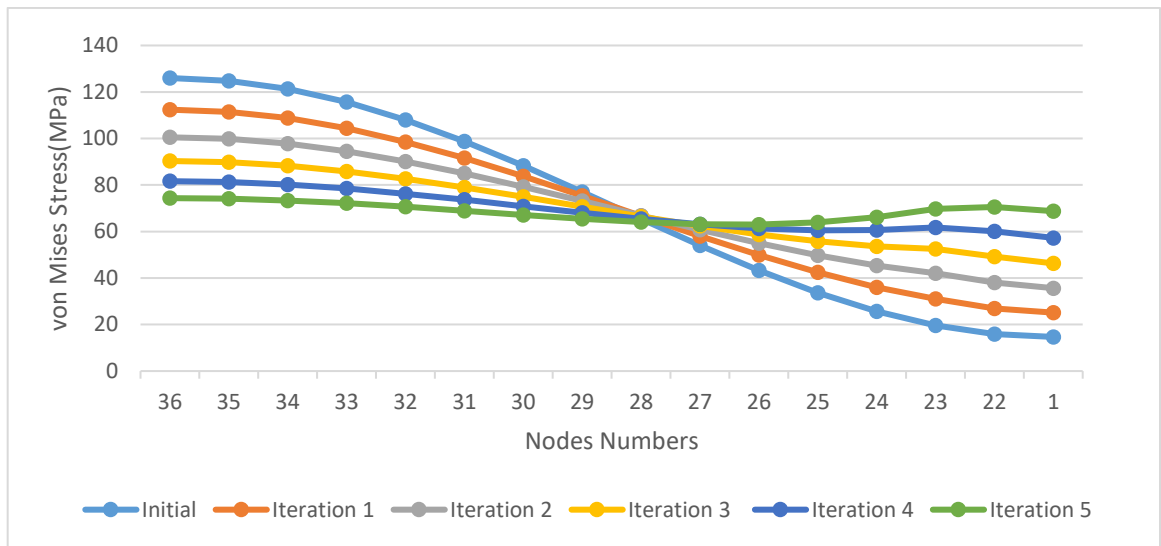


(c) Variation of ellipse axes ratio

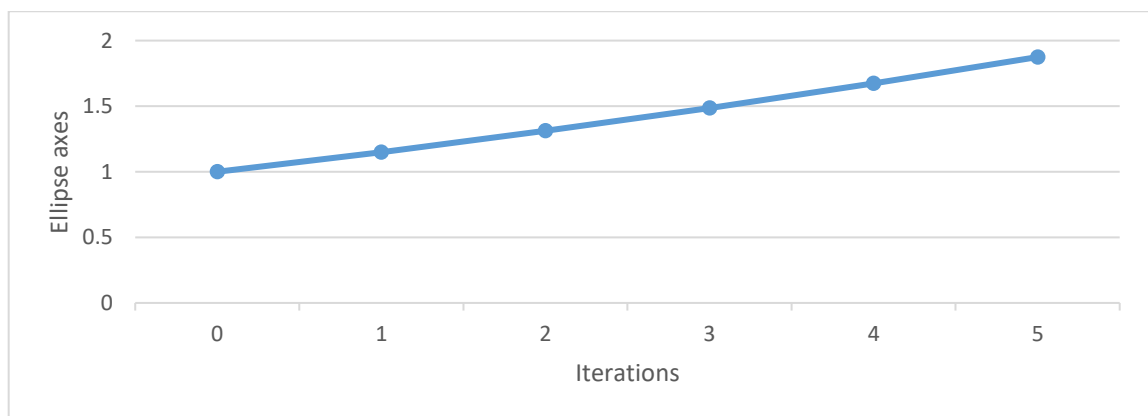
Figure 4.52: Optimization results of a plate with a hole ($D=40$ mm, $K=200$, $\sigma_{ref} = 40$ MPa)



(a) von Mises stresses for first and last iterations: Iteration 1 (left), Iteration 5 (right)

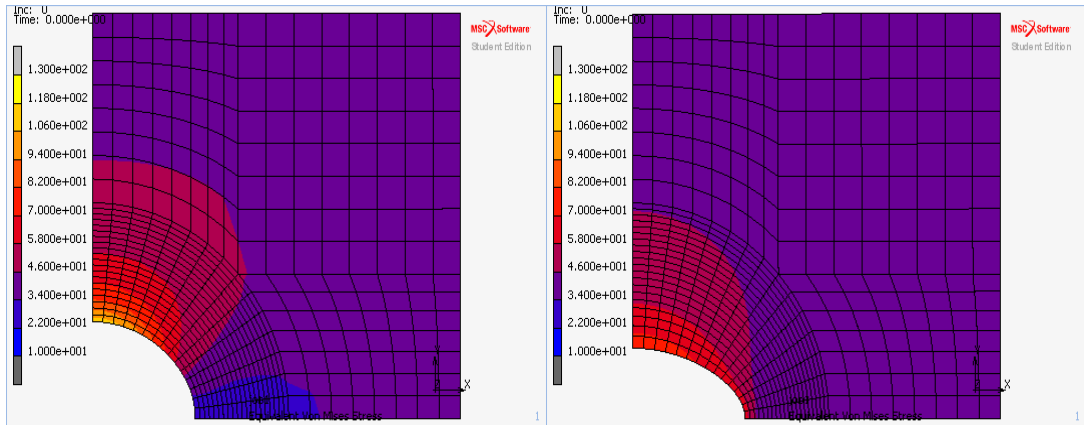


(b) Variation of von Mises stress distribution along the hole boundary

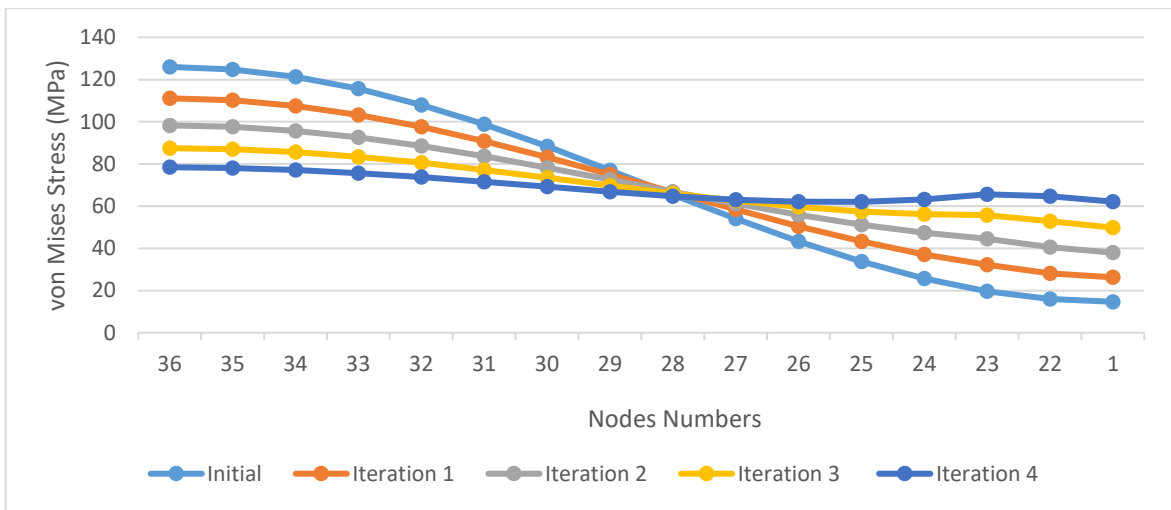


(c) Variation of ellipse axes ratio

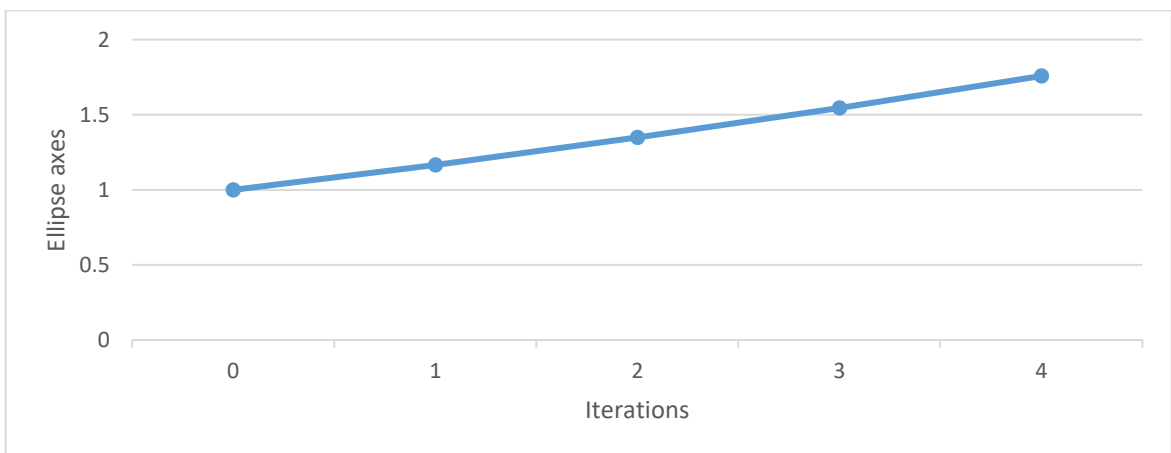
Figure 4.53: Optimization results of a plate with a hole ($D=40$ mm, $K=250$, $\sigma_{ref} = 40$ MPa)



(a) von Mises stresses for first and last iterations: Iteration 1 (left), Iteration 4 (right)

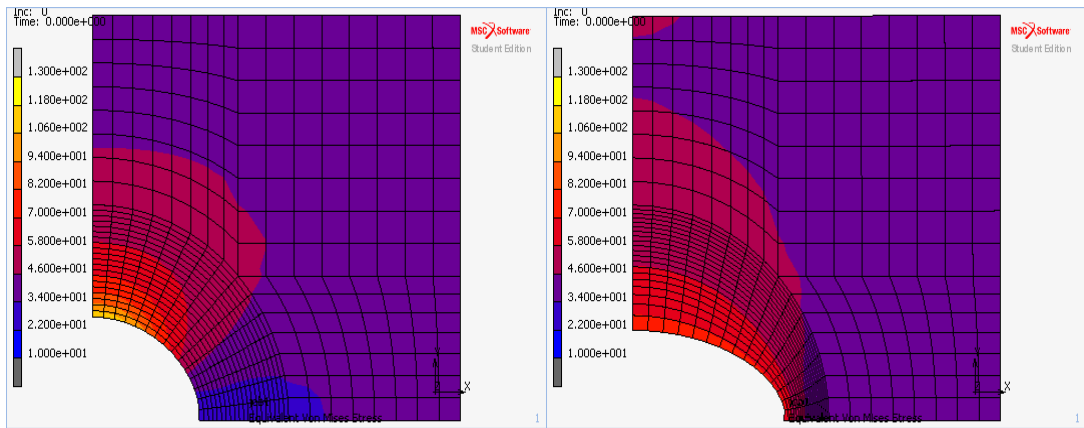


(b) Variation of von Mises stress distribution along the hole boundary

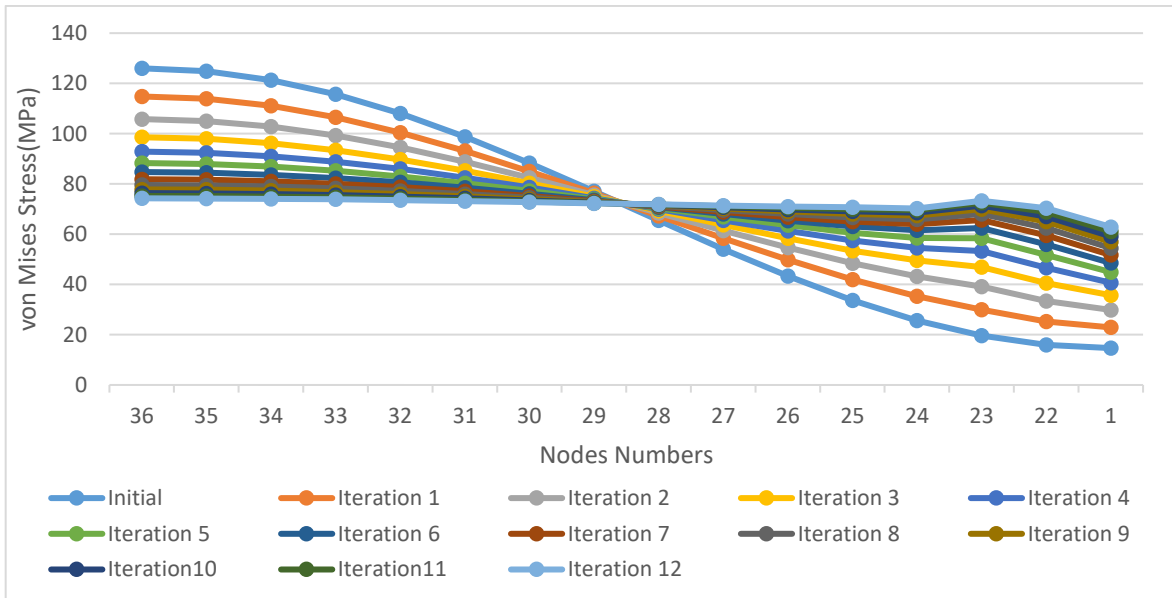


(c) Variation of ellipse axes ratio

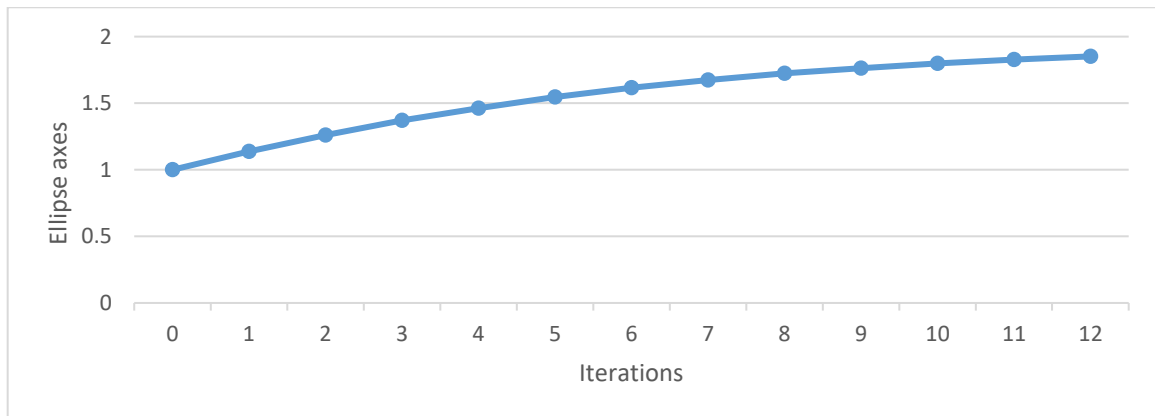
Figure 4.54: Optimization results of a plate with a hole ($D=40$ mm, $K=275$, $\sigma_{ref} = 40$ MPa)



(a) von Mises stresses for first and last iterations: Iteration 1 (left), Iteration 12 (right)

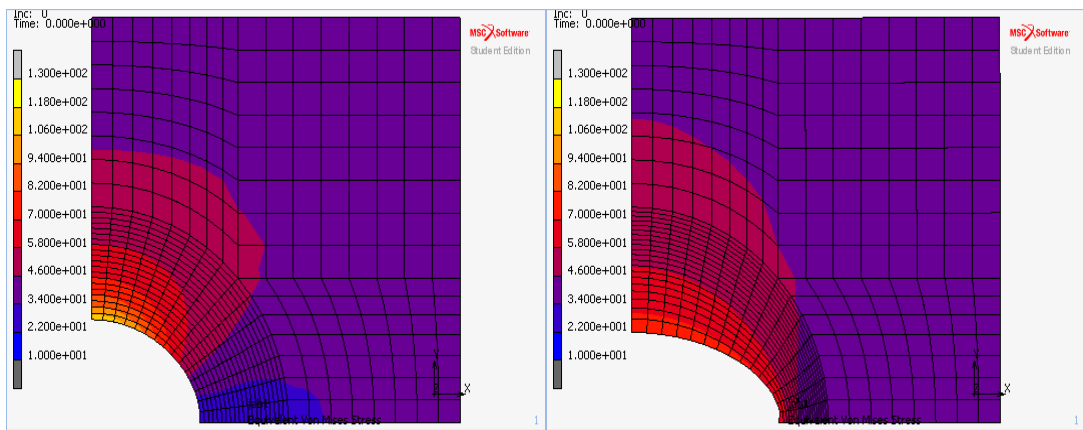


(b) Variation of von Mises stress distribution along the hole boundary

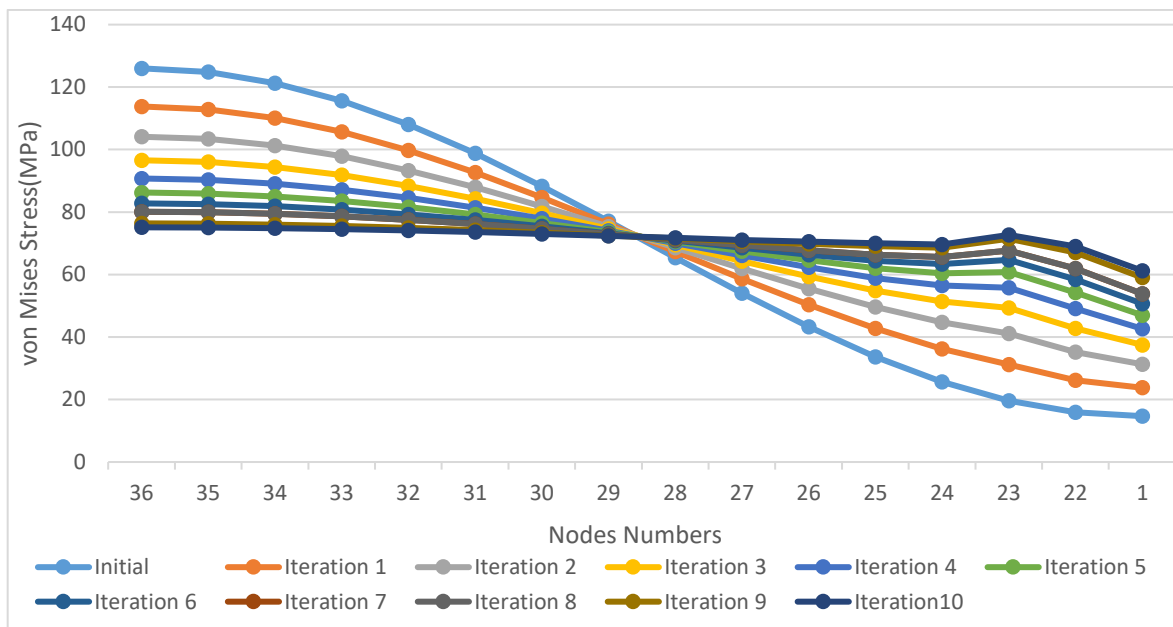


(c) Variation of ellipse axes ratio

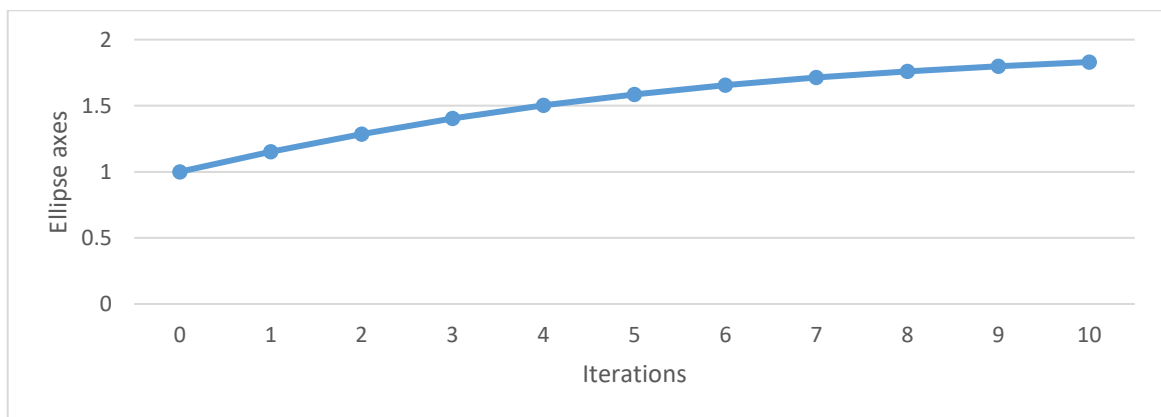
Figure 4.55: Optimization results of a plate with a hole ($D=40$ mm, $K=250$, $\sigma_{ref} = 60$ MPa)



(a) von Mises stresses for first and last iterations: Iteration 1 (left), Iteration 10 (right)

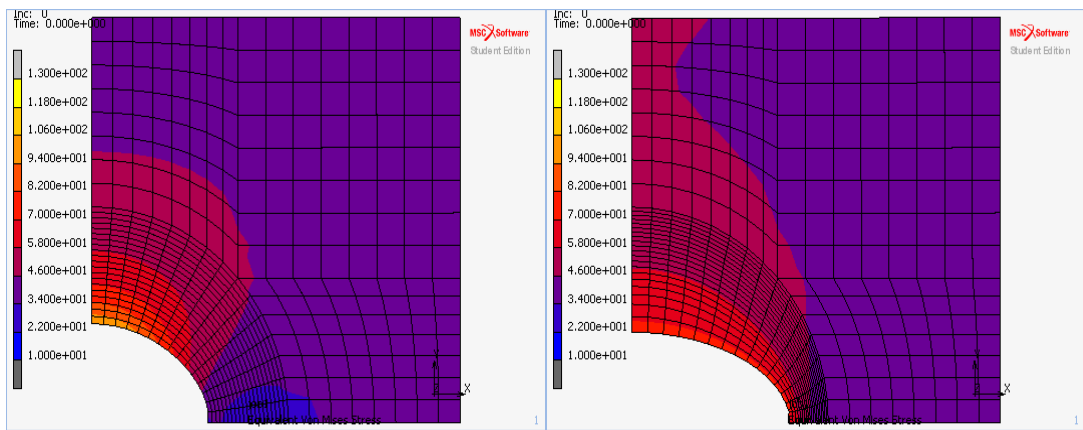


(b) Variation of von Mises stress distribution along the hole boundary

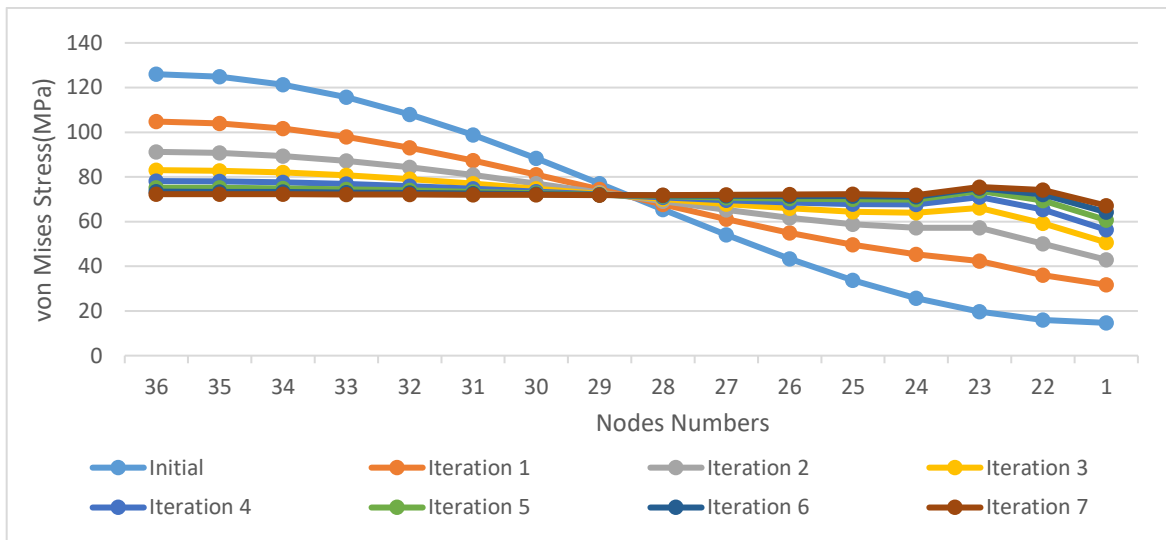


(c) Variation of ellipse axes ratio

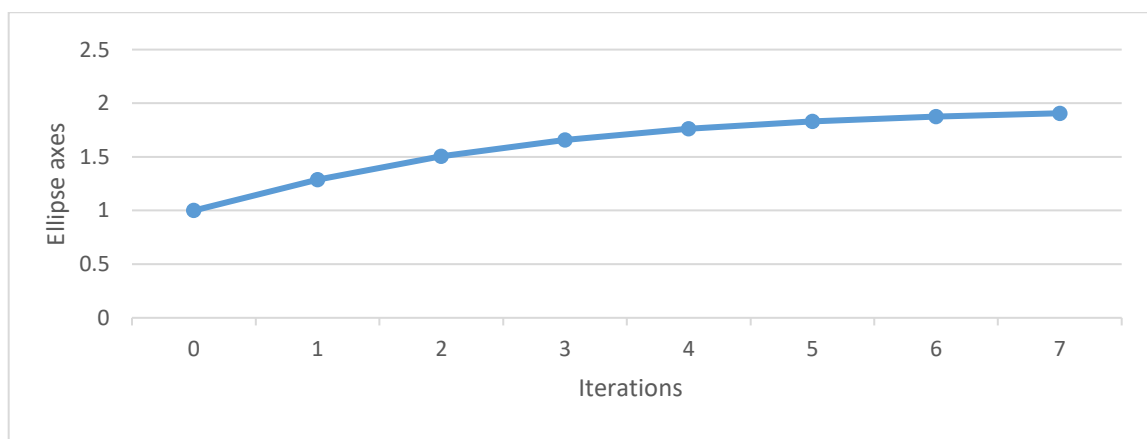
Figure 4.56: Optimization results of a plate with a hole ($D=40$ mm, $K=275$, $\sigma_{ref} = 60$ MPa)



(a) von Mises stresses for first and last iterations: Iteration 1 (left), Iteration 7 (right)



(b) Variation of von Mises stress distribution along the hole boundary



(c) Variation of ellipse axes ratio

Figure 4.57: Optimization results of a plate with a hole ($D=40$ mm, $K=500$, $\sigma_{ref} = 60$ MPa)

Table 4.5: Summary of results with domain thickness 40mm

		Magnification factor k				
σ_{ref}		100	200	250	275	500
10	Iterations	--	--	3	2	--
	Max stress	--	--	79.05	89.36	--
	Ellipse axes ratio	--	--	1.85	1.49	--
40	Iterations	13	7	5	4	--
	Max stress	73.88	75.48	74.35	76.03	--
	Ellipse axes ratio	1.87	1.98	1.87	1.75	--
60	Iterations	--	--	12	10	7
	Max stress	--	--	74.89	75.11	80.09
	Ellipse axes ratio	--	--	1.85	1.87	1.90

4.4 Optimization of a Plate with a Hole with Auto-Mesh

The finite element models and the boundary conditions for stress and optimization domain in the thermal analysis are shown in Figure 4.58. The area indicated by material2 was considered as the optimization domain and a reduced Young's modulus was assigned as given in Table 4.1. Optimization domain was defined as the area effected by the dislocations in the continuum, i.e. the area effected in the plane by the hole, and determined from the results of initial stress analysis of the geometry as shown in Figure 4.59. The stress far away from the hole was about 40 MPa and therefore $\sigma_{ref} = 40 \text{ MPa}$ was selected.

The results obtained for magnification factor $k = 200, 250$, given in Figures 4.60 to 4.61 and summarized in Table 4.6, were very close to the analyses conducted before in the present study and also by Tekkaya (1996).

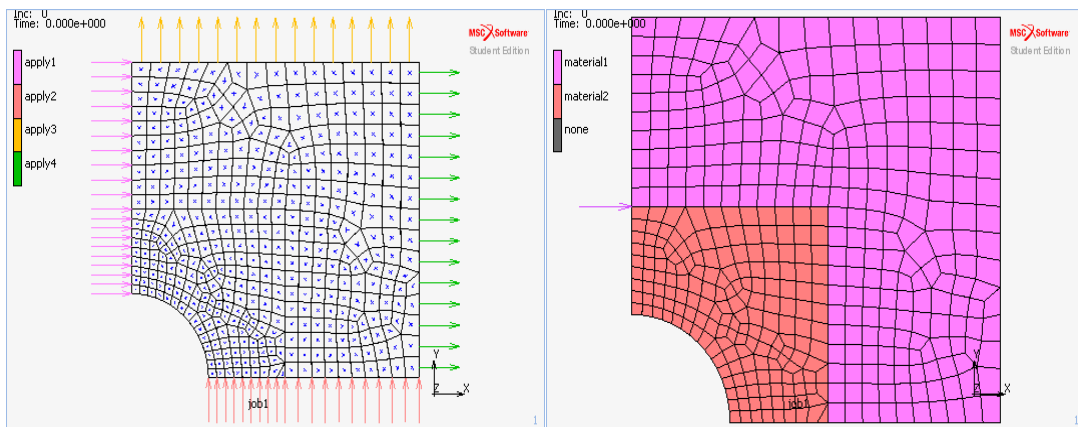


Figure 4.58: Finite element model for stress (left) and thermal (right) analyses (Auto-mesh)

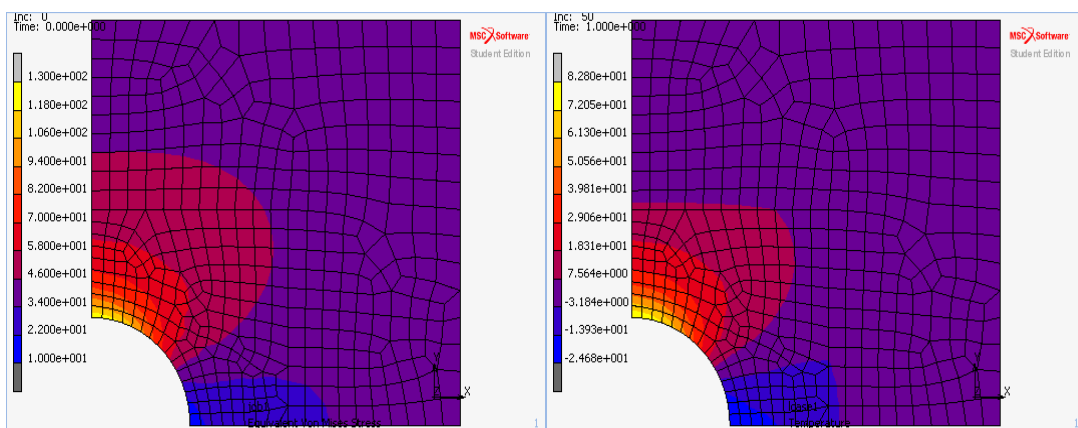
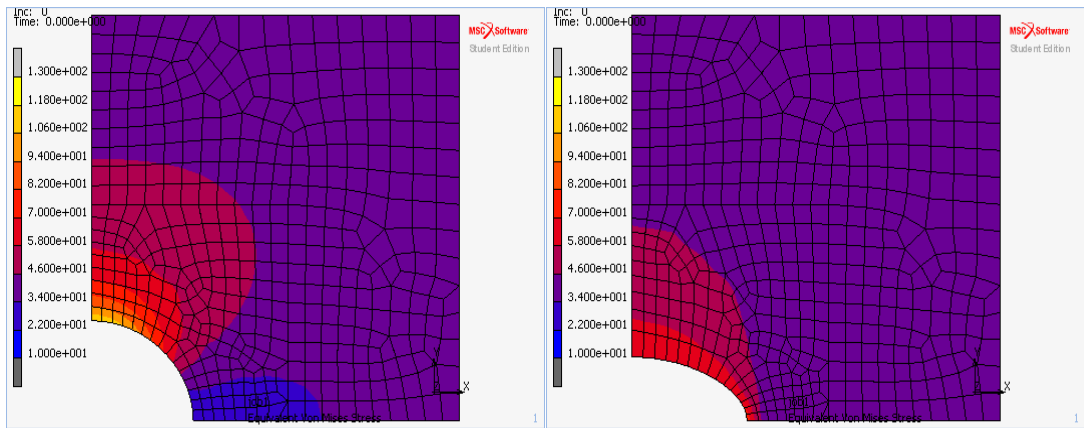
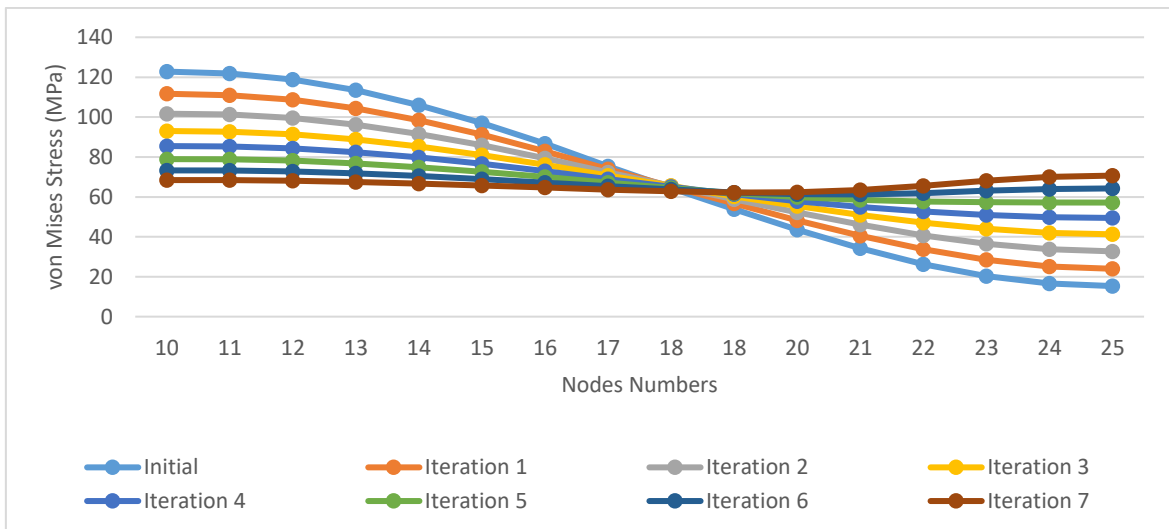


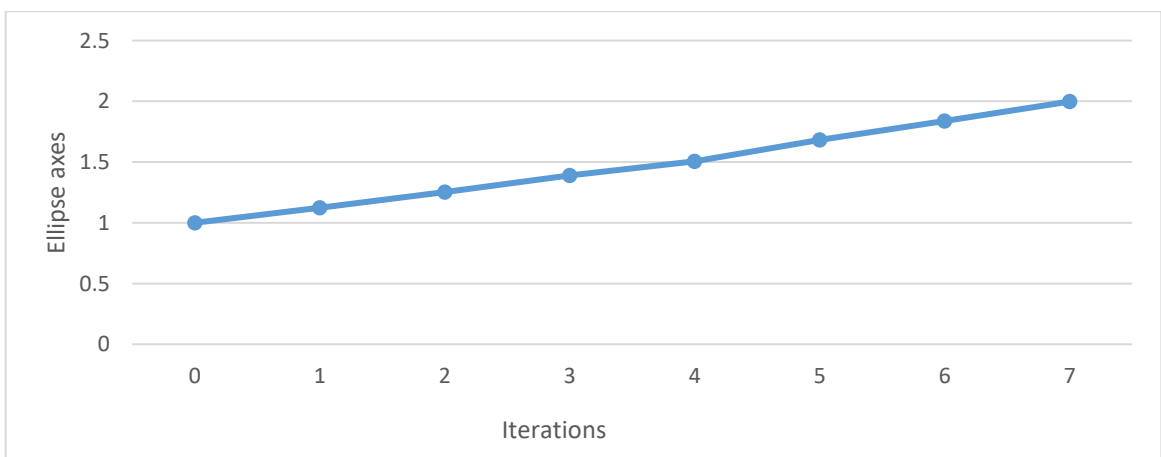
Figure 4.59: von Mises stresses (left) and thermal deformations (right) of the original shape (Auto-mesh)



(a) von Mises stresses for first and last iterations: Iteration 1 (left), Iteration 7 (right)

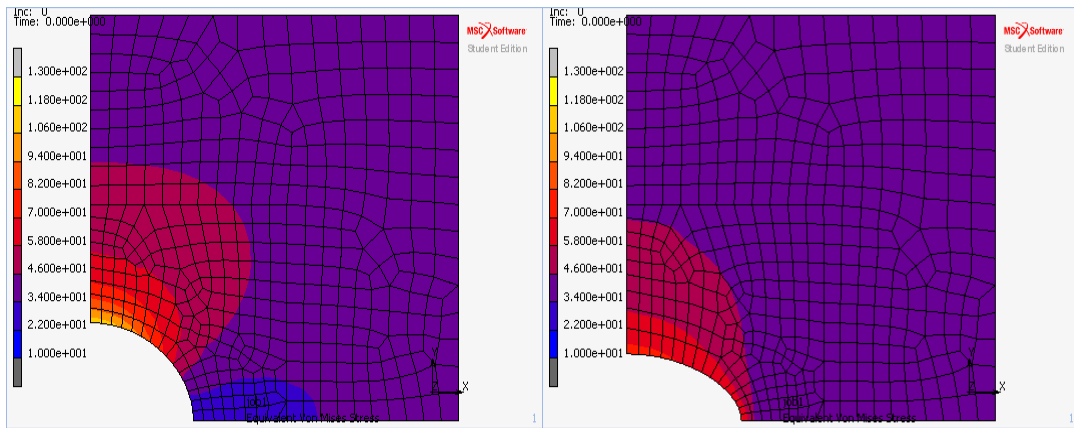


(b) Variation of von Mises stress distribution along the hole boundary

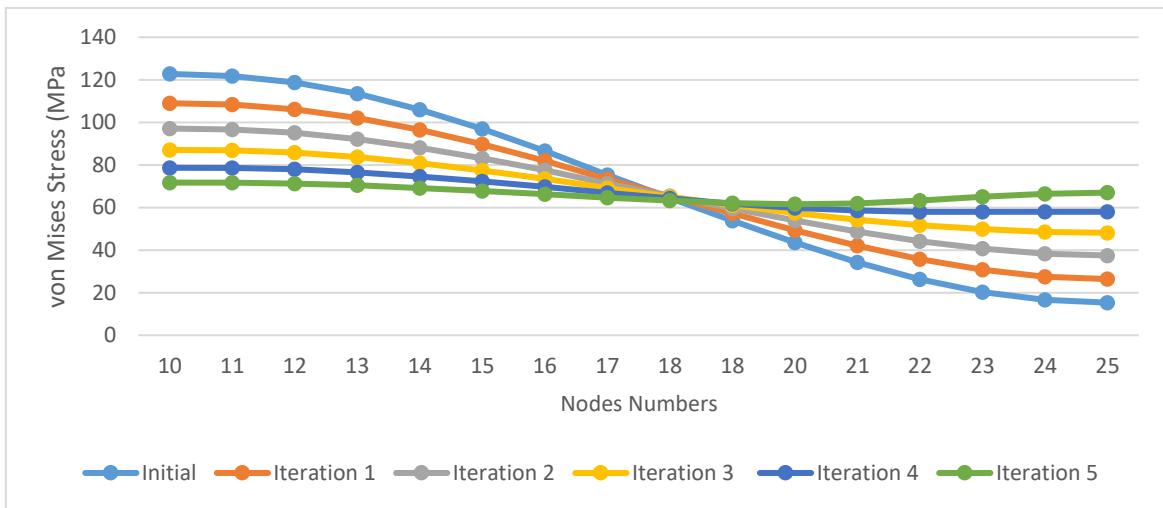


(c) Variation of ellipse axes ratio

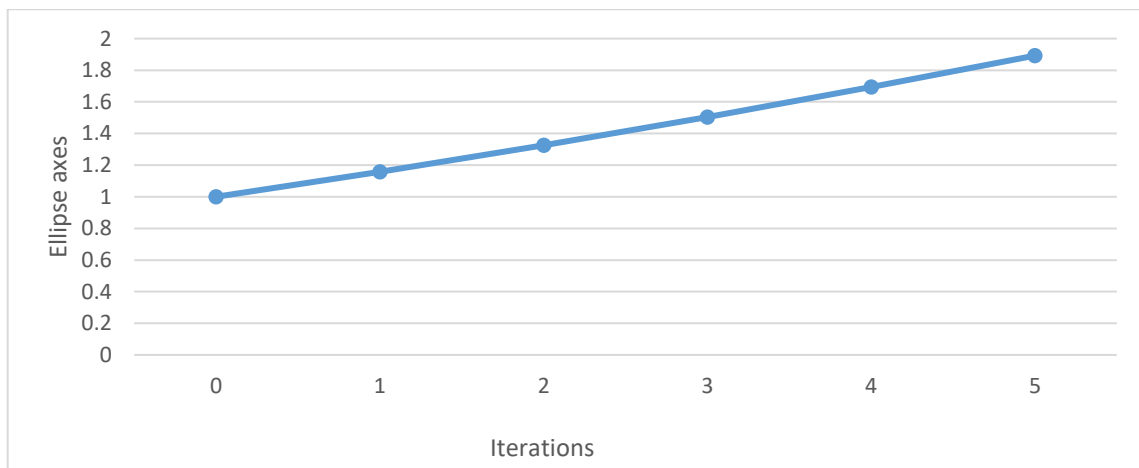
Figure 4.60: Optimization results of a plate with a hole (Auto-mesh K=200, $\sigma_{ref} = 40$ MPa)



(a) von Mises stresses for first and last iterations: Iteration 1 (left), Iteration 5 (right)



(b) Variation of von Mises stress distribution along the hole boundary



(c) Variation of ellipse axes ratio

Figure 4.61: Optimization results of a plate with a hole (Auto-mesh $K=250$, $\sigma_{ref} = 40$ MPa)

Table 4.6: Summary of results with auto-mesh

		Magnification factor k	
σ_{ref}		200	250
40	Iterations	7	5
	Max stress	70.68	71.73
	Ellipse axes ratio	1.99	1.89

CHAPTER 5

CONCLUSIONS

Biological Growth Method (BGM) is a structural shape optimization method, generally based on the natural optimization of trees under their own weights or external loads. Swelling or shrinking takes place at their outer layers decreasing the localized stresses in their body. In BGM, the outer layer that will shrink or swell is called the optimization domain. The von Mises stresses developed in the optimization domain during structural stress analyses were related to temperature differences in the consequent thermal expansion analysis to determine the magnitudes of swelling and shrinking. The study aimed to investigate the effect of domain thickness on BGM.

During the application of the method the finite element code, pre- and post-processor MARC-MENTAT student version was used. A software named Biological Growth Interface (BGI) was developed to interactively control and modify the data in the input and output files. The procedure was verified by conducting the parametric study of the plane with a hole problem of Tekkaya (1996). In the study, the effects of magnification factor and the reference stress were investigated with a constant domain thickness of 10 mm.

From the interpretation of the results of the verification analyses, it was concluded that as the magnification factor increased the number of iterations required for the optimization decreased. On the other hand, increasing the reference stress towards the maximum stress level expected after the optimization, increased the number of iterations. As the number of iterations increased the method gave better results. A minimum of 5-6 iterations seemed to be a must for the plane with a hole problem. 130 MPa of maximum von Mises stress around the hole before the optimization dropped down to about 70 MPa, the ellipse axes ratio being 1 for the circular hole resulted around 2 after the optimization procedure was applied.

The maximum stress before the optimization was at the hole boundary and generally the stress concentration was in the optimization domain of thickness 10 mm. Far away from the hole, the stress level drops down to the values that the plane would have without the hole. However, the stress levels in the vicinity of the 10 mm domain were still remarkable. To

include the effect, the method was applied to the same problem with domain thicknesses 20, 30 and 40 mm. The maximum von-Mises stresses and ellipse axes ratios were determined to be between 70-75 MPa and 1.7-2.0, respectively. The number of iterations required decreased. Still, a minimum of 5-6 iterations seemed to be a must for better results.

It should be noted that the main difference between the present study and that of Tekkaya (1996) was that in the second, the mesh was re-generated after each iteration to keep the domain thickness at 10 mm and to eliminate the distortion of elements. In the present study, the mesh was not re-generated but the coordinates of the nodes were changed according to the deflections, i.e. so-called swelling and shrinking action, resulting in distorted or high aspect ratio elements effecting the results in a negative way.

The problem of mesh distortion can be resolved by adopting an automatic mesh generation scheme after each iteration and may be considered as a future work. However, the outcomes of the study turned the attention to form a model with larger elements to prevent distortion and aspect ratio problems with automatic mesh generation to have the benefit of easiness in modelling. The optimization domain roughly selected to include remarkable stress changes around the hole boundary. Reference stress was assigned as the stress level far away from the hole. Since the optimization domain is large magnification factor was taken as low to have enough number of iterations for acceptable results. A magnification factor of 200 resulted with a maximum von Mises stress of 70.68 MPa and an ellipse ratio of 1.99 after 7 iterations.

REFERENCES

- Baumgartner, A., Harzheim, L., & Mattheck, C. (1992). SKO (soft kill option): the biological way to find an optimum structure topology. *International Journal of Fatigue*, 14(6), 387-393.
- Budynas, R. G., & Nisbett, J. K. (2008). *Shigley's mechanical engineering design* (Vol. 9). New York: McGraw-Hill.
- Cai, R., Cai, S., Yang, X., & Lu, F. (1998). A novel method of structural shape optimization coupling BEM with an optimization method based on biological growth. *Structural and Multidisciplinary Optimization*, 15(3), 296-300.
- Cardona, A., Nigro, N., Sonzogni, V., & Storti, M. (2006). The coupling of the biological growth method and the boundary element method for structural shape optimization. *Mecánica Computacional*, 25, 2827-2834
- Chen, J. L., & Tsai, W. C. (1993). Shape optimization by using simulated biological growth approaches. *AIAA journal*, 31(11), 2143-2147.
- Le Riche, R., & Cailletaud, G. (1998). A mixed evolutionary / heuristic approach to shape optimization. *International Journal for Numerical methods in Engineering*, 41, 1463-1484.
- MARC-MENTAT Finite Element Software, Newport Beach, CA 92660, USA. Retrieved November 19, 2017 from <http://www.mscsoftware.com/page/msc-software>
- Mattheck, C., Burkhardt, S., & Erb, D. (1991). Shape optimization of engineering components by adaptive biological growth. *In Engineering optimization in design processes* (pp. 15-24). Berlin: Proceedings of the International Conference
- Mattheck, C., Moldenhauer, H. (1990). An intelligent CAD method based on biological growth. *Fatigue and Fracture of Engineering Materials & Structures*, 13(1), 41-51.
- Peng, D., & Jones, R. (2009). A CAD-based on biological method for designing optimal fatigue life. *Structural and Multidisciplinary Optimization*, 37(3), 295-304.

- Tang, J. (2011). Developing evolutionary structural optimization techniques for civil engineering applications Retrieved November 19, 2017 from <https://researchbank.rmit.edu.au/view/rmit:160087>.
- Tekkaya, A. Erman, & Güneri, A. (1996). Shape optimization with the biological growth method: a parameter study. *Engineering computations*, 13(8), 4-18.
- Tian, Z. M. H., & Shangjin, W. (2004). Modified biological growth method and its application to shape optimization of centrifugal impellers. *Chinese Journal of Mechanical Engineering*, 12, 1-6.
- Wessel, C., Cisilino, A., & Sensale, B. (2004). Structural shape optimization using boundary elements and the biological growth method. *Structural and Multidisciplinary Optimization*, 28(2), 221-227.
- Zehsaz, M., Torkanpouri, K. E., & Paykani, A. (2013). Convergence of shape optimization calculations of mechanical components using adaptive biological growth and iterative finite element methods. *Journal of Central South University*, 20(1), 76-82.

APPENDICES

APPENDIX 1

StressV1.dat

```

title          job1
$....MARC input file produced by Marc Mentat 2016.0.0 (64bit) Student Edition
$.....
$....input file using extended precision
extended
$.....
sizing          0          629          680          0
alloc          25
elements       3
version        11
table          0          0          2          1          1          0          0          1
processor      1          1          1          0
$no list
elastic        0
all points
no echo        1          2          3
end
$.....
solver
      8          0          0          0          0          0          0          0          0          0
0      0          0          0          0          0
optimize      11
connectivity
      0          0          1
      1          3          28          29          85          27
      2          3          29          30          86          85
      3          3          30          31          87          86
      ;          ;          ;          ;          ;          ;
      ;          ;          ;          ;          ;          ;
      ;          ;          ;          ;          ;          ;
      627         3          704          684          701          710
      628         3          688          709          703          700
      629         3          709          688          680          656
coordinates
      3          680          0          1
      1 1.0000000000000000+2 0.0000000000000000+0 0.0000000000000000+0
      2 1.1000000000000000+2 0.0000000000000000+0 0.0000000000000000+0

```

```

3 1.2000000000000000+2 0.0000000000000000+0 0.0000000000000000+0
; ; ; ; ; ;
; ; ; ; ; ;
; ; ; ; ; ;
709 3.990607755390000+1 5.560678049811000+1 0.0000000000000000+0
710 5.830118186922000+1 4.358156739948000+1 0.0000000000000000+0
711 5.258083798993000+1 5.388790137404000+1 0.0000000000000000+0
define node set apply1_nodes
50 51 52 53 54 55 358 359
360 361 362 363 364 c 369 370 371 372
365 366 367 368 369 370
define node set apply2_nodes
1 2 3 4 5 6 312 313
314 315 316 317 318 c 323 324 325 326
319 320 321 322 323 324
define edgemt set apply3_edges
1:0 2:0 3:0 4:0 5:0
6:0 7:0 8:0 c 11:0 12:0 13:0
9:0 10:0 11:0 12:0 13:0
14:0 15:0 16:0 c 19:0 20:0 21:0
17:0 18:0 19:0 20:0 21:0
22:3
define edgemt set apply4_edges
1:3 53:0 54:0 55:0 56:0
57:0 58:0 59:0 c 62:0 63:0 64:0
60:0 61:0 62:0 63:0 64:0
65:0 66:0 67:0 c 70:0 71:0 72:0
68:0 69:0 70:0 71:0 72:0
73:0
define ndsq set Domain_Nodes
1 55 56 57 58 59 60 61
62 63 64 65 66 c 71 72 73 74
75 76 77 78 79 c 84 312 313 314
315 316 317 318 319 c 667 668 669 670
663 664 665 666 667 668 669 670

```

```

671      672      673      674      675  c
      676      677      678      679      680      681      682      683
684      685      686      687      688  c
      689      690      691      692      693      694      695      696
697      698      699      700      701  c
      702      703      704      705      706      707      708      709
710      711
define      element      set      Domain_Elements
      269      to      629
isotropic

      lelastic      10      0      0      0material1
2.1000000000000000+5 3.0000000000000000-1 0.0000000000000000+0 0.0000000000000000+0 0.0000000000000000+0
0.0000000000000000+0 0.0000000000000000+0 0.0000000000000000+0
      0      0      0      0      0      0      0      0
      1      to      629
geometry

5.0000000000000000+0 0.0000000000000000+0 0.0000000000000000+0 0.0000000000000000+0 0.0000000000000000+0
0.0000000000000000+0 0.0000000000000000+0
      1      to      629
fixed disp

      1      0      0      0      1      0apply1
0.0000000000000000+0
      0
      1
      2
apply1_nodes
      1      0      0      0      1      0apply2
0.0000000000000000+0
      0
      2
      2
apply2_nodes
dist loads

```

```

      1      0      0      0      0      0      0      0      0      0      0      0
-2.2500000000000000+1      0      0      0      0      0      0      0      0      0      0
      0
      0      1
      13
apply3_edges
      1      0      0      0      0      0      0      0      0      0      0      0
-4.5000000000000000+1      0      0      0      0      0      0      0      0      0      0
      0
      0      1
      13
apply4_edges
loadcase      job1
      4

apply1
apply2
apply3
apply4
post
      1      16      17      2      0      19      20      0      1      0
0      0      0      0      0      0      0      0      0      0
      17      0

parameters
1.0000000000000000+0 1.0000000000000000+9 1.0000000000000000+2 1.0000000000000000+6 2.5000000000000000-1
5.0000000000000000-1 1.5000000000000000+0-5.0000000000000000-1
8.6250000000000000+0 2.0000000000000000+1 1.0000000000000000-4 1.0000000000000000-6 1.0000000000000000+0
1.0000000000000000-4
8.3140000000000000+0 2.7315000000000000+2 5.0000000000000000-1 0.0000000000000000+0 5.6705100000000000-8
1.4387690000000000-2 2.9979000000000000+8 1.0000000000000000+30
0.0000000000000000+0 0.0000000000000000+0 1.0000000000000000+2 0.0000000000000000+0 1.0000000000000000+0-
2.0000000000000000+0 1.0000000000000000+6 3.0000000000000000+0
0.0000000000000000+0 0.0000000000000000+0 1.2566370610000000-6 8.8541878170000000-12 1.2000000000000000+2
1.0000000000000000-3 1.6000000000000000+2 0.0000000000000000+0
3.0000000000000000+0
end option
$.

```

APPENDIX 2

StressV1.out

M		M
W		W
MMMM		MMMM
WWWW		WWWW
MMMMMMMM		MMMMMMMM
WWWWWWWWW		WWWWWWWWW
MMMMMMMMMMMM		MMMMMMMMMMMM
WWWWWWWWWWWWW		WWWWWWWWWWWWW
MM		MM
WW		WW
MMMMMMMM	MMMMMMMMMMMMMMMMMMMM	MMMMMMMM
WWWWWWWWW	WWWWWWWWWWWWWWW	WWWWWWWWW
MMMMM	MMMMMMMM	MMMMM
WWWWW	WWWWWWWWW	WWWWW
MM	MMM	MM
WW	WWW	WW
M	M	M
W	W	W
MM	MMM	MM
WW	WWW	WW
MMMM	MMMMMMMM	MMMM
WWWWW	WWWWWWWWW	WWWWW
MMMMMMMM	MMMMMMMMMMMMMMMM	MMMMMMMM
WWWWWWW	WWWWWWWWWWWWW	WWWWWWW
MMMMMMMMMM	MMMMMMMMMMMMMMMMMMMM	MMMMMMMMMM
WWWWWWWWW	WWWWWWWWWWWWWWW	WWWWWWWWW
MM		MM
WW		WW
MMMMMMMMMMMMMMMMMMMM	MMMMMMMMMMMMMMMMMMMM	MMMMMMMMMMMMMMMMMMMM
WWWWWWWWWWWWWWW	WWWWWWWWWWWWWWW	WWWWWWWWWWWWWWW
MMMMMMMMMMMM	MMMMMMMMMMMM	MMMMMMMMMMMM
WWWWWWWWWWW	WWWWWWWWWWW	WWWWWWWWWWW

```
MMMMM      MMMMM
WWWWW      WWWWW
  M         M
  W         W
```

version: Marc - Student Edition 2016.0.0, build 430850 (2016/08/12)

machine type: WINDOWS

integer*8 version: integers are 64-bits

date: Tue Oct 31 19:43:26 2017

Student Edition

Maximum number of nodes in the model: 5000

Expiration date: July 15, 2018

(c) COPYRIGHT 2016 MSC Software Corporation, all rights reserved

Marc - Student Edition - W i n d o w s

i n p u t d a t a

p a g e 1

80	90	100	110	120	130	140	150	160	70
----	----	-----	-----	-----	-----	-----	-----	-----	----


```

title                                job1
$. . . .MARC input file produced by Marc Mentat 2016.0.0 (64bit) Student Edition
$. . . .
$. . . .input file using extended precision
card      5  extended
$. . . .
sizing                                0      629      680      0
alloc      25
elements   3
card      10 version      11
table      0      0      2      1      1
0          0      1
processor  1      1      1      0
-----
-----
10      20      30      40      50      60      70
80      90      100     110     120     130     140     150     160
-----
-----
-----

```

1
 general memory increasing from 25 MByte to 106 MByte

memory increased to 28003864 words during
 pre-reading of sets

MSC Customer Entitlement ID
 N/A

program sizing and options requested as follows

element type requested*****	3
number of elements in mesh*****	629
number of nodes in mesh*****	680
load correction was suppressed*****	
elastic re-analysis flagged*****	
values stored at all integration points*****	
tape no.for input of coordinates + connectivity	5
no.of different materials 1 max.no of slopes	5
number of points on shell section *****	11
new style input format will be used*****	
requested number of element threads*****	1
requested number of solver threads*****	1
extended precision input is used *****	
Marc input version *****	11
maximum number of boundary conditions *****	4
suppress echo of list items *****	
suppress echo of bc summary *****	
suppress echo of nurbs data *****	

end of parameters and sizing

key to stress, strain and displacement output

element type 3

4-node isoparametric plane stress

stresses and strains in global directions

1=xx

2=yy

3=xy

displacements in global directions

1=u global x direction

2=v global y direction

allocated	76172 words of memory due to nodal vectors
allocated	1940 words of memory due to boundary conditions
allocated	12 words of memory due to geometric points
allocated	46 words of memory due to geometric curves
allocated	28 words of memory due to geometric surfaces

allocated 2720 words of memory due to shell, user or contact transformations

workspace needed for input and stiffness assembly: 34746

internal core allocation parameters
degrees of freedom per node (ndeg) 2
max. number of coordinates per node 2
max. nodes per element (nnodmx) 4
max. invariants per int. points (neqst) 1
max. stress components per int. point (nstrmx) 3
strains per integration point (ngens) 3

flag for element storage (ielsto) 0
element data in core

memory usage per element group

group	# elements	nelsto	MByte	words
1	629	410	1	257890

total	629		1	257890

internal element variables

internal element number 1 library code type 3
number of nodes= 4
stresses stored per integration point = 3

```
direct continuum components stored = 2
shear continuum components stored = 1
shell/beam flag = 0
curvilinear coord. flag = 0
int.points for elem. stiffness 4
number of local inertia directions 2
int.point for print if all points not flagged 5
int. points for dist. surface loads (pressure) 2
library code type = 3
large disp. row counts 4 4 7
```

residual load correction is switched off

\$.

solver

multifrontal direct sparse solver invoked

optimize 11

metis nested dissection algorithm

connectivity

```

    meshr1, iprnt
        5      1
    elem no., type,      nodes

coordinates
-----

ncrd1 ,meshr1,iprnt
    2      5      1
    node      coordinates

define      node      set      apply1_nodes
-----

a list of nodes given below
360      361      50      51      52      53      54      55      358      359
362      363      364
    echo suppressed for      8 items
    total number of items read:      21

define      node      set      apply2_nodes
-----

a list of nodes given below
314      315      1      2      3      4      5      6      312      313
316      317      318
    echo suppressed for      8 items
    total number of items read:      21

define      edgmt      set      apply3_edges
-----

    1: 0      2: 0      3: 0      4: 0      5: 0      6: 0

```

```

7: 0      8: 0      echo suppressed for      14 items
          total number of items read:      22

          define      edgmt      set      apply4_edges
          -----

          1: 3      53: 0      54: 0      55: 0      56: 0      57: 0
58: 0      59: 0      echo suppressed for      14 items
          total number of items read:      22

          define      ndsq      set      Domain_Nodes
          -----

          a list of nodes given below
          1      55      56      57      58      59      60      61
62      63      64      65      66
          echo suppressed for      387 items
          total number of items read:      400

          define      element      set      Domain_Elements
          -----

          from element      269 to element      629 by      1

          isotropic
          -----

          isotropic material material id =      1
          elastic      yield criteria
          isotropic      hardening rule

```

material name is: material1

structural property	value	table id
Youngs modulus	2.10000E+05	0
Poissons ratio	3.00000E-01	0
mass density	0.00000E+00	0
shear modulus	8.07692E+04	0
coefficient of thermal expansion	0.00000E+00	0
Yield stress	1.00000E+20	0
cost per unit volume	0.00000E+00	0
cost per unit mass	0.00000E+00	0

from element 1 to element 629 by 1

geometry

from element 1 to element 629 by 1

geometry id = 1

geometric parameter	value
1	5.00000E+00
2	0.00000E+00
3	0.00000E+00
4	0.00000E+00
5	0.00000E+00
6	0.00000E+00
7	0.00000E+00
8	0.00000E+00

fixed disp

read data from unit 5

name of boundary condition apply1

Displacements are applied incrementally relative to current position

Prescribed Displacement for dof 1 = 0.00000E+00 table id is 0

applied to node ids

apply1_nodes

name of boundary condition apply2

Displacements are applied incrementally relative to current position

Prescribed Displacement for dof 2 = 0.00000E+00 table id is 0

applied to node ids

apply2_nodes

dist loads

read data from unit 5

name of boundary condition apply3

```

Load Type      1
Prescribed Distributed Pressure =    -2.25000E+01  table id is      0
Prescribed Distributed Pressure =     0.00000E+00  table id is      0
Prescribed Distributed Pressure =     0.00000E+00  table id is      0
applied to elem mn-edge
apply3_edges
name of boundary condition apply4

Load Type      1
Prescribed Distributed Pressure =    -4.50000E+01  table id is      0
Prescribed Distributed Pressure =     0.00000E+00  table id is      0
Prescribed Distributed Pressure =     0.00000E+00  table id is      0
applied to elem mn-edge
apply4_edges

loadcase          job1
-----

activate boundary condition apply1
activate boundary condition apply2

```

activate boundary condition apply3

activate boundary condition apply4

post

number of element variables on post file: 1

both binary and formatted post file will be used

initial output frequency of post file: 1

Marc 2005 style post file (default)

post variable 1 is post code 17 =

maximum record length on binary post file= 680

approximate no. of words per increment on file= 2532

maximum record length on formatted post file= 80

approximate no. of records per increment on file= 3200

parameters

parameters set as follows

predictor used for stress-strain calculation 1.00000E+00

penalty factor for boundary conditions 1.00000E+09

penalty for incompressibility - r-p flow 1.00000E+02

penalty for incompressibility - fluid flow 1.00000E+06

beta parameter for Newmark operator	2.50000E-01
gamma parameter for Newmark operator	5.00000E-01
gamma parameter for Single-Step-Houbolt	1.50000E+00
gamma parameter for Single-Step-Houbolt	-5.00000E-01
sharp angle for sticking/separating - 2D	8.62500E+00
sharp angle for sticking/separating - 3D	2.00000E+01
initial strain rate for r-p flow	1.00000E-04
lowest strain rate cut-off for r-p flow	1.00000E-06
fraction of dilatational stress neglected	1.00000E+00
factor for drilling d.o.f for shells	1.00000E-04
factor for displacement after rezoning	1.00000E+00
universal gas constant	8.31400E+00
absolute temperature offset	2.73150E+02
thermal properties evaluation weight	5.00000E-01
surface projection factor in ssh dynamics	0.00000E+00
Stefan Boltzmann constant	5.67051E-08
Planck's second radiation constant	1.43877E-02
Speed of light in vacuum	2.99790E+08
Permeability of vacuum	1.25664E-06
Permittivity of vacuum	8.85419E-12
maximum iterative displacement component	1.00000E+30
initial stiffness to simulate sticking	0.00000E+00
minimum angle between the normal vectors of contacting segments	1.20000E+02
radiation reflection cut-off	1.00000E-03
angle for averaging adjacent beams (s2s)	1.60000E+02
stabilizer stiffness for model sections	0.00000E+00
maximum change in temperature per iteration	1.00000E+02
maximum rbe3 conditioning number	0.10000E+07
end option	

wall time = 0.00

wall time = 0.00

direct symmetric multi-frontal sparse solver is invoked for region 1

number of element groups used: 1

formulation	group	# elements	element type	material
S	1	629	3	1

formulation:
S: small displacement

**** note ****

can not find the following flow-data file
in job directory or in the material library:
C:\MSC.Software\Marc_Student_Edition\2016.0.0\marc2016\AF_flowmat\material1.mat
This is ok if no separate flow-data file is required.
Otherwise please provide the data file or result
will be wrong.

maximum connectivity in stiffness matrix is 10 at node 704

maximum half-bandwidth is 373 between nodes 1 and 404
number of profile entries excluding fill-in is 3246

total workspace needed with in-core matrix storage = 92122
part of solver workspace is allocated separately

allocated 840 words of memory due to kinematic boundary conditions

load increments for each degree of freedom
summed over the whole model

from distributed loads

dist. loads on undeformed configuration - increments for dist. loads

increments for point loads

3.375000E+04 1.687500E+04

point loads

0.000000E+00 0.000000E+00

start of assembly cycle number is 0

wall time = 0.00

0.07 MByte)	solver workspace for phase1 (matrix input)	(64bit words) =	8546 (
	Metis nested dissection ordering used		
0.19 MByte)	solver workspace for phase2 (nodal ordering)	(64bit words) =	25194 (
0.27 MByte)	solver workspace for phase3 (symbolic factor)	(64bit words) =	35511 (
0.45 MByte)	solver workspace for phase4 (factorization)	(64bit words) =	59606 (
	(MINIMUM)		
0.84 MByte)	solver workspace for phase4 (factorization)	(64bit words) =	110322 (
	(MAXIMUM)		
7.63 MByte)	solver workspace available and used	(64bit words) =	1000000 (

start of matrix solution
wall time = 0.00

singularity ratio 2.9111E-01

end of matrix solution
wall time = 0.00

element with highest stress relative to yield is 283
where equivalent stress is 1.235E-18 of yield

WINDOWS version
 Marc - Student Edition 2016.0.0
 output for increment 0. " job1"

total strain energy is 6.07713E+02
 within which:
 elastic strain energy is 6.07713E+02
 total ext-force work is 6.07713E+02
 within which:
 work by appl. force/disp. is 6.07713E+02
 work by frictional forces is 0.00000E+00

tresca mises mean principal values physical c
 o m p o n e n t s
 intensity intensity normal minimum intermediate maximum 1 2 3
 4 5 6
 intensity

element 1 point 1 integration pt. coordinate= 0.149E+03 0.149E+03
 section thickness = 0.500E+01
 engsts 4.497E+01 3.895E+01 2.248E+01 0.000E+00 2.247E+01 4.497E+01 4.497E+01 2.247E+01 1.548E-02
 engstn 2.784E-04 1.718E-04 0.000E+00-9.635E-05 4.277E-05 1.821E-04 1.821E-04 4.277E-05 1.916E-07

element 1 point 2 integration pt. coordinate= 0.145E+03 0.149E+03
 section thickness = 0.500E+01
 engsts 4.498E+01 3.895E+01 2.249E+01 0.000E+00 2.249E+01 4.498E+01 4.498E+01 2.249E+01 2.205E-02
 engstn 2.784E-04 1.718E-04 0.000E+00-9.639E-05 4.285E-05 1.821E-04 1.821E-04 4.285E-05 2.730E-07

```

element          1 point  3      integration pt. coordinate=      0.149E+03      0.145E+03
section thickness = 0.500E+01
engsts  4.499E+01 3.896E+01 2.249E+01 0.000E+00 2.248E+01 4.499E+01 4.499E+01 2.248E+01 2.227E-02
engstn  2.785E-04 1.718E-04 0.000E+00-9.639E-05 4.277E-05 1.821E-04 1.821E-04 4.277E-05 2.758E-07

element          1 point  4      integration pt. coordinate=      0.145E+03      0.145E+03
section thickness = 0.500E+01
engsts  4.500E+01 3.897E+01 2.250E+01 0.000E+00 2.250E+01 4.500E+01 4.500E+01 2.250E+01 2.882E-02
engstn  2.786E-04 1.719E-04 0.000E+00-9.642E-05 4.285E-05 1.821E-04 1.821E-04 4.285E-05 3.568E-07
      ;          ;          ;          ;          ;
      ;          ;          ;          ;          ;
      ;          ;          ;          ;          ;
element          629 point  1      integration pt. coordinate=      0.390E+02      0.545E+02
section thickness = 0.500E+01
engsts  6.383E+01 5.769E+01 2.642E+01 0.000E+00 1.542E+01 6.383E+01 6.173E+01 1.752E+01-9.864E+00
engstn  3.952E-04 2.485E-04 0.000E+00-1.132E-04-1.777E-05 2.819E-04 2.689E-04-4.764E-06-1.221E-04

element          629 point  2      integration pt. coordinate=      0.362E+02      0.544E+02
section thickness = 0.500E+01
engsts  6.377E+01 5.774E+01 2.627E+01 0.000E+00 1.505E+01 6.377E+01 6.164E+01 1.718E+01-9.956E+00
engstn  3.948E-04 2.486E-04 0.000E+00-1.126E-04-1.942E-05 2.822E-04 2.690E-04-6.247E-06-1.233E-04

element          629 point  3      integration pt. coordinate=      0.391E+02      0.517E+02
section thickness = 0.500E+01
engsts  6.361E+01 5.752E+01 2.629E+01 0.000E+00 1.526E+01 6.361E+01 6.145E+01 1.742E+01-9.989E+00
engstn  3.938E-04 2.477E-04 0.000E+00-1.127E-04-1.821E-05 2.811E-04 2.677E-04-4.839E-06-1.237E-04

element          629 point  4      integration pt. coordinate=      0.364E+02      0.517E+02
section thickness = 0.500E+01
engsts  6.354E+01 5.756E+01 2.614E+01 0.000E+00 1.488E+01 6.354E+01 6.135E+01 1.707E+01-1.009E+01
engstn  3.933E-04 2.478E-04 0.000E+00-1.120E-04-1.990E-05 2.813E-04 2.677E-04-6.342E-06-1.249E-04

```

1

n o d a l p o i n t d a t a

t o t a l d i s p l a c e m e n t s

		1	2.90842E-02	4.03022E-13		2	3.05130E-02	5.85636E-13
3	3.20504E-02	6.06750E-13						
		4	3.36153E-02	6.40419E-13		5	3.52212E-02	6.86812E-13
6	3.68172E-02	3.64991E-13						
		<i>i</i>		<i>i</i>			<i>i</i>	<i>i</i>
<i>i</i>								
		<i>i</i>		<i>i</i>			<i>i</i>	<i>i</i>
<i>i</i>								
		<i>i</i>		<i>i</i>			<i>i</i>	<i>i</i>
<i>i</i>								
		704	2.00663E-02	3.16076E-03		705	1.71486E-02	3.27788E-03
706	1.52546E-02	3.14671E-03						
		707	1.47720E-02	3.19445E-03		708	1.63233E-02	3.33722E-03
709	1.24337E-02	2.77517E-03						
		710	1.88602E-02	3.23357E-03		711	1.58645E-02	3.24955E-03

total equivalent nodal forces (distributed plus point loads)

		1	0.0000	0.0000		2	0.0000	0.0000
3	0.0000	0.0000						
		4	0.0000	0.0000		5	0.0000	0.0000
6	767.05	0.0000						
		7	1534.1	0.0000		8	1534.1	0.0000
9	1534.1	0.0000						

```

;
;
;
;
704 0.0000 0.0000 705 0.0000 0.0000
706 0.0000 0.0000
707 0.0000 0.0000 708 0.0000 0.0000
709 0.0000 0.0000
710 0.0000 0.0000 711 0.0000 0.0000

```

elsewhere reaction forces at fixed boundary conditions, residual load correction

```

1 -5.00222E-12 -1061.3 2 -5.22959E-12 -1542.2
3 -4.78906E-12 -1597.8
4 2.95586E-12 -1686.4 5 -1.25056E-12 -1808.6
6 3.29692E-12 -961.14
7 3.18323E-12 -1.13687E-12 8 -1.81899E-12 -1.13687E-13
9 -1.15961E-11 4.88853E-12
;
;
;
;
;
;
701 1.21076E-11 5.11591E-13 702 1.81899E-12 6.53699E-13
706 -1.25056E-12 -2.55795E-12
707 -3.29692E-12 1.25056E-12 708 3.36797E-12 1.36424E-12
709 1.13687E-12 -1.36424E-12

```

710 9.54969E-12 7.95808E-13 711 6.36646E-12 2.55795E-13

summary of externally applied loads

3.37500E+04 1.68750E+04

summary of reaction/residual forces

-3.37500E+04 -1.68750E+04

memory usage:	MByte	words	% of total
within general memory:			
element stiffness matrices:	0	30126	0.1
solver: first part	0	57376	0.2
overallocation initial allocation	106	27911746	74.5
other:	0	4616	0.0
allocated separately:			
solver 8	8	1982908	5.3
nodal vectors:	0	77532	0.2
defined sets:	0	2068	0.0
transformations:	0	2720	0.0
kinematic boundary conditions:	0	2780	0.0
points, curves and surfaces:	0	86	0.0
mem_none:	0	89366	0.2
element storage:	1	280862	0.8
material properties:	0	3568	0.0
executable and common blocks:	27	7000000	18.7
miscellaneous	0	212	0.0

total:	143	37445966	
general memory allocated:	107	28003864	

```

general memory used:          0      92118
peak memory usage:          159    41557520
e n d   o f   i n c r e m e n t      0
binary post data at increment      0.  subincrement      0.  on file 16
formatted post data at increment    0.  subincrement    0.  on file 19
wall time =                    1.00

```

\$.....

*** end of input deck - job ends

memory usage:	MByte	words	% of total
within general memory:			
element stiffness matrices:	0	30126	0.1
solver: first part	0	57376	0.2
overallocation initial allocation	106	27911746	74.5
other:	0	4616	0.0
allocated separately:			
solver 8	8	1982908	5.3
nodal vectors:	0	77532	0.2
defined sets:	0	2068	0.0
transformations:	0	2720	0.0
kinematic boundary conditions:	0	2780	0.0
points, curves and surfaces:	0	86	0.0
mem_none:	0	89366	0.2
element storage:	1	280862	0.8

material properties:	0	3568	0.0
executable and common blocks:	27	7000000	18.7
miscellaneous	0	212	0.0

total:	143	37445966	
general memory allocated:	107	28003864	
general memory used:	0	92118	
peak memory usage:	159	41557520	

timing information:	wall time	cpu time
total time for input:	0.05	0.05
total time for stiffness assembly:	0.02	0.02
total time for stress recovery:	0.01	0.00
total time for matrix solution:	0.06	0.02
total time for output:	0.05	0.06
total time for miscellaneous:	0.09	0.09

total time:	0.28	0.23

This is a successful completion to a Marc simulation,
indicating that no additional incremental data was
found and that the analysis is complete.

Marc - Student Edition 2016.0.0

Exit number 3004

APPENDIX 3

ThermalV1.dat

```

title          job1
$....MARC input file produced by Marc Mentat 2016.0.0 (64bit) Student Edition
$.....
$....input file using extended precision
extended
$.....
sizing          0          585          633          0
alloc           25
elements        3
version         11
table           0          0          2          1          1          0          0          1
processor       1          1          1          0
$no list
couple          0
all points
no echo         1          2          3
end
$.....
solver
      8          0          0          0          0          0          0          0          0
0      0          0          0          0          0
optimize        11
connectivity
      0          0          1
      1          3          55          56          91          54
      2          3          56          57          92          91
      3          3          57          58          93          92
      ;          ;          ;          ;          ;          ;
      ;          ;          ;          ;          ;          ;
      ;          ;          ;          ;          ;          ;
      ;          ;          ;          ;          ;          ;
      583         3          55          54          647          612
      584         3          666          649          52          51
      585         3          649          666          607          608
coordinates
      3          633          0          1

```

```

1 4.000000000000000+1 0.000000000000000+0 0.000000000000000+0
2 4.500000000000000+1 0.000000000000000+0 0.000000000000000+0
3 5.000000000000000+1 0.000000000000000+0 0.000000000000000+0

666 3.389361435619000+1 1.449949264039000+2 0.000000000000000+0
667 1.449969631442000+2 2.552391971165000+1 0.000000000000000+0
668 1.449985816417000+2 1.703941592972000+1 0.000000000000000+0

define      node      set      applyT1_nodes
1
define      node      set      applyT2_nodes
2
define      node      set      applyT3_nodes
3
; ; ; ; ;
; ; ; ; ;
; ; ; ; ;
define      node      set      applyT572_nodes
572
define      node      set      applyT573_nodes
573
define      node      set      applyT574_nodes
574
define      node      set      apply1_nodes
55      56      57      58      59      60      61      62
63      64      65      66      67      c      72      73      74      75
68      69      70      71
611      612
define      node      set      apply2_nodes
1      2      3      4      5      6      7      8
9      10      11      12      13      c      18      19      20      21
14      15      16      17
576      577
define      ndsq      set      Domain_Nodes
1      2      3      4      5      6      7      8
9      10      11      12      13      c      18      19      20      21
14      15      16      17
22      23      24      25      26      c

```

```

35      27      28      29      30      31      32      33      34
      36      37      38      39      c
542    534    535    536    537    538    539    540    541
      543    544    545    546    c
555    547    548    549    550    551    552    553    554
      556    557    558    559    c
568    560    561    562    563    564    565    566    567
      569    570    571    572    c
      573    574
define      element      set      Domain_Elements
      1      to      528
isotropic
      1elastic      10      0      0      0material1
2.1000000000000000+5 3.0000000000000000-1 0.0000000000000000+0 0.0000000000000000+0 0.0000000000000000+0
0.0000000000000000+0 0.0000000000000000+0 0.0000000000000000+0
      0      0      0      0      0      0      0      0      0
0.0000000000000000+0 0.0000000000000000+0 0.0000000000000000+0 0.0000000000000000+0 0.0000000000000000+0
0.0000000000000000+0 0.0000000000000000+0
      0      0      0      0      0      0      0      0
      529      to      585
isotropic
      2elastic      10      0      0      0material2
5.2500000000000000+2 3.0000000000000000-1 0.0000000000000000+0 1.0800000000000000-5 0.0000000000000000+0
0.0000000000000000+0 0.0000000000000000+0 0.0000000000000000+0
      0      0      0      0      0      0      0      0      0
0.0000000000000000+0 0.0000000000000000+0 0.0000000000000000+0 0.0000000000000000+0 0.0000000000000000+0
0.0000000000000000+0 0.0000000000000000+0
      0      0      0      0      0      0      0      0
      1      to      528
geometry
      5.0000000000000000+0 0.0000000000000000+0 0.0000000000000000+0 0.0000000000000000+0 0.0000000000000000+0

```

```

0.0000000000000000+0 0.0000000000000000+0
      1          to          585
fixed temperature

      1          0          0          0          0          0applyT1
0.0000000000000000+0
      0
      1
      2
applyT1_nodes
      1          0          0          0          0          0applyT2
0.0000000000000000+0
      0
      1
      2
applyT2_nodes
      1          0          0          0          0          0applyT3
0.0000000000000000+0
      0
      1
      2
applyT3_nodes

      1          0          0          0          0          0applyT574
0.0000000000000000+0
      0
      1
      2
applyT574_nodes
fixed disp

      1          0          0          0          1          0apply1
0.0000000000000000+0
      0

```

```

      1
      2
apply1_nodes
      1      0      0      0      1      0apply2
0.0000000000000000+0
      0
      2
      2
apply2_nodes
loadcase      job1
      576
applyT1
applyT2
applyT3

applyT574
apply1
apply2
post
      0      16      17      2      0      19      20      0      1      0
0      0      0      0      0      0      0      0      0      0
parameters
1.0000000000000000+0 1.0000000000000000+9 1.0000000000000000+2 1.0000000000000000+6 2.5000000000000000-1
5.0000000000000000-1 1.5000000000000000+0-5.0000000000000000-1
8.6250000000000000+0 2.0000000000000000+1 1.0000000000000000-4 1.0000000000000000-6 1.0000000000000000+0
1.0000000000000000-4
8.3140000000000000+0 2.7315000000000000+2 5.0000000000000000-1 0.0000000000000000+0 5.6705100000000000-8
1.4387690000000000-2 2.9979000000000000+8 1.0000000000000000+30
0.0000000000000000+0 0.0000000000000000+0 1.0000000000000000+2 0.0000000000000000+0 1.0000000000000000+0-
2.0000000000000000+0 1.0000000000000000+6 3.0000000000000000+0
0.0000000000000000+0 0.0000000000000000+0 1.2566370610000000-6 8.8541878170000000-12 1.2000000000000000+2
1.0000000000000000-3 1.6000000000000000+2 0.0000000000000000+0
3.0000000000000000+0
end option
$.

```

\$. . . . start of loadcase lcase1

title lcase1

loadcase lcase1

576

applyT1

applyT2

applyT3

applyT574

apply1

apply2

control

99999 10 0 0 0 1 0 0 1 0

1 0 0 0

1.0000000000000000-1 0.0000000000000000+0 0.0000000000000000+0 0.0000000000000000+0 0.0000000000000000+0

0.0000000000000000+0 0.0000000000000000+0 0.0000000000000000+0

2.0000000000000000+1 1.0000000000000000+2 0.0000000000000000+0 1.0000000000000000+2 1.0000000000000000-1

1.0000000000000000-1 1.0000000000000000-1 1.0000000000000000+30

parameters

1.0000000000000000+0 1.0000000000000000+9 1.0000000000000000+2 1.0000000000000000+6 2.5000000000000000-1

5.0000000000000000-1 1.5000000000000000+0-5.0000000000000000-1

8.6250000000000000+0 2.0000000000000000+1 1.0000000000000000-4 1.0000000000000000-6 1.0000000000000000+0

1.0000000000000000-4

8.3140000000000000+0 2.7315000000000000+2 5.0000000000000000-1 0.0000000000000000+0 5.6705100000000000-8

1.4387690000000000-2 2.9979000000000000+8 1.0000000000000000+30

0.0000000000000000+0 0.0000000000000000+0 1.0000000000000000+2 0.0000000000000000+0 1.0000000000000000+0-

1.0000000000000000+0 1.0000000000000000+6 3.0000000000000000+0

0.0000000000000000+0 0.0000000000000000+0 1.2566370610000000-6 8.8541878170000000-12 1.2000000000000000+2

1.0000000000000000-3 1.6000000000000000+2 0.0000000000000000+0

3.0000000000000000+0

transient non auto

2.0000000000000000-2 1.0000000000000000+0 50 0 0 0 0.0000000000000000+0

continue

\$. . . . end of loadcase lcase1

\$.

APPENDIX 4
ThermalV1.out

M M
W W
MMMM MMMM
WWWWW WWWWW
MMMMMMMMM MMMMMMMMM
WWWWWWWWW WWWWWWWW
MMMMMMMMMMMMM MMMMMMMMMMMMM
WWWWWWWWWWWWW WWWWWWWWWWWW
MM
WW
MMMMMMMMM MMMMMMMMMMMMMMMMM MMMMMMMMM
WWWWWWW WWWWWWWWWWWWWW WWWWWWWW
MMMMMM MMMMMMMMMMMM MMMMMMM
WWWWW WWWWWWWW WWWWWW
MM MMM MMM MM
WW WWW WWW WW
M M M
W W W
MM MMM MM
WW WWW WW
MMMM MMMMMMMM MMMM
WWWWW WWWWWW WWWWW
MMMMMM MMMMMMMMMMMMM MMMMMMM
WWWWWWW WWWWWWWWWW WWWWWW
MMMMMMMMM MMMMMMMMMMMMMMMMM MMMMMMMMM
WWWWWWWWW WWWWWWWWWWWWWW WWWWWWWW
MM
WW
MMMMMMMMMMMMMMMMM MMMMMMMMMMMMMMMM
WWWWWWWWWWWWWWW WWWWWWWWWWWWWW
MMMMMMMMMM MMMMMMMMMMM
WWWWWWWWW WWWWWWWWWW

```
MMMMM      MMMMM
WWWWW      WWWWW
  M         M
  W         W
```

version: Marc - Student Edition 2016.0.0, build 430850 (2016/08/12)

machine type: WINDOWS

integer*8 version: integers are 64-bits

date: Sun Aug 13 17:48:29 2017

Student Edition

Maximum number of nodes in the model: 5000

Expiration date: July 15, 2018

(c) COPYRIGHT 2016 MSC Software Corporation, all rights reserved

Marc - Student Edition - W i n d o w s

i n p u t d a t a

p a g e 1

80	90	100	110	120	130	140	150	160	70
----	----	-----	-----	-----	-----	-----	-----	-----	----

program sizing and options requested as follows

element type requested*****	3
element type requested*****	39
number of elements in mesh*****	439
number of nodes in mesh*****	486
thermal stress analysis flagged*****	
load correction flagged or set*****	
values stored at all integration points*****	
tape no.for input of coordinates + connectivity	5
no.of different materials 2 max.no of slopes	5
heat transfer analysis, extrapolation flag, **	1
gradient of scaler field printed*****	
number of points on shell section *****	11
new style input format will be used*****	
coupled thermal-mechanical analysis flagged****	
requested number of element threads*****	1
requested number of solver threads*****	1
extended precision input is used *****	
Marc input version *****	11
maximum number of boundary conditions *****	98
suppress echo of list items *****	
suppress echo of bc summary *****	
suppress echo of nurbs data *****	

end of parameters and sizing

element type 3

4-node isoparametric plane stress

stresses and strains in global directions

1=xx

2=yy

3=xy

displacements in global directions

1=u global x direction

2=v global y direction

element type 39

4-node heat transfer planar element

1 degree of freedom per node - temperature

allocated 64164 words of memory due to nodal vectors

allocated 51552 words of memory due to boundary conditions


```
int.points for elem. stiffness 4
number of local inertia directions 1
int.point for print if all points not flagged 5
int. points for dist. surface loads (pressure) 2
library code type = 39
large disp. row counts 0 0 0
number of nodes 4
number of gradient components at each int. point 2
integration points for conductivity 4
integration point for print-out 5
integration points for surface b.c.s 2
```

residual load correction is invoked

\$.....

solver

multifrontal direct sparse solver invoked

optimize 11

metis nested dissection algorithm

connectivity

```

-----
meshr1, iprnt
      5      1
elem no., type,      nodes

coordinates
-----

ncrd1 ,meshr1,iprnt
      2      5      1
      node      coordinates

define      node      set      applyT17_nodes
-----

a list of nodes given below
      19

define      node      set      applyT18_nodes
-----

      95

      ;      ;      ;
      ;      ;      ;
      ;      ;      ;
      ;      ;      ;

define      node      set      apply1_nodes
-----

a list of nodes given below

```

```

404      405      1      2      3      4      5      6      97      403
         406      407      408
         echo suppressed for      6 items
         total number of items read:      19

         define      ndsq      set      apply2_nodes
         -----

         a list of nodes given below
308      309      21      36      51      66      81      96      106      307
         310      311      312
         echo suppressed for      6 items
         total number of items read:      19

         define      node      set      apply2_nodes_1
         -----

         a list of nodes given below
308      309      21      36      51      66      81      96      106      307
         310      311      312
         echo suppressed for      6 items
         total number of items read:      19

define      ndsq      set      Domain_nodes
-----

a list of nodes given below
9      10      1      2      3      4      5      6      7      8
11      12      13
         echo suppressed for      83 items
         total number of items read:      96

define      element      set      Domain_elements

```

a list of elements given below

9 10 11 12 13 14 15 16 17 18

 1 2 3 4 5 6 7 8

 11 12 13

 echo suppressed for 78 items

 total number of items read: 91

isotropic

isotropic material material id = 1
 elastic yield criteria
 isotropic hardening rule

material name is: material1

property	value	table id
Youngs modulus	2.10000E+05	0
Poissons ratio	3.00000E-01	0
mass density	0.00000E+00	0
shear modulus	8.07692E+04	0
coefficient of thermal expansion	0.00000E+00	0
Yield stress	1.00000E+20	0
cost per unit volume	0.00000E+00	0
cost per unit mass	0.00000E+00	0
thermal conductivity	0.00000E+00	0
specific heat	0.00000E+00	0
mass density - heat transfer	0.00000E+00	0
emissivity	0.00000E+00	0

from element 76 to element 439 by 1

isotropic

isotropic material material id = 2
elastic yield criteria
isotropic hardening rule

material name is: material2

property	value	table id
Youngs modulus	5.25000E+02	0
Poissons ratio	3.00000E-01	0
mass density	0.00000E+00	0
shear modulus	2.01923E+02	0
coefficient of thermal expansion	1.08000E-05	0
Yield stress	1.00000E+20	0
cost per unit volume	0.00000E+00	0
cost per unit mass	0.00000E+00	0
thermal conductivity	0.00000E+00	0
specific heat	0.00000E+00	0
mass density - heat transfer	0.00000E+00	0
emissivity	0.00000E+00	0

from element 1 to element 75 by 1

geometry

from element 1 to element 439 by 1

geometry id = 1

geometric parameter	value
1	5.00000E+00
2	0.00000E+00
3	0.00000E+00
4	0.00000E+00
5	0.00000E+00
6	0.00000E+00
7	0.00000E+00
8	0.00000E+00

fixed temperature

read data from unit 5

name of boundary condition applyT1

Prescribed Temperature for dof 1 = 7.92350E+01 table id is 0

applied to node ids

applyT1_nodes

name of boundary condition applyT2

Prescribed Temperature for dof 1 = 8.63000E+01 table id is 0

applied to node ids

applyT2_nodes

fixed disp

read data from unit 5

name of boundary condition apply1

Displacements are applied incrementally relative to current position

Prescribed Displacement for dof 2 = 0.00000E+00 table id is 0

applied to node ids

apply1_nodes

name of boundary condition apply2

Displacements are applied incrementally relative to current position

Prescribed Displacement for dof 1 = 0.00000E+00 table id is 0

applied to node ids

apply2_nodes_1

loadcase job1

```

activate boundary condition apply1
activate boundary condition apply2
activate boundary condition applyT1
;           ;           ;
;           ;           ;
;           ;           ;
;           ;           ;
activate boundary condition applyT95
activate boundary condition applyT96

post
-----

both binary and formatted post file will be used

initial output frequency of post file:      1

Marc 2005 style post file (default)

maximum record length on binary post file=      486
approximate no. of words per increment on file=      16

maximum record length on formatted post file=      80
approximate no. of records per increment on file=      490

parameters

```

parameters set as follows

predictor used for stress-strain calculation	1.00000E+00
penalty factor for boundary conditions	1.00000E+09
penalty for incompressibility - r-p flow	1.00000E+02
penalty for incompressibility - fluid flow	1.00000E+06
beta parameter for Newmark operator	2.50000E-01
gamma parameter for Newmark operator	5.00000E-01
gamml parameter for Single-Step-Houbolt	1.50000E+00
gamma parameter for Single-Step-Houbolt	-5.00000E-01
sharp angle for sticking/separating - 2D	8.62500E+00
sharp angle for sticking/separating - 3D	2.00000E+01
initial strain rate for r-p flow	1.00000E-04
lowest strain rate cut-off for r-p flow	1.00000E-06
fraction of dilatational stress neglected	1.00000E+00
factor for drilling d.o.f for shells	1.00000E-04
factor for displacement after rezoning	1.00000E+00
universal gas constant	8.31400E+00
absolute temperature offset	2.73150E+02
thermal properties evaluation weight	5.00000E-01
surface projection factor in ssh dynamics	0.00000E+00
Stefan Boltzmann constant	5.67051E-08
Planck's second radiation constant	1.43877E-02
Speed of light in vacuum	2.99790E+08
Permeability of vacuum	1.25664E-06
Permittivity of vacuum	8.85419E-12
maximum iterative displacement component	1.00000E+30
initial stiffness to simulate sticking	0.00000E+00
minimum angle between the normal vectors of contacting segments	1.20000E+02

```
radiation reflection cut-off          1.00000E-03
angle for averaging adjacent beams (s2s) 1.60000E+02
stabilizer stiffness for model sections 0.00000E+00
```

```
maximum change in temperature per iteration 1.00000E+02
maximum rbe3 conditioning number          0.10000E+07
```

```
end option
-----
```

```
wall time =          1.00
```

```
wall time =          1.00
```

```
direct symmetric multi-frontal sparse solver is invoked for region 1
```

```
number of element groups used:          2
```

formulation	group	# elements	element type	material
S	1	364	3	1
S	2	75	3	2

```
formulation:
  S:  small displacement
```

```
**** note ****
can not find the following flow-data file
```

in job directory or in the material library:
C:\MSC.Software\Marc_Student_Edition\2016.0.0\marc2016\AF_flowmat\material1.mat
This is ok if no separate flow-data file is required.
Otherwise please provide the data file or result
will be wrong.

**** note ****
can not find the following flow-data file
in job directory or in the material library:
C:\MSC.Software\Marc_Student_Edition\2016.0.0\marc2016\AF_flowmat\material2.mat
This is ok if no separate flow-data file is required.
Otherwise please provide the data file or result
will be wrong.

maximum connectivity in stiffness matrix is 9 at node 390

maximum half-bandwidth is 402 between nodes 2 and 403

number of profile entries excluding fill-in is 2288

total workspace needed with in-core matrix storage = 89594
part of solver workspace is allocated separately

allocated 760 words of memory due to kinematic boundary conditions

allocated 1920 words of memory due to kinematic boundary conditions

load increments for each degree of freedom
summed over the whole model

from distributed loads

dist. loads on undeformed configuration - increments for dist. loads

increments for point loads

0.000000E+00 0.000000E+00

point loads

0.000000E+00 0.000000E+00

start of assembly cycle number is 0

wall time = 1.00

0.05 MByte)	solver workspace for phase1 (matrix input)	(64bit words) =	6048 (
	Metis nested dissection ordering used		
0.14 MByte)	solver workspace for phase2 (nodal ordering)	(64bit words) =	18782 (
0.19 MByte)	solver workspace for phase3 (symbolic factor)	(64bit words) =	25341 (
0.32 MByte)	solver workspace for phase4 (factorization)	(64bit words) =	41381 (
	(MINIMUM)		

0.56 MByte) solver workspace for phase4 (factorization) (64bit words) = 74047 (
(MAXIMUM)
7.63 MByte) solver workspace available and used (64bit words) = 1000000 (
(MAXIMUM)

start of matrix solution
wall time = 1.00

singularity ratio 1.6829E-01

end of matrix solution
wall time = 1.00

element with highest stress relative to yield is 1
where equivalent stress is 1.000E-20 of yield

WINDOWS version
Marc - Student Edition 2016.0.0
output for increment 0. " job1"

total strain energy is 0.00000E+00

within which:
 elastic strain energy is 0.00000E+00
 total ext-force work is 0.00000E+00
 within which:
 work by appl. force/disp. is 0.00000E+00
 work by frictional forces is 0.00000E+00

				p r i n c i p a l v a l u e s			p h y s i c a l c			
o m p o n e n t s				1	2	3				
4	5	6	intensity	normal	minimum	intermediate	maximum			
				intensity						

element 1 point 1 integration pt. coordinate= 0.404E+02 0.893E+00
 section thickness = 0.500E+01

element 1 point 2 integration pt. coordinate= 0.415E+02 0.918E+00
 section thickness = 0.500E+01

element 1 point 3 integration pt. coordinate= 0.402E+02 0.333E+01
 section thickness = 0.500E+01

element 1 point 4 integration pt. coordinate= 0.414E+02 0.343E+01
 section thickness = 0.500E+01

; ; ;
 ; ; ;
 ; ; ;

element 439 point 1 integration pt. coordinate= 0.143E+03 0.364E+02
 section thickness = 0.500E+01

element 439 point 2 integration pt. coordinate= 0.143E+03 0.342E+02

		1	0.0000	0.0000		2	0.0000	0.0000
3	0.0000		0.0000					
		4	0.0000	0.0000		5	0.0000	0.0000
6	0.0000		0.0000					
	;		;			;		;
	;		;			;		;
		481	0.0000	0.0000		482	0.0000	0.0000
483	0.0000		0.0000					
		484	0.0000	0.0000		485	0.0000	0.0000
486	0.0000		0.0000					

t o t a l n o d a l t e m p e r a t u r e s

		1	0.0000		2	0.0000		3	0.0000
4	0.0000			5	0.0000				
		6	0.0000		7	0.0000		8	0.0000
9	0.0000			10	0.0000				
		11	0.0000		12	0.0000		13	0.0000
14	0.0000			15	0.0000				
	;		;		;				;
	;		;		;				;
	;		;		;				;
					481	0.0000		482	0.0000
483	0.0000		484	0.0000					
		486	0.0000		485	0.0000			

t o t a l n o d a l f l u x e s

4	0.0000	1	0.0000	5	0.0000	2	0.0000	3	0.0000
9	0.0000	6	0.0000	10	0.0000	7	0.0000	8	0.0000
14	0.0000	11	0.0000	15	0.0000	12	0.0000	13	0.0000
;		;		;		;		;	
;		;		;		;		;	
484	0.0000	481	0.0000	485	0.0000	482	0.0000	483	0.0000
		486	0.0000						

total equivalent nodal forces (distributed plus point loads)

3	0.0000	1	0.0000	0.0000	2	0.0000	0.0000
6	0.0000	4	0.0000	0.0000	5	0.0000	0.0000
		7	0.0000	0.0000	8	0.0000	0.0000
;		;		;		;	
;		;		;		;	

		481	0.0000	0.0000	482	0.0000	0.0000
483	0.0000		0.0000				
		484	0.0000	0.0000	485	0.0000	0.0000
486	0.0000		0.0000				

elsewhere reaction forces at fixed boundary conditions, residual load correction

		1	0.0000	0.0000	2	0.0000	0.0000
3	0.0000		0.0000				
		4	0.0000	0.0000	5	0.0000	0.0000
6	0.0000		0.0000				
			<i>i</i>	<i>i</i>		<i>i</i>	<i>i</i>
<i>i</i>		<i>i</i>					
			<i>i</i>	<i>i</i>		<i>i</i>	<i>i</i>
<i>i</i>		<i>i</i>					
483	0.0000		0.0000				
		484	0.0000	0.0000	485	0.0000	0.0000
486	0.0000		0.0000				

summary of externally applied loads

0.00000E+00 0.00000E+00

summary of reaction/residual forces

0.00000E+00 0.00000E+00

memory usage: MByte words % of total

within general memory:			
element stiffness matrices:	0	21554	0.1
solver: first part	0	63376	0.2
overallocation initial allocation	106	27914276	74.6
other:	0	4660	0.0
allocated separately:			
solver 8	8	1987904	5.3
nodal vectors:	0	64166	0.2
defined sets:	0	3620	0.0
transformations:	0	1944	0.0
kinematic boundary conditions:	0	54232	0.1
points, curves and surfaces:	0	86	0.0
mem_none:	0	42438	0.1
element storage:	1	259576	0.7
material properties:	0	5150	0.0
executable and common blocks:	27	7000000	18.7
miscellaneous	0	212	0.0

total:	143	37423194	
general memory allocated:	107	28003866	
general memory used:	0	89590	
peak memory usage:	159	41557522	
e n d o f i n c r e m e n t	0		
binary post data at increment	0.	subincrement	0. on file 16
formatted post data at increment	0.	subincrement	0. on file 19
wall time =	1.00		

```

$......
$....start of loadcase lcase1
title                lcase1
-----

loadcase             lcase1
-----

activate boundary condition apply1
activate boundary condition apply2
activate boundary condition applyT1
    ;                ;                ;                ;
    ;                ;                ;                ;
    ;                ;                ;                ;
activate boundary condition applyT95
activate boundary condition applyT96

control
-----

control information for region 1

maximum number of increments 100000
maximum number of recycles   10

```

minimum number of recycles 0

control of residual convergence:

relative tolerance:	1.00000E-01
cut-off value :	0.00000E+00
absolute tolerance:	0.00000E+00
relative moment tolerance:	0.00000E+00
moment cut-off value :	0.00000E+00
absolute moment tolerance:	0.00000E+00

full newton-raphson technique chosen

convergence testing is automatically switched between
residual and displacement testing if reactions or displacements
become too small

maximum nodal temperature change per time step = 2.00000E+01

maximum nodal temperature change before reassembly = 1.00000E+02

control messages will be written to log file

parameters

parameters set as follows

predictor used for stress-strain calculation	1.00000E+00
penalty factor for boundary conditions	1.00000E+09
penalty for incompressibility - r-p flow	1.00000E+02
penalty for incompressibility - fluid flow	1.00000E+06

beta parameter for Newmark operator	2.50000E-01
gamma parameter for Newmark operator	5.00000E-01
gamma parameter for Single-Step-Houbolt	1.50000E+00
gamma parameter for Single-Step-Houbolt	-5.00000E-01
sharp angle for sticking/separating - 2D	8.62500E+00
sharp angle for sticking/separating - 3D	2.00000E+01
initial strain rate for r-p flow	1.00000E-04
lowest strain rate cut-off for r-p flow	1.00000E-06
fraction of dilatational stress neglected	1.00000E+00
factor for drilling d.o.f for shells	1.00000E-04
factor for displacement after rezoning	1.00000E+00
universal gas constant	8.31400E+00
absolute temperature offset	2.73150E+02
thermal properties evaluation weight	5.00000E-01
surface projection factor in ssh dynamics	0.00000E+00
Stefan Boltzmann constant	5.67051E-08
Planck's second radiation constant	1.43877E-02
Speed of light in vacuum	2.99790E+08
Permeability of vacuum	1.25664E-06
Permittivity of vacuum	8.85419E-12
maximum iterative displacement component	1.00000E+30
initial stiffness to simulate sticking	0.00000E+00
minimum angle between the normal vectors of contacting segments	1.20000E+02
radiation reflection cut-off	1.00000E-03
angle for averaging adjacent beams (s2s)	1.60000E+02
stabilizer stiffness for model sections	0.00000E+00
maximum change in temperature per iteration	1.00000E+02
maximum rbe3 conditioning number	0.10000E+07
transient non auto	

time increment	time period	maximum steps	assembly interval	max iter mcreep
1.000E+00	5.000E+01	50	0	5

continue

auto control specified for time of 5.000E+01

s t a r t o f i n c r e m e n t 1

space needed for incremental backup: 63677

thermal pass

fluxes summed over the whole model

from distributed fluxes
magnitudes based upon undeformed configuration
0.000000E+00

concentrated fluxes
0.000000E+00

start of assembly cycle number is 0
wall time = 1.00

0.05 MByte)	solver workspace for phase1 (matrix input)	(64bit words) =	6048 (
	Metis nested dissection ordering used		
0.02 MByte)	solver workspace for phase2 (nodal ordering)	(64bit words) =	2262 (
0.01 MByte)	solver workspace for phase3 (symbolic factor)	(64bit words) =	1761 (
0.02 MByte)	solver workspace for phase4 (factorization)	(64bit words) =	2275 (
0.02 MByte)	(MINIMUM)		
0.02 MByte)	solver workspace for phase4 (factorization)	(64bit words) =	2276 (
0.02 MByte)	(MAXIMUM)		
7.63 MByte)	solver workspace available and used	(64bit words) =	1000000 (

start of matrix solution
wall time = 1.00

singularity ratio 1.0000E+00

end of matrix solution
wall time = 1.00

maximum nodal temperature change is 1.000E-20 at node 1

this is 5.000E-20 percent of change allowed on control option

automatic time stepping is switched off
init. thermal energy is 0.00000E+00
total thermal energy is 0.00000E+00

stress pass

load increments for each degree of freedom
summed over the whole model

from distributed loads
dist. loads on undeformed configuration - increments for dist. loads
increments for point loads
0.000000E+00 0.000000E+00

point loads
0.000000E+00 0.000000E+00

start of assembly cycle number is 0

wall time = 1.00

0.05 MByte)	solver workspace for phase1 (matrix input)	(64bit words) =	6048 (
	Metis nested dissection ordering used		
0.14 MByte)	solver workspace for phase2 (nodal ordering)	(64bit words) =	18782 (
0.19 MByte)	solver workspace for phase3 (symbolic factor)	(64bit words) =	25341 (
0.32 MByte)	solver workspace for phase4 (factorization)	(64bit words) =	41381 (
	(MINIMUM)		
0.56 MByte)	solver workspace for phase4 (factorization)	(64bit words) =	74047 (
	(MAXIMUM)		
7.63 MByte)	solver workspace available and used	(64bit words) =	1000000 (

start of matrix solution
wall time = 1.00

singularity ratio 1.6829E-01

end of matrix solution
wall time = 1.00

maximum residual force at node 443 degree of freedom 1 is equal to 4.030E-

6.614E+00 maximum reaction force at node 307 degree of freedom 1 is equal to
 residual convergence ratio 6.093E-15
 dynamic change has reached time of 1.000E+00 of total time period 5.000E+01
 total transient time = 1.00000E+00

WINDOWS version
 Marc - Student Edition 2016.0.0
 output for increment 1. " lcase1"

total strain energy is 4.87682E-01
 within which:
 elastic strain energy is 4.87682E-01
 total ext-force work is 4.87682E-01
 within which:
 work by appl. force/disp. is 4.87682E-01
 work by frictional forces is 0.00000E+00

Thermal Results

flux	element	point	temp	gradient components		
				1	2	3
1	2	3				
	1	1	5.387	1.521	0.3793	

```

0.000      0.000
           1      2      7.152      1.522      0.3591
;          ;          ;          ;          ;
;          ;          ;          ;          ;
0.000      0.000
           11     4      89.92     -3.401     -2.504
0.000      0.000

```

```

WINDOWS version
Marc - Student Edition 2016.0.0
output for increment 1. " lcase1"

```

```

           element      point      temp      gradient components
flux components
           1          2          3          1          2          3
0.000      12          1      97.65     -3.025     -2.992
           0.000
           12          2      93.11     -2.872     -3.056
;          ;          ;          ;          ;
;          ;          ;          ;          ;
0.000      0.000
           439         4      0.000     0.000     0.000
0.000      0.000

```

Structural Results

```

           tresca      mises      mean      p r i n c i p a l      v a l u e s      p h y s i c a l      c

```

o m p o n e n t s

	intensity	intensity	normal	minimum	intermediate	maximum	1	2	3
4	5	6							
			intensity						

element 1 point 1 integration pt. coordinate= 0.404E+02 0.893E+00
 section thickness = 0.500E+01
 engsts 1.407E-01 1.401E-01-4.601E-02-1.394E-01 0.000E+00 1.351E-03 1.304E-03-1.393E-01 2.582E-03
 engstn 3.485E-04 2.148E-04 0.000E+00-2.081E-04 7.888E-05 1.404E-04 1.403E-04-2.080E-04 1.279E-05
 thermal 5.818E-05 1.164E-04 0.000E+00 0.000E+00 5.818E-05 5.818E-05 5.818E-05 5.818E-05 0.000E+00

element 1 point 2 integration pt. coordinate= 0.415E+02 0.918E+00
 section thickness = 0.500E+01
 engsts 1.392E-01 1.351E-01-4.927E-02-1.392E-01-8.602E-03 0.000E+00-8.673E-03-1.391E-01 3.042E-03
 engstn 3.234E-04 2.006E-04 0.000E+00-1.830E-04 8.446E-05 1.404E-04 1.402E-04-1.828E-04 1.506E-05
 thermal 7.724E-05 1.545E-04 0.000E+00 0.000E+00 7.724E-05 7.724E-05 7.724E-05 7.724E-05 0.000E+00

element 1 point 3 integration pt. coordinate= 0.402E+02 0.333E+01
 section thickness = 0.500E+01
 engsts 1.446E-01 1.442E-01-4.770E-02-1.438E-01 0.000E+00 7.400E-04-5.680E-04-1.425E-01 1.369E-02
 engstn 3.580E-04 2.198E-04 0.000E+00-2.083E-04 8.178E-05 1.497E-04 1.464E-04-2.051E-04 6.780E-05
 thermal 6.608E-05 1.322E-04 0.000E+00 0.000E+00 6.608E-05 6.608E-05 6.608E-05 6.608E-05 0.000E+00

element 1 point 4 integration pt. coordinate= 0.414E+02 0.343E+01
 section thickness = 0.500E+01
 engsts 1.436E-01 1.393E-01-5.086E-02-1.436E-01-8.976E-03 0.000E+00-1.041E-02-1.422E-01 1.384E-02

;

;

;

;

```

element      439 point  3      integration pt. coordinate=      0.148E+03      0.364E+02
section thickness = 0.500E+01
engsts  4.391E-02 4.350E-02 1.491E-02 0.000E+00 8.206E-04 4.391E-02 9.511E-04 4.378E-02-2.367E-03
engstn  2.718E-07 1.840E-07 0.000E+00-6.390E-08-5.882E-08 2.079E-07-5.801E-08 2.071E-07-2.931E-08

element      439 point  4      integration pt. coordinate=      0.148E+03      0.342E+02
section thickness = 0.500E+01
engsts  4.378E-02 4.373E-02 1.462E-02 0.000E+00 9.855E-05 4.378E-02 3.176E-04 4.356E-02-3.086E-03
engstn  2.710E-07 1.847E-07 0.000E+00-6.268E-08-6.207E-08 2.083E-07-6.071E-08 2.070E-07-3.820E-08

```

n o d a l p o i n t d a t a

i n c r e m e n t a l d i s p l a c e m e n t s

```

          1 -1.58077E-15  1.08567E-16          2 -1.72493E-15  4.12865E-16
3 -1.60566E-15  1.69533E-16
          4 -1.62224E-15  1.06395E-16          5 -1.63117E-15  4.77400E-17
6 -1.64503E-15 -7.49572E-18
;          ;          ;          ;          ;          ;
;          ;          ;          ;          ;          ;
;          ;          ;          ;          ;          ;

485 -2.27958E-21 -9.44609E-22          486 -2.26694E-21 -7.45146E-22

```

t o t a l d i s p l a c e m e n t s

		1	-1.40311E-03	3.06355E-34		2	5.10222E-05	-2.49421E-32
3	-1.12704E-03		-2.51387E-33					
			4	-8.22878E-04	-9.81830E-34	5	-5.11124E-04	2.27280E-33
6	-2.15670E-04			-3.25327E-34				
	;							
				;				;
				;				;
483	3.39817E-05		4.37533E-06					
			484	3.35310E-05	5.04756E-06	485	3.30855E-05	5.95247E-06
486	3.26170E-05			7.18174E-06				

t o t a l n o d a l t e m p e r a t u r e s

		1	4.4700		2	14.325		3	7.5450
4	10.330			5	12.150				
		6	13.335		7	5.7550		8	9.5400
9	15.655			10	23.770				
	;								
		481	0.0000		482	0.0000		483	0.0000
484	0.0000			485	0.0000				
		486	0.0000						

t o t a l n o d a l f l u x e s

4	0.0000	1	0.0000	5	0.0000	2	0.0000	3	0.0000
		6	0.0000			7	0.0000	8	0.0000
			;		;		;		;
			;		;		;		;
479	0.0000			480	0.0000				
484	0.0000	481	0.0000	482	0.0000	483	0.0000		
		486	0.0000	485	0.0000				

total equivalent nodal forces (distributed plus point loads)

3	0.0000	1	0.0000	0.0000	2	0.0000	0.0000
		0.0000					
		4	0.0000	0.0000	5	0.0000	0.0000
			;		;		;
			;		;		;
483	0.0000		0.0000				
486	0.0000	484	0.0000	0.0000	485	0.0000	0.0000
			0.0000				

elsewhere reaction forces at fixed boundary conditions, residual load correction

		1	1.04083E-17	0.72903		2	0.0000	2.2342
3	1.38778E-17	1.3763						
		4	0.0000	1.3266		5	0.0000	1.2314
6	5.55112E-17	1.1027						
			;	;			;	;
;	;		;	;			;	;
			;	;			;	;
;	;		;	;			;	;
		478	0.0000	1.11022E-16		479	-2.22045E-16	5.55112E-17
480	-3.33067E-16	1.38778E-17						
		481	-1.11022E-16	0.0000		482	2.22045E-16	2.77556E-17
483	1.66533E-16	-3.33067E-16						
		484	2.22045E-16	1.11022E-16		485	8.32667E-17	1.11022E-16
486	2.77556E-17	1.11022E-16						

summary of externally applied loads

0.00000E+00 0.00000E+00

summary of reaction/residual forces

1.17796E-14 -3.10862E-15

memory usage: MByte words % of total

within general memory:			
element stiffness matrices:	0	21554	0.1
solver: first part	0	63376	0.2
overallocation initial allocation	106	27914276	74.3
other:	0	4660	0.0
allocated separately:			
incremental backup:	0	127354	0.3
solver 8	8	1987904	5.3
nodal vectors:	0	64166	0.2
defined sets:	0	3620	0.0
transformations:	0	1944	0.0
kinematic boundary conditions:	0	54232	0.1
points, curves and surfaces:	0	86	0.0
mem_none:	0	43410	0.1
element storage:	1	259576	0.7
material properties:	0	5150	0.0
executable and common blocks:	27	7000000	18.6
miscellaneous	0	212	0.0

total:	143	37551520	
general memory allocated:	107	28003866	
general memory used:	0	89590	
peak memory usage:	159	41557522	
e n d o f i n c r e m e n t	50		
binary post data at increment	50.	subincrement	0. on file 16
formatted post data at increment	50.	subincrement	0. on file 19
wall time =	10.00		

\$....end of loadcase lcase1

\$.....

*** end of input deck - job ends

memory usage:	MByte	words	% of total
within general memory:			
element stiffness matrices:	0	21554	0.1
solver: first part	0	63376	0.2
overallocation initial allocation	106	27914276	74.3
other:	0	4660	0.0
allocated separately:			
incremental backup:	0	127354	0.3
solver 8	8	1987904	5.3
nodal vectors:	0	64166	0.2
defined sets:	0	3620	0.0
transformations:	0	1944	0.0
kinematic boundary conditions:	0	54232	0.1
points, curves and surfaces:	0	86	0.0
mem_none:	0	43410	0.1
element storage:	1	259576	0.7
material properties:	0	5150	0.0
executable and common blocks:	27	7000000	18.6
miscellaneous	0	212	0.0

total:	143	37551520	
general memory allocated:	107	28003866	
general memory used:	0	89590	

peak memory usage: 159 41557522

timing information:	wall time	cpu time
total time for input:	0.16	0.14
total time for stiffness assembly:	1.32	1.19
total time for stress recovery:	1.24	1.12
total time for matrix solution:	1.64	1.39
total time for output:	3.85	3.45
total time for miscellaneous:	0.86	0.70

total time:	9.08	8.00

This is a successful completion to a Marc simulation,
indicating that no additional incremental data was
found and that the analysis is complete.

Marc - Student Edition 2016.0.0

Exit number 3004